




2019

BIOINFORMATIC AND EXPERIMENTAL ANALYSES OF AXOLOTL REGENERATION

Nour W. Al Haj Baddar

University of Kentucky, nwal222@uky.edu

Author ORCID Identifier:

 <https://orcid.org/0000-0003-1496-2561>

Digital Object Identifier: <https://doi.org/10.13023/etd.2019.470>

[Right click to open a feedback form in a new tab to let us know how this document benefits you.](#)

Recommended Citation

Al Haj Baddar, Nour W., "BIOINFORMATIC AND EXPERIMENTAL ANALYSES OF AXOLOTL REGENERATION" (2019). *Theses and Dissertations--Biology*. 61.
https://uknowledge.uky.edu/biology_etds/61

This Doctoral Dissertation is brought to you for free and open access by the Biology at UKnowledge. It has been accepted for inclusion in Theses and Dissertations--Biology by an authorized administrator of UKnowledge. For more information, please contact UKnowledge@lsv.uky.edu.

STUDENT AGREEMENT:

I represent that my thesis or dissertation and abstract are my original work. Proper attribution has been given to all outside sources. I understand that I am solely responsible for obtaining any needed copyright permissions. I have obtained needed written permission statement(s) from the owner(s) of each third-party copyrighted matter to be included in my work, allowing electronic distribution (if such use is not permitted by the fair use doctrine) which will be submitted to UKnowledge as Additional File.

I hereby grant to The University of Kentucky and its agents the irrevocable, non-exclusive, and royalty-free license to archive and make accessible my work in whole or in part in all forms of media, now or hereafter known. I agree that the document mentioned above may be made available immediately for worldwide access unless an embargo applies.

I retain all other ownership rights to the copyright of my work. I also retain the right to use in future works (such as articles or books) all or part of my work. I understand that I am free to register the copyright to my work.

REVIEW, APPROVAL AND ACCEPTANCE

The document mentioned above has been reviewed and accepted by the student's advisor, on behalf of the advisory committee, and by the Director of Graduate Studies (DGS), on behalf of the program; we verify that this is the final, approved version of the student's thesis including all changes required by the advisory committee. The undersigned agree to abide by the statements above.

Nour W. Al Haj Baddar, Student

Dr. S. Randal Voss, Major Professor

Dr. David Weisrock, Director of Graduate Studies

BIOINFORMATIC AND EXPERIMENTAL ANALYSES OF AXOLOTL
REGENERATION

DISSERTATION

A dissertation submitted in partial fulfillment of the
requirements for the degree of Doctor of Philosophy in the
College of Arts and Sciences
at the University of Kentucky

By

Nour Al Haj Baddar

Lexington, Kentucky

Director: Dr. S. Randal Voss, Professor of Neuroscience
Lexington, Kentucky

2019

Copyright © Nour Al Haj Baddar 2019

<https://orchid.org/0000-0003-1496-2561>

ABSTRACT OF DISSERTATION

BIOINFORMATIC AND EXPERIMENTAL ANALYSES OF AXOLOTL REGENERATION

Salamanders have an extraordinary ability to regenerate appendages after loss or amputation, irrespective of age. My dissertation research explored the possibility that regenerative ability is associated with the evolution of novel, salamander-specific genes. I utilized transcriptional and genomic databases for the axolotl to discover previously unidentified genes, to the exclusion of other vertebrate taxa. Among the genes identified were multiple *mmps* (Matrix metalloproteases) and a *jnk1/mapk8* (c-jun-N-terminal kinase) paralog. MMPs function in extracellular matrix remodeling (ECM) and tissue histolysis, processes that are essential for successful regeneration. *Jnk1/mapk8* plays a pivotal role in regulating transcription in response to cellular stress stimuli, including ROS (reactive oxygen species). Discovery of these novel genes motivated further bioinformatic studies of *mmps* and wet-lab experiments to characterize JNK and ROS signaling. The paralogy of the newly discovered *mmps* and orthology of 15 additional *mmps* was established by analyses of predicted, protein secondary structures and gene phylogeny. A microarray-analysis identified target genes downstream of JNK signaling that are predicted to function in cell proliferation, cellular stress response, and ROS production. These inferences were validated by additional experiments that showed a requirement for NOX (NADPH oxidase) activity, and thus presumably ROS production for successful tail regeneration. In summary, my dissertation identified novel, salamander-specific genes. The functions of these genes suggest that regenerative ability is associated with a diverse extracellular matrix remodeling and/or tissue histolysis response, and also stress-associated signaling pathways. The bioinformatic findings and functional assays that were developed to quantify ROS, cell proliferation, and mitosis will greatly empower the axolotl embryo model for tail regeneration research.

KEYWORDS: Regeneration, paralogs, ROS, JNK, MMPs

Nour Al Haj Baddar

06/29/2019

BIOINFORMATIC AND EXPERIMENTAL ANALYSES OF AXOLOTL
REGENERATION

By
Nour Al Haj Baddar

S. Randal Voss
Director of Dissertation
David Weiserock
Director of Graduate
Studies
06/29/2019

ACKNOWLEDGMENTS

I would like to express my utmost gratitude to my doctoral advisor, Randal Voss, for giving me the opportunity to work in his lab and providing the environment to support and guide me throughout my research. I would like to thank him for allowing me to independently think and formulate hypotheses, tackle arising problems and research solutions. This work could not have been possible without his support, help, and guidance.

I would also like to thank the rest of my dissertation committee members (Vincent Cassone, Jeramiah Smith, Sasha Rabchevsky) for their invaluable help and advice. Beside my committee members, I would like to thank Mike Fried for serving as an external examiner and for all his insightful advice.

Additionally, I would like to thank all past and present members of the Voss lab for their help throughout my dissertation, especially; Laura Muzinic, Chris Muzininc, Maria Torres-Sanchez, Ryan Woodcock, Varun Dwaraka, Jennifer Wolfe, Alex Palumbo, and Kevin Kump.

I count myself very lucky to have such a supportive and loving family in Jordan! I am in debt for my parents who taught me the value of science, hard work, and independence. I express my thanks to my awesome brothers and sisters for their endless support and encouragement, especially my sister Zeinah!

TABLE OF CONTENTS

ACKNOWLEDGMENTS	iii
LIST OF TABLES.....	vii
LIST OF FIGURES	viii
LIST OF SUPPLEMENTARY FILES	ix
Chapter 1: Introduction.....	1
1.1 Axolotl as a model for regeneration.....	1
1.2 Gene duplication as an engine of novelty	3
1.3 Salamander-specific genes with proven roles during regeneration	4
1.4 Injury induced signaling in regeneration (ROS and JNK signaling)	6
1.5 Establishing methods to empower studies of tail regeneration using axolotl embryos	7
Chapter 2: Sal-Site: Research Resources for the Mexican Axolotl	9
2.1 Introduction.....	9
2.2 Sal-Site Website.....	10
2.2.1 Homepage	10
2.2.2 Axolotl Research.....	10
2.2.3 Genome Resources.....	11
2.2.3.1 Gene and EST Database.....	11
2.2.3.2 Genetic Map and Marker Information	13
2.2.3.3 Blast	14
2.2.3.4 Gene Expression	16
2.3 Ambystoma Genetic Stock Center.....	17
2.4 Education	17
Chapter 3: Identification of Presumptive Lineage-Specific Duplicated Genes in The Mexican Axolotl (<i>Ambystoma Mexicanum</i>)	34
3.1 Introduction.....	34
3.2 Materials and Methods.....	35
3.2.1 Identification of human: axolotl orthologous gene pairs using Sal-site	35
3.2.2 Identification of putative lineage-specific duplicates in the axolotl using the recently published axolotl genome	37
3.2.3 Gene ontology enrichment analysis	37
3.3 Results.....	37
3.3.1 Identification of orthologs and candidate lineage-specific duplicates in the axolotl.....	38
3.3.2 Gene ontology analysis of presumptive axolotl paralogs.....	38
3.4 Discussion.....	41
3.5 Acknowledgments.....	43
Chapter 4: Identification of Axolotl MMP Gene Family Members, Including Novel Salamander-Specific MMP Paralogs	44
4.1 Introduction.....	44
4.2 Materials and Methods.....	46
4.2.1 Bioinformatics search for axolotl MMPs.....	46
4.2.2 Phylogenetic analyses.....	46

4.2.3 Temporal and spatial gene expression of axolotl MMPs.....	47
4.3 Results and Discussion	48
4.3.1 Identification of MMP genes in the axolotl.....	48
4.3.2 Salamander-specific MMP3 duplicates.....	49
4.3.3 Salamander-specific collagenases	49
4.3.4 Salamander-specific MMP13 duplicates.....	50
4.3.5 Salamander-specific MMPe	50
4.3.6 Gene expression profiles of MMPs in the axolotl.	51
4.3.7 Salamander-specific molecular sequence signatures in MMP3 paralogs	53
4.4 Conclusions.....	54
4.5 Acknowledgments.....	55
Chapter 5: Role of JNK Signaling During Axolotl Embryo Tail Regeneration:	
A Microarray Study to Identify Downstream Targets	68
5.1 Introduction.....	68
5.2 Materials and Methods.....	69
5.2.1 Chemical treatment with a JNK inhibitor and regeneration assays.....	69
5.2.2 Microarray gene expression analysis	69
5.2.3 Statistical analyses	70
5.2.4 Nanostring nCounter® SPRINT Profiler development and analysis	70
5.3 Results and Discussion.....	71
5.3.1 JNK activity is essential for axolotl embryo tail regeneration.....	71
5.3.2 Identification of transcripts that changed as a result of JNK inhibition	
at 1dpa	71
5.3.3 GO enrichment analysis of genes that were upregulated in the JNK	
inhibitor treatment group	72
5.3.4 GO enrichment analysis of genes that were downregulated in the JNK	
inhibitor treatment group	75
5.4 Conclusions	78
Chapter 6: Amputation-induced ROS signaling is required for axolotl tail regeneration .	83
6.1 Introduction.....	83
6.2 Materials and Methods.....	85
6.2.1 Ethical procedure	85
6.2.2 Regeneration assay.....	85
6.2.3 Histology and immunohistochemistry	86
6.2.4 <i>In vivo</i> ROS imaging.....	86
6.2.5 Cellular proliferation assay	87
6.3 Results and Discussion	88
6.3.1 Histology of axolotl embryo tail regeneration	88
6.3.2 Association of ROS with axolotl embryo tail regeneration	89
6.3.3 NOX activity is required for amputation-induced ROS production	90
6.3.4 ROS as early injury-induced signal and its role in cellular proliferation.	91
6.4 Conclusions.....	93
Chapter 7: Conclusions and Future directions	101
References.....	104

Vita.....	120
-----------	-----

LIST OF TABLES

Table 4.1. Transcriptome resources used to extract MMP sequences from the organisms listed	56
Table 4.2. Refined analysis showing the best candidate sequences for salamander MMP3 genes	57
Table 5.1. Gene Ontology Enrichment for differentially expressed genes as a result of SP600125 treatment	79

LIST OF FIGURES

Figure 2.1 The Sal-Site homepage.	19
Figure 2.2 Axolotl research webpage provides hyperlinks to axolotl research projects and selected publications.	20
Figure 2.3 Axolotl BAC project.....	21
Figure 2.4 Genome resources main webpage.	22
Figure 2.5 Gene and EST database.....	23
Figure 2.6 An example search of the Gene and EST database.	24
Figure 2.7 An example gene card for <i>Ambystoma mexicanum</i> <i>erg1</i>	25
Figure 2.8 Axolotl genetic map and marker information.	26
Figure 2.9 The Sal-Site NCBI-BLAST tool is used to identify axolotl contigs that share sequence identity with query sequences.....	27
Figure 2.10 BLAST output.	28
Figure 2.11 Continuation of BLAST output from Fig. 10.....	29
Figure 2.12 Gene expression during axolotl limb regeneration.....	30
Figure 2.13 Comprehensive microarray analysis of gene expression during axolotl limb regeneration is available on the Sal-Site genome resources page....	31
Figure 2.14 The <i>Ambystoma</i> Genetic Stock Center (AGSC).....	32
Figure 2.15 The Education hyperlink.	33
Figure 4.1 The MMP gene family.....	58
Figure 4.2 Cladogram showing MMPs from the axolotl and other vertebrates.....	59
Figure 4.3 A magnified view of the salamander MMP3 clade and human collagenase and stromelysin clades shown in Fig 4.2.....	60
Figure 4.4 A magnified view of the salamander-specific collagenase, MMPe, and MMP13 clades shown in Fig 4.2.....	61
Figure 4.5 Gene expression of salamander specific <i>mmps</i> during limb regeneration	62
Figure 4.6 Gene expression analysis of <i>mmps</i> across different tissues in the axolotl	64
Figure 4.7 Hinge domain sequence variation within salamanders MMP3 proteins.	67
Figure 5.1 JNK inhibitor SP600125 treatment blocks tail regeneration in axolotl.....	80
Figure 5.2 Experimental design used to collect tissues for microarray analysis... ..	81
Figure 5.3 Correlation of normalized log ₂ fold change estimates across gene platforms: ncounter Nanostring and <i>Ambystoma</i> Affymetrix.....	82
Figure 6.1 H&E stained longitudinal sections of axolotl embryo tail regeneration	94
Figure 6.2 Association of ROS production with axolotl embryo tail regeneration	96
Figure 6.3 DPI and VAS2870 reduced ROS production during tail regeneration.....	97
Figure 6.4 Treatment with 4 μ m DPI (NOX inhibitor) significantly inhibits axolotl embryo tail regeneration	98
Figure 6.5 ROS signaling is important for mitosis during axolotl embryo tail regeneration.....	99
Figure 6.6 ROS signaling is required for DNA synthesis and cell cycle re-entry during axolotl tail regeneration.....	100

LIST OF SUPPLEMENTARY FILES

Table 3.1 Human: axolotl putative orthologs based on Sal-Site.....	[XLSX 146 KB]
Table 3.2 Putative lineage specific paralogs in axolotl based on Sal-Site ...	[XLSX 33 KB]
Table 3.3 Presumptive lineage-specific paralogs using (Nowoshilow et al., 2018) and (Smith et al., 2019) genomic/transcriptomic resources	[XLSX 197 KB]
Table 3.4 Gene Ontology (GO) enriched terms of lineage-specific paralogs in the axolotl	[XLSX 33 KB]
Table 4.1 Axolotl MMPs with their corresponding transcript IDS from three axolotl transcriptome databases; (Nowoshilow et al., 2018; Bryant et al., 2017, and Sal-Site (Baddar et al., 2015).....	[XLSX 37 KB]
Table 4.2 Candidate homologs of axolotl mmps in other salamanders and caecilian transcriptomes	[XLSX 37 KB]
Supplementary File 4.1 The mmps transcript IDs of the selected organisms for the study	[TXT 67 KB]
Supplementary File 4.2 The mmp gene coding sequences used for the study	[TXT 468 KB]
Table 5.1 Differentially expressed genes in Sp600125-treated embryos	[XLSX 17 KB]
Table 5.2 Validation of gene expression of selected genes in Sp600125-treated embryo using Nanostring codeset	[XLSX 25 KB]

CHAPTER 1: INTRODUCTION

Although regeneration is widespread among metazoans, relatively few vertebrates possess an ability to regenerate lost or injured appendages. What explains variation in regenerative ability is a long-standing mystery. One possibility is that regenerative ability is associated with the evolution of novel, lineage-specific genes. However, there has not been a systematic and comprehensive search for salamander-specific genes that may function in regeneration. Among salamanders, axolotls are the primary model for studies of tissue regeneration. Considerable progress has been made in developing transcriptional and genomic databases for the axolotl, and much has been learned about gene expression during regeneration. Thus, the axolotl is the most logical salamander species to exploit in the search for novel, duplicated genes. I summarize below the features that make axolotls especially good models for tissue regeneration. I then review literature supporting the existence of salamander specific genes and their roles in regeneration. Next, I introduce two injury-induced signaling pathways that are essential for successful regeneration: JNK and ROS (reactive oxygen species). Finally, I introduce assays developed in my research that empower the axolotl embryo model for tail regeneration research.

1.1 The axolotl as a model of regeneration

Lower vertebrates possess an unparalleled ability to regenerate complex tissues and appendages after traumatic injury. Among these, the Mexican Axolotl, *Ambystoma mexicanum*, is the primary salamander model in biomedical research (Putta et al., 2004; Denis et al., 2013; Voss et al., 2015). Several features make axolotls ideal for experimental procedures and regeneration studies, better for example than frog and fish models. First,

axolotl larvae and adults faithfully regenerate appendages like limbs and tail, and various internal organs including the spinal cord, brain, and heart. This contrasts with anuran amphibians that have limited adult regenerative potential and developmentally restricted windows wherein regeneration can occur (Beck et al., 2009). Although fish (e.g. zebrafish) can regenerate appendages like fins, axolotls have limbs that are homologous among tetrapods, including mammals. Zebrafish fins lack tissues found in tetrapod limbs, including muscle and cartilage (Gemberling et al., 2013; Ceci et al., 2018).

Axolotls are among the best characterized vertebrate models for appendage regeneration. Recently, Ponomareva et al (2015) established a tail regeneration model using axolotl embryos for chemical genetic screening. They showed that developmental stage 42 embryos (Bordzilovskaya et al., 1989) completely regenerate a 2 mm piece of their amputated tail in 7 days. Furthermore, they showed that this model provides an efficient assay for characterizing gene expression changes associated with tail regeneration. This model offers a very quick regeneration assay, much quicker than working with older axolotls. Also, embryos used in this assay do not require feeding and can be reared individually in cell culture plates. Importantly, chemicals that inhibit specific signaling pathways can be tested for effects on tissue regeneration in a timely and cost-effective manner.

Axolotl transcriptomic/genomic resources and databases have matured greatly over last decade. Prior to recent advances in genome sequencing and assembly (Keinath et al., 2015; Nowoshilow et al., 2018; Smith et al., 2019), transcript sequences were the primary data from which to develop tools for genetic, genomic, and developmental studies (Putta et al., 2004; Smith et al., 2005). The Voss lab developed many resources from

transcript data, including EST databases, an axolotl linkage map, Affymetrix microarrays (Huggins et al., 2012), and gene expression databases (Monaghan, 2009; Voss et al., 2015). All these resources were made publicly available via a web portal called Sal-Site (www.Ambystoma.org) (Baddar et al., 2015). These constitute essential resources for axolotl research. In this dissertation, I describe Sal-Site resources and best approaches to extract useful information (Baddar et al., 2015). In summary, the advantages highlighted above establish the axolotl as the best salamander model for regeneration research.

1.2. Gene duplication as an engine of novelty

Genes that arise uniquely within lineages by gene duplication provide the raw material for functional novelties and species-specific adaptations (Force et al., 1999; Remm et al., 2001; Kaessmann, 2010; Khaltrurin et al., 2009; Voordeckerers et al., 2015). Indeed, the evolutionary retention of duplicated genes is known to be associated with changes in genetic pathways, developmental programs, physiological systems, and the origin of novel phenotypes (Han et al., 2009, Ravi et al., 2013; Shukla et al., 2014). Duplicated genes contribute to the evolution and expansion of existing (sub) cellular machineries and genetic pathways by introducing gene products with the ability to fold into stable structures, with established functions and the potential to interact with their ancestor's interaction partners (Voordeckerers, et al., 2015). Mutations are thought to accumulate in newly duplicated sequences that may engender new functions that did not exist before (neofunctionalization). Also, the functions of duplicated genes can be temporally and spatially partitioned to achieve more exacting gene regulation (subfunctionalization)

(Force et al., 1999). There are many examples of lineage specific duplication, I focus below on those identified in salamanders within the context of regeneration.

1.3. Salamander-specific genes with proven roles during regeneration

Salamanders show a remarkable ability to regenerate limbs and complex organs throughout life, an ability that might reflect the evolution of lineage specific genes that are associated with regeneration (Graza-Garcia et al., 2010; Zhao et al., 2016; Slack, 2017). Several salamander-specific genes that presumably arose by duplication have been identified and shown to play essential roles during regeneration. For example, Prod 1 and nAG orchestrate nerve-dependent signaling that supports blastema growth and limb patterning (da Silva et al., 2002; Kumar et al., 2007; Blassberg et al., 2010). *Prod1* (proximal distal 1) is a novel member of the TFP (Three Finger Protein) gene family and encodes a cell surface protein that is expressed on blastema cells in a proximodistal gradient in newts and axolotls (da Silva et al., 2002; Graza-Garica, et al., 2009, Blassberg et al., 2010). nAG (newt anterior gradient) protein, another novel member in the highly conserved gene family of anterior gradient proteins, was identified as the ligand that binds PROD1 in newts (Kumar et al., 2007). nAG is secreted in Schwann cells around nerves in the stump and later in the wound epidermis (Kumar et al., 2007). It was subsequently shown that *prod1* is found in species of many salamander families, including a species (*Batrachuperus longdongensis*) from a family at the base of the salamander tree (Geng et al., 2015). This suggests that fundamental mechanisms of limb regeneration are associated with the evolution of novel genes.

The CCN gene family (Connective tissue growth factor - *ctgf*, Cystein rich protein-*cry61*, and Nephroblastoma overexpressed gene- *nov*) provides another example of novel genes with regeneration-specific functions in newts (Losso et al., 2012). These genes are stimulated by growth factors (e.g. TGF- β) and changes in their expression are correlated with cell proliferation, adhesion, migration, and angiogenesis (Leask and Abraham, 2003). A newt-specific CCN (*NvCCN*) is only up regulated during heart regeneration, while two other presumptive paralogs of CCN do not change their expression levels (Looso et al., 2012). This suggests that *NvCCN* arose by gene duplication and diverged in a way that allowed it to be functionally integrated in a regeneration-specific gene network (Tanaka and Galliot, 2009). More recently, *Newtic1*, also a salamander-specific gene, was found to be expressed in a subset of circulating erythrocyte-monocyte clumps (EryC) in a newt (Casco-Robles et al., 2018). These clumps were found to be formed in stump tissue following limb amputation and around the blastema. More importantly, EryC were found to also harbor a host of secretory molecules commonly involved in angiogenesis and ECM remodeling (TGFB1, Bmp2, VEGF, several MMPs, and the aforementioned (*NvCCN*), that may be delivered to the blastema (Casco-Robles et al., 2018).

The recent development of genomic and transcriptomic resources for the axolotl (Bryant et al., 2017; Nowoshilow et al., 2018; Smith et al., 2019) now make it possible to mine novel salamander genes in a more efficient manner. In my dissertation research, I searched computationally-predicted axolotl protein coding sequences in Sal-Site (Baddar et al., 2015) and the newly released axolotl transcriptome (Nowoshilow et al., 2018) to identify a comprehensive list of salamander-specific genes. Surprisingly, I discovered multiple, novel MMPs (Matrix metalloprotease genes) with no apparent homologs in

mammals. These MMPs retain conserved MMP family domain signatures but have additional novel sequence features that seem to be specific to salamanders (Miyazakai et al; 1996; Kato et al, 2003). MMPs mediate tissue histolysis and ECM (extracellular matrix) remodeling during limb regeneration in salamanders (Yang and Bryant, 1994; Miyazakai et al; 1996; Yang et al., 1999; Chernoff et al., 2000; Kato et al., 2003; Vinarsky et al., 2005; Monaghan, 2009; Stocum et al., 2017). Furthermore, pharmacological inhibition of MMPs blocks regeneration, highlighting their indispensability (Vinarsky et al., 2005). I utilized axolotl transcriptomic databases to identify 24 MMP genes, including novel, salamander-specific genes. These salamander-specific MMP genes may enable tissue and ECM remodeling mechanisms that create regeneration permissive environments, environments that are lacking in mammals.

1.4. Injury-induced signaling pathways

Appendage regeneration is governed by complex biological processes and signaling pathways that are highly conserved in all vertebrates (Stoick-Cooper et al., 2007; Lévesque, et al., 2007; McCusker and Gardiner, 2011). Our results in Chapter 3 identify a duplication of the conserved *jnk1* gene. Upon phosphorylation by upstream kinases, JNK1 proteins phosphorylate and activate downstream targets, including transcription factors (Weston and Davis, 2007; Zeke et al., 2016). JNK signaling is highly conserved among organisms and helps regulate cellular responses to a myriad of stimuli (Davis, 2000). Inhibition of JNK signaling has been shown to perturb blastema formation, wound healing, patterning, and apoptosis in different regeneration models, beyond salamanders (Sugiura et al, 2009; Tasaki et al., 2011; Gauron et al., 2013). However, JNK pathway signaling

during regeneration in the axolotl has not been rigorously explored (Sabin et al., 2015; Sader et al., 2019). Described in Chapter 5, I inhibited JNK signaling in axolotl embryos and identified target genes that are predicted to function in cell proliferation, pathogenicity, cellular stress response, and ROS production. ROS are chemically reactive oxygen-containing molecules, generated endogenously by several cellular components, including mitochondria, lysosomes, and the plasma membrane (Di Meo et al. 2016). ROS are well recognized components of metazoan innate immune responses and may provide cues for activating cell signaling pathways (Weidinger and Kozlov, 2015). Indeed, recent reports show that ROS are injury-induced signaling molecules essential for triggering tissue regeneration processes in amphibia (Love et al., 2013; Gauron et al., 2013). Therefore, I investigated the role of ROS in the axolotl embryo model and found that ROS are required for tail regeneration. Understanding how these early signaling pathways initiate and facilitate regeneration programs relative to non-regenerating vertebrates is key to identifying the most efficient paths toward developing regenerative/reparative therapies for humans.

1.5. Establishing methods to empower studies of tail regeneration using axolotl embryos

The axolotl embryo tail regeneration model provides important advantages over other models (Ponomareva et al., 2015). The Voss lab has screened thousands of chemicals for effect on tail regeneration and many hits have been identified. To advance this research effort, there is need to develop assays that can identify the mechanisms that are associated with chemical inhibition of tail regeneration. To this end, I developed and present new

assays in this dissertation that bring us closer to understanding how axolotls are able to successfully regenerate tissues.

Chapter 2: Sal-Site: Research Resources for the Mexican Axolotl

Nour W. Al Haj Baddar^{a,b}, M. Rayan Woodcock^c, Shivam Khatri^a, Kevin Kump^a, and S.

Randal Voss^{b,d}

^aDepartment of Biology, University of Kentucky, Lexington, KY, 40506

^bDepartment of Neuroscience and Spinal Cord and Brain Injury Research Center (SCoBIRC), University of Kentucky, Lexington, Kentucky, 40536

^cDepartment of Biology, Keene State College, Keene, NH 03431

^dAmbystoma Genetic Stock Center, University of Kentucky, Lexington, KY 40536

Previously published:

Al Haj Baddar N, Woodcock M, Khatri S, Kump K, and Voss R. (2015). Sal-Site: Research Resources for the Mexican Axolotl. *Methods in molecular biology* (Clifton, N.J.). 1290. 321-36. 10.1007/978-1-4939-2495-0_25. DOI: 10.1007/978-1-4939-2495-0_25.

2.1 Introduction

Salamanders are important models in basic and biomedical research. Over the last 100 years, salamanders have figured prominently in studies of development, neurophysiology, ecology, evolution, and tissue regeneration. To enhance efforts in these and other research areas, genome resource development is underway for the primary salamander model—the Mexican axolotl (*Ambystoma mexicanum*). A bioinformatics Web-base—Sal-Site—was created to make axolotl genomic data and information available to the community. Here we describe Sal-Site content and best practices for extracting useful information.

2.2 Sal-Site Website

2.2.1 Homepage

The Sal-Site homepage provides hyperlinks to access axolotl genome resources and information (Fig. 2.1). The header tab (Fig. 2.1A) indexes major sections of the website: axolotl research, genome resources, *Ambystoma* Genetic Stock Center (AGSC), education, about, and photo gallery. In addition, an orientation video (Fig. 2. 1B) introduces the Mexican axolotl (*Ambystoma mexicanum*) and highlights its remarkable ability to regenerate complex tissues and organs. The video also details general functions of the AGSC. This unique facility houses, breeds, and maintains a large inbred axolotl population, providing axolotls nationally and inter- nationally. The homepage also displays additional summary information regarding the axolotl's type location (Lake Xochimilco, Mexico), general phenotypic characteristics, and Sal-Site support mechanisms (Fig. 2.1C). The Fun Facts section (Fig. 2.1D) provides quick informational statements regarding axolotls that periodically change. Finally, the home page provides quick links for the most highly accessed Sal-Site links (Fig. 2.1E).

2.2.2 Axolotl Research

The significance of the axolotl model will grow with genome resource development and further advances in the field. The axolotl research section of Sal-Site (Fig. 2.2) details projects and publications associated with axolotl resource development. Over the last 10 years, the axolotl transcriptome has been deeply sequenced, microarrays have been developed and used to study regeneration and metamorphosis, and a meiotic map was constructed. Current projects include transgenic axolotl development, sequencing of whole axolotl chromosomes, and creation of large insert DNA libraries

using Bacterial Artificial Chromosome (BAC) vectors. With respect to the BAC project, a workflow is in place to screen BAC super pools by next generation sequencing to create an inventory of potential candidate genes for isolation. This initiative is developing regulatory sequence information for key developmental genes, information that is useful for developing reporter constructs for transgenic development (Fig. 2.3). This and the other initiatives will enable sequence-based methods of inquiry that are typical of genetic model organisms. The axolotl research section of Sal-Site will continually evolve to keep the community abreast of new resources as they become available.

2.2.3 Genome Resources

The Genome Resources section of Sal-Site (Fig. 2.4) organizes resources into four main subsections: gene and EST databases (Fig. 2.4A), genetic map and marker information (Fig. 2.4B), BLAST (Fig. 2.4C), and limb regeneration microarray databases (Fig. 2.4D). Each subsection is discussed below.

2.2.3.1 Gene and EST Database

An EST represents a partial sequence of a complementary DNA (cDNA) synthesized from a messenger RNA (mRNA). ESTs enable multiple lines of research, including transcript assembly, protein sequence annotation, genome mapping, and design of oligonucleotide probes for PCR and microarrays. Sal-Site presents transcriptome data for the Mexican axolotl and eastern tiger salamander (*A. tigrinum tigrinum*) (Fig. 2.5), and in the future, for additional ambystomatid species. The *A. mexicanum* transcriptome includes transcripts sampled from a variety of tissues and exists as two separate transcript assemblies (Version 3.0 and 4.0) (Putta et al., 2004; Smith et al., 2005; Voss et al., 2011).

When a sufficient number of ESTs are generated for a specific mRNA, it is possible to assemble these into a contiguous nucleotide sequence that provides a model of the protein-coding sequence. However, if EST depth is not sufficient to build a contiguous sequence (contig), which is problematic in working with expanded genic regions of the axolotl genome (Smith et al., 2009), a contig may only partially cover an mRNA, or independent contigs may map to nonoverlapping portions of the same mRNA. ESTs may also assemble into multiple overlapping reads that are suggestive of splice variants. When there is sequence contiguity among a group of contigs, they are classified into a common isogroup. For a given isogroup, any inferred splice variants (which would putatively represent individual transcripts) are reported as isotigs. The Sal-Site genome resources webpage enables visitors to search for genes of interest in *A. mexicanum* or *A. t. tigrinum* salamander transcriptome databases. The search for genes in assembly V3.0 and V4.0 (Fig. 2.5) can be conducted by typing a specific contig (Fig. 2.5A), isotig (Fig. 2.5B), or gene symbol identifier (Fig. 2.5C) in the appropriate field, and by selecting a reference database from the drop-down menu (Fig. 2.5D).

Figure 2.6 shows steps that an investigator would follow to identify a gene of interest in the gene and EST database. For example, if a user is interested in searching the *A. mexicanum* V4.0 database for *early growth response 1*, the official gene symbol (*egr1*) is typed in the appropriate field (Fig. 2.6A) using one of the reference databases (Fig. 2.6B). After clicking the submit button, a results page appears to show axolotl contigs (hits) that are annotated for *egr1* (Fig. 2.6C). It is important to note that more than one contig hit may be reported for a query; these may represent split or nonoverlapping contigs for the same gene model, or incomplete transcript models with low quality sequence. Moreover, when

more than one contig shows sequence identity to the same region of a query, it is possible that the contigs are paralogous genes. In this example, two contigs have been assembled for *egr1*. By clicking on the hyperlink provided for the first contig (contig316872), a gene card appears (Fig. 2.7A). The gene card offers an additional hyperlink to open a NCBI page for the corresponding orthologous human protein (Fig. 2.7B). The gene card page also includes a hyperlink to PubMed that reports some of the scientific articles that are related to the gene of interest (Fig. 2.7C). Clicking the contig ID hyperlink opens a sequence annotation page that provides detailed information about the contig, including the number of ESTs in the contig (Fig. 2.7D), contig nucleotide sequence (Fig. 2.7E), and the longest computer predicted open reading frame (ORF) with protein translation (Fig. 2.7F). Additionally, this sequence annotation page contains data for BLAST hits linked to human sequences curated by NCBI, including sequence similarity and alignment statistics (Fig. 2.7G). In this example, EST depth, sequence similarity, and sequence coverage provide very good evidence that contig 316872 corresponds to *egr1*.

2.2.3.2 Genetic Map and Marker Information

Although the Mexican axolotl genome is large, it has been possible to order genes into linkage groups and identify conserved gene orders in comparison to other vertebrate models (Voss et al., 2003; Smith et al., 2009; Voss et al., 2011). Sal-Site provides information about the ordering of 917 genetic markers among 17 linkage groups (LG)—as an example, part of LG3 is shown (Fig. 2.8A). The number of linkage groups approaches the *Ambystoma* haploid chromosome number ($N=14$) and is comprised mostly of EST-based markers. A conserved synteny table provides the positions of orthologous loci from human, axolotl, chicken, and *Xenopus tropicalis* genomes (Fig. 2.8B). Continuing with

the example above, the genome position of *egr1* has not been determined, however it is possible to determine the most likely position by comparing conserved synteny blocks between the axolotl and chicken gene maps. In the chicken genome, *egr1* is found on chromosome 13. Because all but two of the chicken chromosome 13 genes that have been mapped in the axolotl locate to axolotl LG3, the location of these genes within LG3 provide the most likely position for *egr1*. The *Ambystoma* linkage map has been used to establish orthology of key developmental genes (Dixon et al., 2010; Tapia et al., 2012) and identify quantitative trait loci (Voss and Shafer, 1999; Voss and Smith, 2005; Johnson et al., 2013; Page et al., 2013).

2.2.3.3 Blast

The Basic Local Alignment Tool (BLAST) is a powerful tool to identify sequence similarities among nucleotide sequences (Altschul et al., 1997). Sal-Site provides NCBI-BLAST tools to allow sequence similarity searches of *A. mexicanum* and *A. t. tigrinum* nucleotide databases (Fig. 9). To illustrate, we will use human *egr1* (gi|31317226) as a query sequence to identify the axolotl sequences that share nucleotide similarity with it. The input sequence (query) can be pasted as a FASTA formatted sequence, (Fig. 2.9A) or uploaded from a file (Fig. 2.9B). The BLAST search can be conducted using a user-selected algorithm (available options include: blastn, blastp, blastx, tblastx, tblastn; Fig. 2.9C) against a chosen *Ambystoma* database from the drop-down menu (Fig. 2.9D). Clicking the search button submits the sequence data and opens a BLAST results report. Example portions of BLAST reports are displayed in Figs. 2.10 and 11.

The first portion of BLAST output contains header information (Fig. 2.10 I) that reports the algorithm used for the BLAST search task (e.g., blastn) and the database that has been searched. The second portion of BLAST output (Fig. 2.10 II) displays the length of the query input sequence and a graphical representation of the BLAST results summarizing the top hits (i.e., a sequence that shows nucleotide similarity to the query) found in the database. The third portion of the BLAST output report includes a one line description of the best hits found (Fig. 2.11 III). Herein, every line summarizes the information about the contig ID, its length, score, and E-value (Fig. 2.11A–D). The sequences are ordered in this section from greatest to least similar, relative to the query sequence. The score (Fig. 2. 11C) measures similarity between the query and the hit sequences: the greater the value, the greater the similarity between hit sequence and query. The E-value (Fig. 2.11D) is an index of the statistical significance of the hit reported: the lower the number, the greater the similarity between sequence and query. Note that the best axolotl hit recovered for human *egr1* is contig 316872 (Fig. 2.11A), as it has the highest score and the lowest E-value. Clicking on the score hyperlink (Fig. 2.11C) of a selected contig takes the user to the final portion of the BLAST output (Fig. 2.11 IV). This part gives a detailed pairwise alignment of the query to each of the recovered hits. The header (Fig. 2.11E) is a repetition of the header information in the previous output section (Fig. 2.11 III). In this example “identities (89 %)” represent the percentage of nucleotide positions that is fully identical between contig316872 and human *egr1* sequence in the region of alignment. The pairwise alignment (Fig. 2.11G) provides the coordinates of the query and subject (or hit) sequences that are aligned (i.e., nucleotides positions) in addition to a vertical line series that represent identical nucleotides shared between both sequences.

2.2.3.4 Gene Expression

Gene expression technologies have advanced nearly all areas of biological research, providing, for example, greater insight into molecular pathways underlying biological processes. A number of advanced molecular tools for gene expression analysis (including microarray, quantitative-pcr, RNA-seq, and Nanostring) are being used in axolotl studies. Sal-Site provides information that is useful for conducting microarray analyses using a custom Affymetrix GeneChip that is available for purchase from Affymetrix (partnumber:520748) (Huggins et al., 2012) (Fig. 2.12). These microarrays provide a standard platform for conducting gene expression experiments. Data from published microarray experiments are available for download as CEL files. Additional files that are needed to analyze and annotate microarray data are available from Sal-Site, as are instructions for normalizing microarray data using Affymetrix® Expression Console™ or Partek® Genomics Suite™ to implement the Robust Multiarray Average (RMA) approach (Irizzary et al., 2003).

Given growing interest in axolotl regeneration, Sal-Site provides a searchable database (Fig. 2.13) of temporal gene expression profile for the first 28 days of limb regeneration. This study is exemplary in scope and experimental design. The experiment used ten replicate axolotl GeneChips to estimate gene expression for two different amputation injuries and 20 different post-amputation time points (Fig. 2.13 I).

Overall, the database reports 8,000,000 estimates of gene expression. These data can be queried using gene names, gene acronyms, or Affy probe IDs. For example, by typing the gene symbol *egr1* in the appropriate field and clicking the submit button, a gene expression profile is shown with log₂ intensity on the Y-axis and post-amputation time

points along the X-axis (Fig. 2.13 II). Additional experimental details about the microarray probe ID, contig sequence ID, and gene name are included in the output.

2.3 Ambystoma Genetic Stock Center

Approximately 150 years ago, Mexican axolotls (*Ambystoma mexicanum*) were collected from their ancestral aquatic habitats near present day Mexico City to establish laboratory populations in Europe and subsequently the US. The AGSC at University of Kentucky houses a historically significant population of axolotls that was founded by Rufus R. Humphrey in 1936, and successfully propagated by the University of Indiana through 2005. Over time, domestication created homogeneous wild type and mutant stocks that are amenable to laboratory culture and breeding. These stocks provide a sustainable resource for research and educational efforts around the world. The AGSC operates as a premier animal resource center providing *A. mexicanum* embryos, larvae, juveniles, adults to laboratories and classrooms nationally and internationally. Essentially all laboratory axolotls in the USA, and the majority if not all axolotls in labs around the world, descend from the AGSC collection. The AGSC also supplies animals and display aquaria to museums, zoos, workshops, and aquariums. Sal-Site provides contact information for AGSC personnel, pricing for axolotl stocks (embryos, larvae, juveniles, adults, and transgenics), axolotl care supplies, information about animal care and use, ordering, and answers to frequently asked questions (Fig. 2.14).

2.4 Education

Sal-Site provides educational materials about axolotls that are useful to researchers and teachers (Fig. 2.15). Education kits are available to involve students in axolotl experiments. Further, Sal- Site provides descriptions and illustrations for axolotl

embryo stages, limb bud stages, and limb regeneration stages. AGSC staffers provide advice in setting up exhibit aquaria. Locally, the AGSC provides tours for high school and college students.

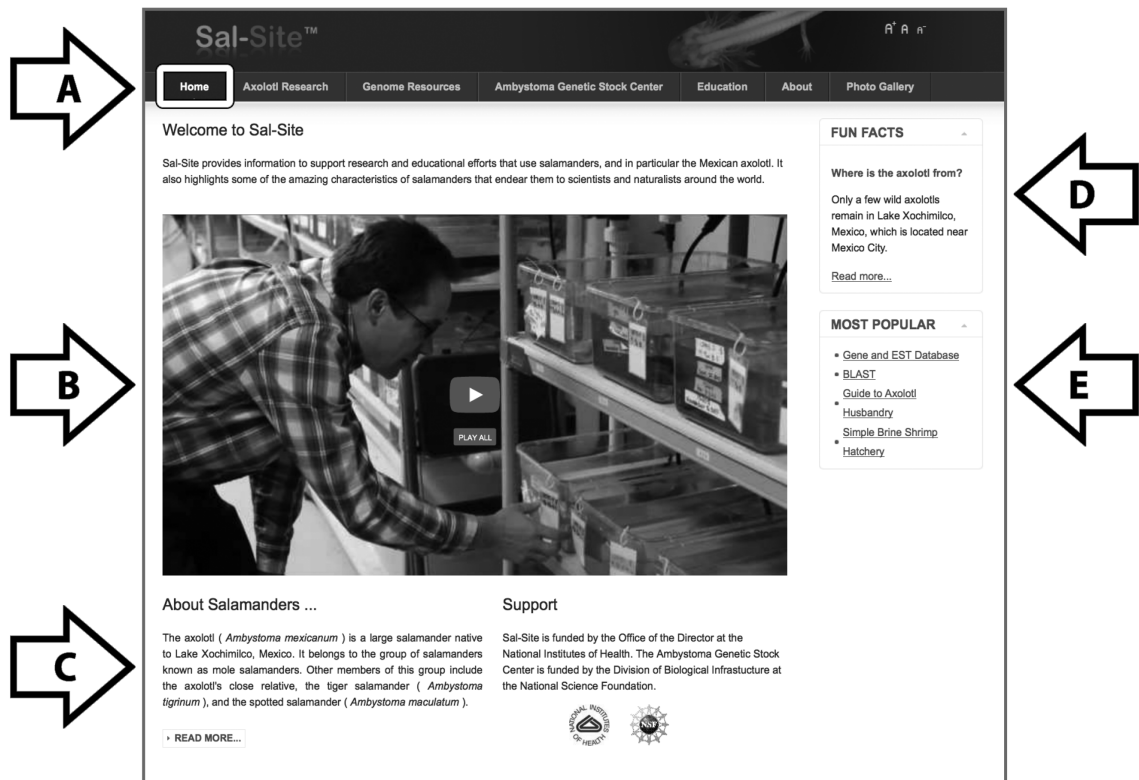


Figure. 2.1 The Sal-Site homepage. This homepage (A) has hyperlinks to orientation video (B) that introduces *Ambystoma mexicanum*, general information about Sal-Site funding mechanisms (C), salamander fun facts (D), and the most highly accessed links of Sal-Site (E).

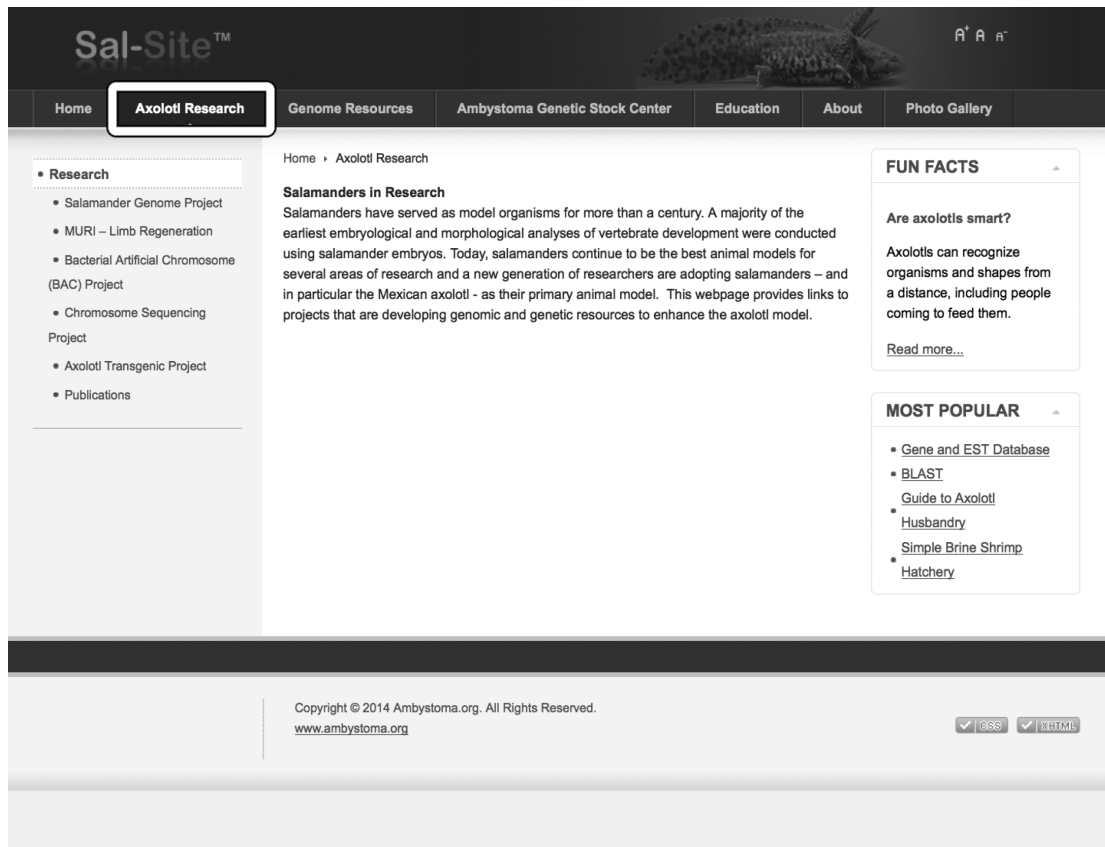


Figure. 2.2. Axolotl research webpage provides hyperlinks to axolotl research projects and selected publications. The axolotl research projects include the salamander genome project, axolotl Bacterial Artificial Chromosome (BAC) project, axolotl chromosome sequencing project, and axolotl transgenic project.

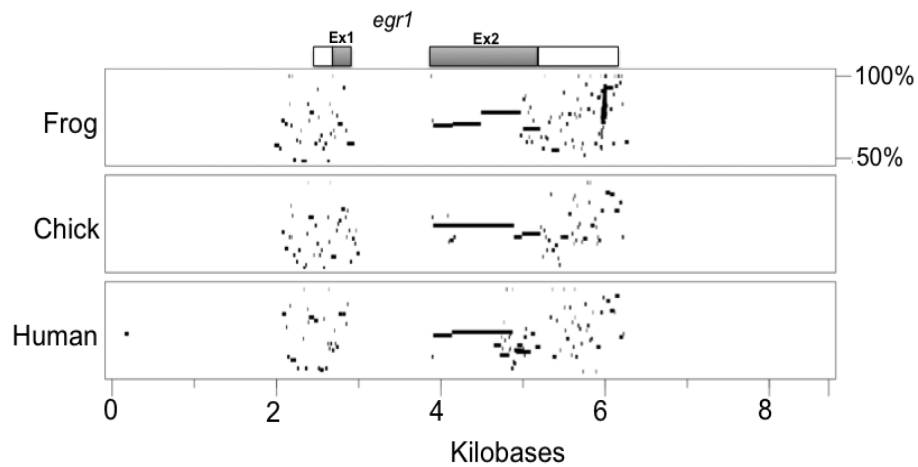


Figure. 2.3. Axolotl BAC project. Alignment of genomic sequences from frog (*Xenopus tropicalis*), chick (*Gallus gallus*), and human (*Homo sapiens*) to an axolotl BAC that contains early growth response 1 (*egr1*). The horizontal black bars show regions of sequence similarity where nucleotide alignments are greater than 50% identical. The white and blue bars at the top show untranslated regions and exons (Ex), respectively.

Sal-Site™

Home Axolotl Research **Genome Resources** Ambystoma Genetic Stock Center Education About Photo Gallery

Home › Genome Resources

Gene and EST Database **A**

Assembly V4.0: The *A. mexicanum* transcriptome has been deep sequenced (15,000,000 Roche 454 short sequence reads and 50K Sanger reads) and assembled. The resulting assembly V4.0 can now be [BLAST searched here](#). Approximately 89.9% of the 14 million high quality sequences were assembled into contigs with a total length of 542 Mb.

▶ [READ MORE...](#)

Genetic Map and Marker Information **B**

Amphibian genomes differ greatly in DNA content and chromosome size, morphology, and number. Investigations of this diversity are needed to identify mechanisms that have shaped the evolution of vertebrate genomes. We used comparative mapping to investigate the organization of genes in the Mexican axolotl (*Ambystoma mexicanum*), a species that presents relatively few chromosomes ($n = 14$) and a gigantic genome (>20 pg/N).

▶ [READ MORE...](#)

NCBI-BLAST **C**

New! We provide NCBI-BLAST (Basic Local Alignment Search Tool) to compare nucleotide or protein sequences to our EST sequence databases. BLAST can be used to infer functional and evolutionary relationships between sequences and help identify members of gene families.

▶ [READ MORE...](#)

Gene Expression **D**

The analysis of gene expression is being studied using microarray, quantitative-pcr, RNA-seq, and nanostring. These resources include:

▶ [READ MORE...](#)

MOST POPULAR

- Gene and EST Database
- BLAST
- Guide to Axolotl Husbandry
- Simple Brine Shrimp
- Hatchery

Copyright © 2014 Ambystoma.org. All Rights Reserved.
www.ambystoma.org

RSS GDS HTML5

Figure 2.4. Genome resources main webpage. This webpage provides hyperlinks to resources and tools. (A) Gene and EST Database, (B) Genetic Map and Marker Information, (C) NCBI-BLAST tool, and (D) Gene Expression.

Sal-Site™

Home Axolotl Research **Genome Resources** Ambystoma Genetic Stock Center Education About Photo Gallery

Home > Genome Resources > Gene and EST Database

Gene and EST Database

Assembly V4.0: The *A. mexicanum* transcriptome has been deep sequenced (15,000,000 Roche 454 short sequence reads and 50K Sanger reads) and assembled. The resulting assembly V4.0 can now be [BLAST searched here](#). Approximately 89.9% of the 14 million high quality sequences were assembled into contigs with a total length of 542 Mb.

These contigs were organized into 921,990 isogroups, representing a total of 1,057,173 isotigs. ([Click here to know more about Isotigs](#)) We have complete (~7K) or incomplete (~10K) protein-coding sequence models for ~17K human refseq proteins. We have 3K additional significant blast hits to non-human protein coding models. With respect to the tissues we have sampled (brain, limb, blood, etc) , we believe we have significant hits to >95% of the transcriptome.

Most Popular

- Gene and EST Database
- BLAST
- Guide to Axolotl
- Husbandry
- Simple Brine Shrimp
- Hatchery

New! Search for Contigs in the Latest V4.0 assembly:

Enter a contig or sequence name (e.g. contig00001, GKJVZ9C02F0B34):

Enter a contig or sequence name (e.g. isotig00001, GKJVZ9C02F0B34):

SEARCH FOR GENES IN ASSEMBLY V4.0:

(Enter a minimum of 3 characters)

Assembly V3.0:

Approximately 74% of the 3.3 million high quality sequences were assembled into contigs with a total length of 71 Mb. The final unique set of contigs and singletons from the assembly was about 12 sequences. We have complete (~3K) or incomplete (~12K) protein-coding sequence models for ~15K human refseq proteins.

SEARCH FOR GENES IN ASSEMBLY V3.0:

If you have a sequence that you want to search against sal-site EST's, you can BLAST search it to our [latest assembly here](#).

If you have a *A. mexicanum* or *A. t. tigrinum* sequence identifier from a prior BLAST search, you can get the sequence information using the below:

Enter *A. mexicanum* sequence id (e.g. contig00001, EPJ1Z2K01CRNZJ, C000001):

Enter *A. t. tigrinum* sequence id (e.g. Tig_NM_000014_Contig_1, TC00001):

Figure 2.5. Gene and EST database. Genes of interest can be searched using the axolotl V4.0 and V3.0 transcriptome assemblies as reference databases. Searches can be conducted by typing a specific contig (A), isotig (B), or gene symbol identifier (C) in the appropriate field, followed by selecting a reference database from the drop-down menu (D).

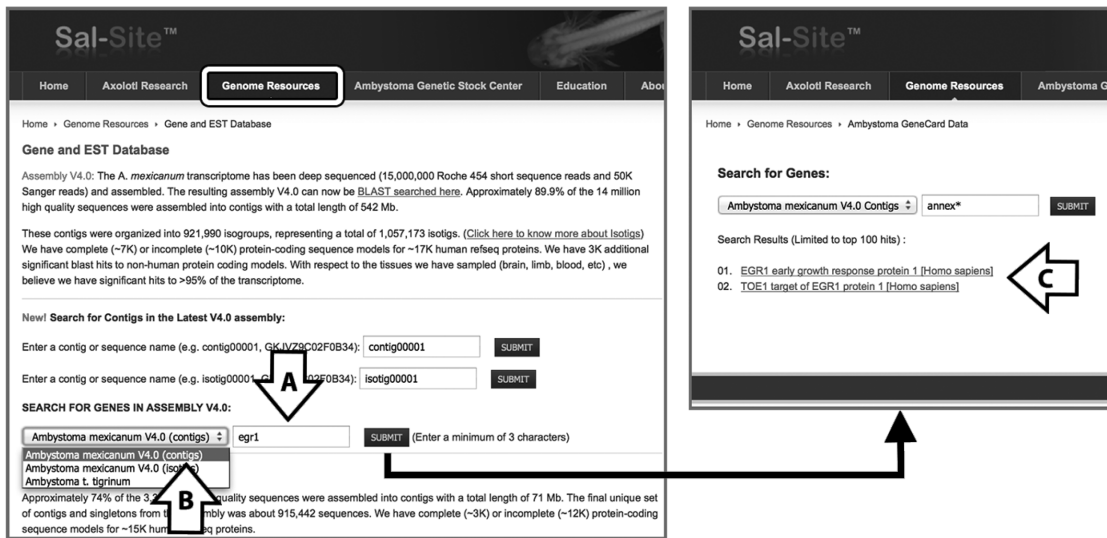


Figure 2.6. An example search of the Gene and EST database. The gene symbol for early growth response —*egr1*— is typed in the appropriate field (A) and a reference database is selected; *Ambystoma mexicanum* V4.0 contigs in this example (B). After clicking the submit button, a result webpage appears showing axolotl hits (contigs) annotated for *egr1* (C).

Panel A: Sal-Site Ambystoma Gene Card

Home • Genome Resources • Ambystoma GeneCard Result

Ambystoma Gene Card (V4.0 contigs) for: **EGR1**

Ambystoma Gene ID : 6006
 RefSeq ID : NP_001955.1
 NCBI ID : 4503493

Gene : EGR1 early growth response protein 1 [Homo sapiens]

A. mexicanum Sequences:

A. mexicanum Sequence	Align Start	Align End	Human Start	Human End
contig316872	232	1740	4	543
contig978315	221	3	78	152

Related Pubmed Articles:
http://www.ncbi.nlm.nih.gov/sites/entrez?cmd=link&db=pubmed&dbFrom=nucleotide&from_uid=4503493

Panel B: NCBI Protein Page

Protein: Advanced

Display Settings: GenPept

early growth response protein 1 [Homo sapiens]

NCBI Reference Sequence: NP_001955.1

FASTA Graphics

Go to:

LOCUS NP_001955 543 aa linear PRI 0

DEFINITION early growth response protein 1 [Homo sapiens].

ACCESSION NP_001955

VERSION NP_001955.1 GI:4503493

DBSOURCE REFSEQ; accession NM_001964.2

KEYWORDS RefSeq.

SOURCE Homo sapiens (human)

ORGANISM Homo sapiens

Bukaryota; Metazoa; Chordata; Craniata; Vertebrata; Euteleostomi;

Panel C: PubMed Search Results

Pubmed Search: Pubmed Advanced

Display Settings: Summary, 20 per page, Sorted by Link Ranking

Results: 11

- Profesione inhibition increases recruitment of Ikb kinase B (IKKb), B3BP-p65, and transcription factor ERF1 to Interleukin-8 (IL-8) promoter, resulting in increased IL-8 production in ovarian cancer.
 - Singh B, Galla HR, Manra S, Chang TP, Sancarova S, Poltorak V, Vancura A, Vancurova I, Park SH, Do KH, Choi HJ, Kim J, Kim KH, Park J, Oh CG, Moon Y.
 - J Biol Chem. 2014 Jan 31;289(5):3581-90. doi: 10.1074/jbc.M113.552841. Epub 2013 Dec 11.
 - PMID: 24337313 (PubMed - indexed for MEDLINE)
 - Related citations
- Early growth response-1 (EGR-1) and nuclear factor of activated T cells (NFAT) cooperate to mediate CD26L expression in neoplastic and dendritic cells.
 - Cole SA, Eddy SD, Ahmann MT, Ruffin TL.
 - J Biol Chem. 2013 Nov 22;288(47):3369-80. doi: 10.1074/jbc.M113.511811. Epub 2013 Oct 8.
 - PMID: 24198272 (PubMed - indexed for MEDLINE)
 - Related citations
- Novel regulatory action of ribosomal inactivation on epithelial Notch-linked proinflammatory signals.
 - Park SH, Do KH, Choi HJ, Kim J, Kim KH, Park J, Oh CG, Moon Y.
 - J Biol Chem. 2013 Nov 22;288(47):3369-80. doi: 10.1074/jbc.M113.511811. Epub 2013 Oct 8.
 - PMID: 24198272 (PubMed - indexed for MEDLINE)
 - Related citations
- Stippled-flow fluorescence kinetic study of protein-actin and intersegment transfer in the target DNA search process.
 - Enozawa A, Inohara J.
 - J Mol Biol. 2014 Jan 9;426(1):230-44. doi: 10.1016/j.jmb.2013.09.019. Epub 2013 Sep 25.
 - PMID: 24017422 (PubMed - indexed for MEDLINE)
 - Related citations

Panel D: Sal-Site Annotation Page

Home • Genome Resources • Ambystoma EST contig

A. mexicanum V4.0 Contig Information:

ID : C0316821

Name : contig316872

Length : 2761

Number of ESTs in Contig : 198

Sequence :

CAGGAGATCCCGAGAGCGAAGCAGAGAAAAAGAGACAAGCGCAGGGGCCAGAGCACCCACCCAGGGCCCTGCGCC1CCCCAACAC
 AACACCCACCCCGAGATCAGGTCAGGCGAGGCGCGAGCTGCAGGGAATCCGCGAGCCCGGAGGCGCCCGCAGAACACCCACAGCCCGGAC
 TGAAAGCCCTCCCGCAATAGGATGATGATGTCACACATCTCTTAATAAATAACTGAA

ORF Start : 229

ORF End : 1743

Frame : 1

Longest ORF :

MAKTEMLLPNSDPPGSPFSPMDSTYLLLEMDLLSVGGQPLGASATGESQYSFQGESGFQLPDTNFDMSLSNKTFFVETSFSNV
 LAYTRGFLSLEPACTHTNTLPEPLFSLVGLVGMANLFTTTPSSPSSSSQSPSLSCVQSDSSPIYSAAPTFPNSASDIFSDQQAQFSSA
 YFPFPAFKSTNFPVSHI PDYLFVQQQELSLSPDQKFFQLSRRGQPLTFLSFKAFATQYGGQKAMSTYQSLMKPQRLKRYKPRP
 EKFPACQFSSKRFNRSBELFBIIRLITGQKFPQCLCHNPFSDLFTHTFTRGFFACIKKPKAPSDKIKTKLHLLKQKTKK
 ASDIFSTFPTTAYSPMDYVSPFPVSYSSPSSSPVSPVSPSPS1ASVTTSTASSFQSLATSPSSIVTNSPSSPFPFSDMAG
 IETC

Blast Results :

align-len	%id	q.start	q.end	s.start	s.end	e-val	Human Match
555	63.42	232	1740	4	543	5e-158	gil4503493 ref NP_001955.1 EGR1 early growth response p...

Figure 2.7. An example gene card for *Ambystoma mexicanum* *erg1*. (A) The Sal-Site gene card for *erg1* provides a hyperlink to human EGR1 at NCBI (B). The gene card page also includes a hyperlink to access related PubMed scientific articles (C). The gene card also provides links of the axolotl contigs annotated for *erg1*. Clicking the first link (contig316872) accesses an annotation webpage that details the number of ESTs associated with the contig (D), contig nucleotide sequence (E), and the longest computer predicted open reading frame (ORF) with protein translation (F). Additionally, this sequence annotation webpage contains data for BLAST hits linked to human sequences curated by NCBI, including sequence similarity and alignment statistics (G). In this example, EST depth and sequence coverage provide very good evidence that contig316872 corresponds to *erg1*.

Sal-Site™

Home Axolotl Research **Genome Resources** Ambystoma Genetic Stock Center Education About

Home > Genome Resources > Genetic Map and Marker Collection

Genetic Map and Marker Information

Amphibian genomes differ greatly in DNA content and chromosome size, morphology, and number. Investigations of this diversity are needed to identify mechanisms that have shaped the evolution of vertebrate genomes. We used comparative mapping to investigate the organization of genes in the Mexican axolotl (*Ambystoma mexicanum*), a species that presents relatively few chromosomes ($n = 14$) and a gigantic genome (>20 pg/N).

We show extensive conservation of synteny between *Ambystoma*, chicken, and human, and a positive correlation between the length of conserved segments and genome size. *Ambystoma* segments are estimated to be four to 51 times longer than homologous human and chicken segments. Strikingly, genes demarcating the structures of 28 chicken chromosomes are ordered among linkage groups defining the *Ambystoma* genome, and we show that these same chromosomal segments are also conserved in a distantly related anuran amphibian (*Xenopus tropicalis*). Using linkage relationships from the amphibian maps, we predict that three chicken chromosomes originated by fusion, nine to 14 originated by fission, and 12-17 evolved directly from ancestral tetrapod chromosomes. We further show that some ancestral segments were fused prior to the divergence of salamanders and anurans, while others fused independently and randomly as chromosome numbers were reduced in lineages leading to *Ambystoma* and *Xenopus*. The maintenance of gene order relationships between chromosomal segments that have greatly expanded and contracted in salamander and chicken genomes, respectively, suggests selection to maintain synteny relationships and/or extremely low rates of chromosomal rearrangement. Overall, the results demonstrate the value of data from diverse, amphibian genomes in studies of vertebrate genome evolution.

[Click here for *A. mexicanum* Linkage Map \(PDF Version\)](#)

[Click here for Conserved gene orders among human, chicken, *X. tropicalis*, and *Ambystoma* \(PDF Version\)](#)

Reference:

Voss SR et al. *Origin of amphibian and avian chromosomes by fission, fusion, and retention of ancestral chromosomes*. Genome Res. 2011 Aug;21(8):1306-12. Epub 2011 Apr 11.

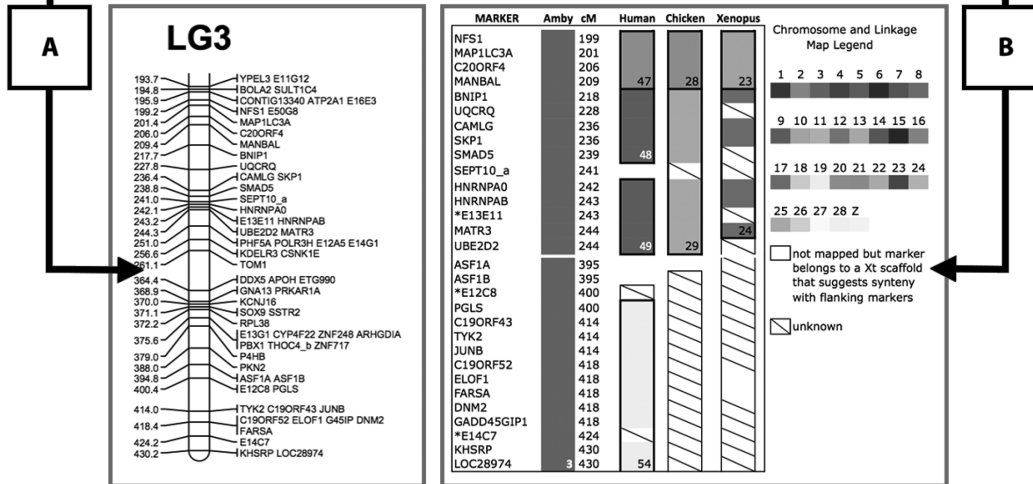


Figure. 2.8. Axolotl genetic map and marker information. This webpage details information about the ordering of 917 genetic markers among 17 linkage groups (LG). A part of LG3 is shown as an example (A). A conserved synteny table provides the positions of orthologous loci from human, axolotl, chicken, and *Xenopus tropicalis* genomes (B).

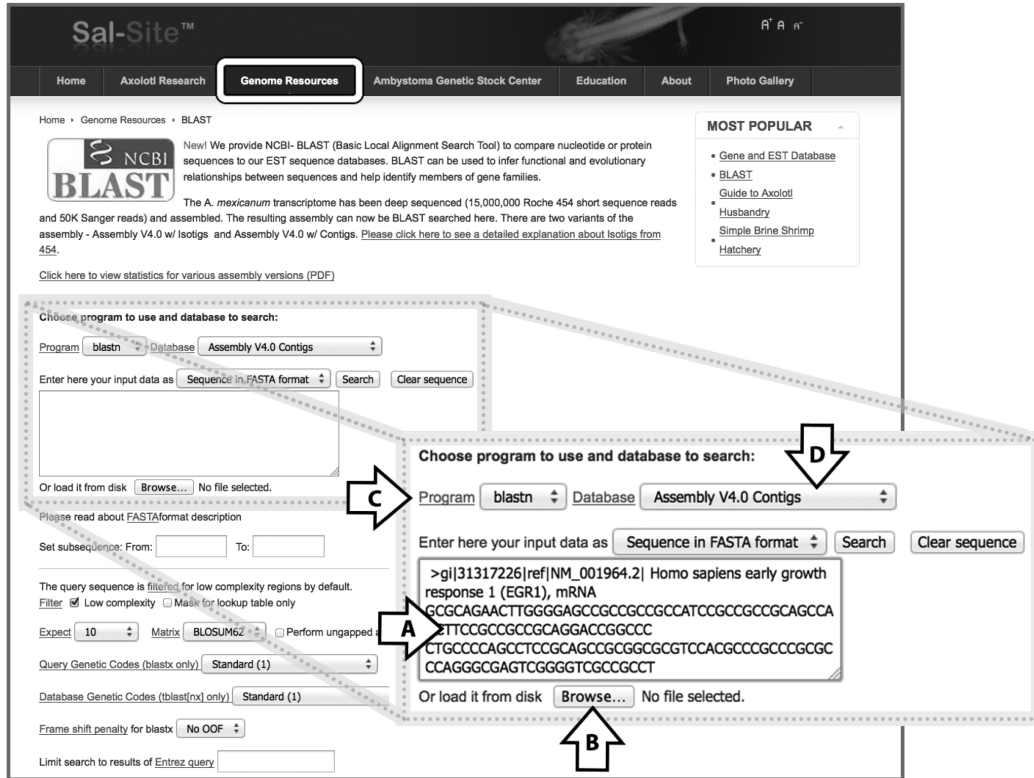


Figure 2.9. The Sal-Site NCBI-BLAST tool is used to identify axolotl contigs that share sequence identity with query sequences. As an example, the human *egr1* (gi|31317226) nucleotide sequence is used as a query and pasted into the appropriate field (A). Alternatively, the query sequence can be uploaded from a file (B). The BLAST can be performed using one of several algorithms (C); the BLASTN algorithm is selected here. The reference data-base is chosen through a drop-down menu (D).

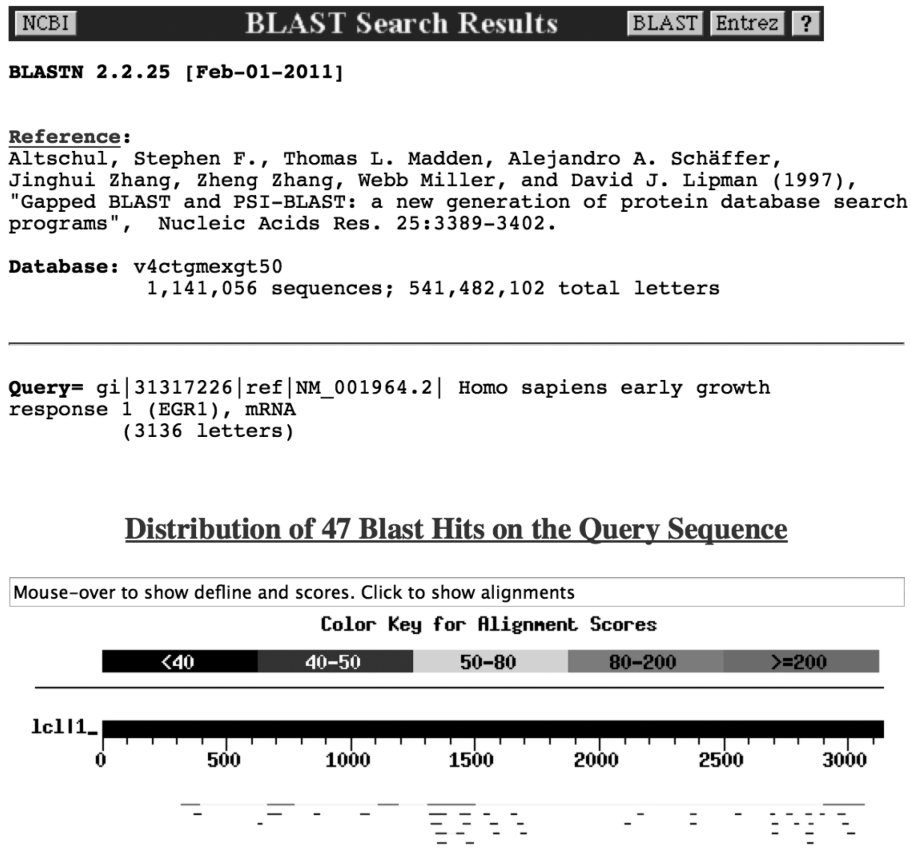


Figure. 2.10. BLAST output. The human *egr1* nucleotide sequence (gi|31317226) was used as a query to identify the most likely *axolotl* orthologous sequence in the V4 transcript assembly. (I) The report shows the algorithm that was used for the BLAST search and the database that was searched. (II) A graphical representation of results that summarizes the top hits to the query sequence. The color bar shows the alignment score. Each of the bars below the query corresponds to a hit. By moving the cursor over these hit bars, it is possible to display a short summary of the sequence ID and alignment.

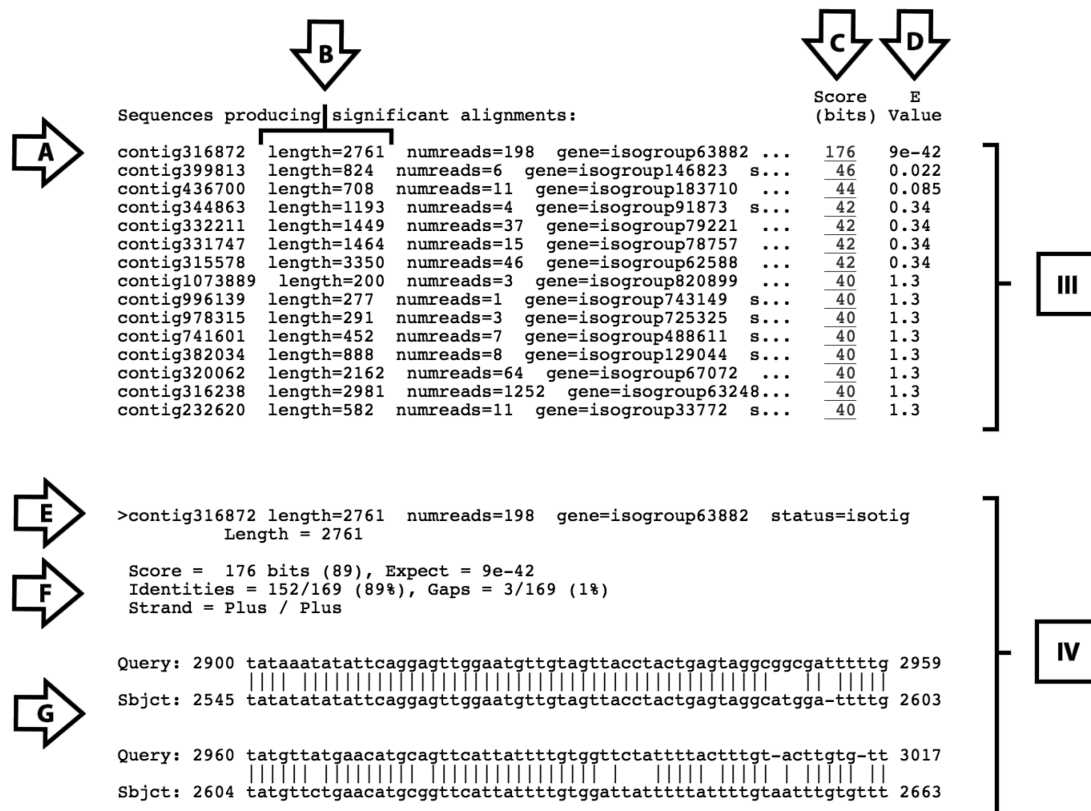


Figure. 2.11. Continuation of BLAST output from Fig. 10. (III) Summary of information for each hit (contig), including length, score, and E-value (A–D). The score (C) measures similarity between the query and the hit sequence. The E-value (D) is an index of the statistical significance of the hit reported. (IV) A detailed pairwise alignment of the query to each of the recovered hits. The header (E) is a repetition of the header information in the previous output section. This final output also provides the identities and the strand directionality of both sequences for which the alignment was performed (F). Identities refer to the number and percentage of identical nucleotides in the alignment. The pairwise alignment (G) provides the coordinates of the query and hit sequences that are aligned (i.e., nucleotides positions) in addition to a vertical line series that represent identical nucleotides shared between both sequences. As shown, the best hit recovered for human *egr1* is contig316872.

Sal-Site™ A A A

Home Axolotl Research **Genome Resources** Ambystoma Genetic Stock Center Education About Photo Gallery

Home » Genome Resources » Gene Expression

Gene Expression

The analysis of gene expression is being studied using microarray, quantitative-pcr, RNA-seq, and nanostring. These resources include:

New! Comprehensive analysis of gene expression during axolotl limb regeneration.

The following database shows temporal gene expression profiles from the largest microarray experiment ever performed for limb regeneration. Ten replicate Amby002 GeneChips (Huggins et al., 2012) were used to estimate gene expression for 20 different time points during limb regeneration. Two different amputation injuries were performed: amputation through the stylopod and zeugopod of the forelimb. One millimeter of the distal-most tissue of regenerating limbs was sampled for RNA isolation and microarray analysis. Overall, the database reports 8,000,000 estimates of gene expression during the first 28 days of limb regeneration.

Search for Genes, Gene Symbol or Probe ID:

Amby001: A custom Affymetrix GeneChip® with approximately 4500 perfect and mismatch probesets. [Library Files](#) [Probe Annotation File \(Original\)](#) [Probe Annotations \(Updated\)](#)

Amby002: A custom Affymetrix GeneChip® with approximately 20,000 perfect probesets. For more information, contact your local Affymetrix representative with the array name (AMBY_002a520748F) and part number - 520748. [Library Files](#) [Probe Annotation File](#)

Nanostring Codesets: The N-Counter is a gene expression analysis system that uses gene-specific capture and reporter probes. Code-set designs are listed for a growing collection of genes.....

Q-PCR: A list of qPCR primers designed for Ambystoma genes.

RNA-Seq: Coming soon.

[Instructions for performing RMA analyses in Expression console](#)

[Instructions for performing RMA analyses using Partek Genomics Suite](#)

Recent Microarray Experiments and Data:

Page RB, Boley MA, Kump DK, Voss SR. 2013. **Genomics of a metamorphic timing QTL: met1 maps to a unique genomic position and regulates morph and species-specific patterns of brain transcription.** *Genome Biology and Evolution*, In Press. [Download_CEL files](#)

Huggins P, Johnson CK, Schoergendorfer A, Putta S, Bathke AC, Stromberg AJ, Voss SR. 2011. **Identification of differentially expressed thyroid hormone responsive genes from the brain of the Mexican Axolotl (Ambystoma mexicanum).** *Comparative Biochemistry and Physiology, Part C*. doi:10.1016/j.cbpc.2011.03.006. [Download_CEL files](#)

MOST POPULAR

- [Gene and EST Database](#)
- [BLAST](#)
- [Guide to Axolotl Husbandry](#)
- [Simple Brine Shrimp Hatching](#)

Figure. 2.12. Gene expression during axolotl limb regeneration. This webpage provides a searchable database of gene expression profiles during axolotl limb regeneration using gene symbol or Affymetrix probe ID. In addition, axolotl microarray library, probe annotation, and raw microarray data files are provided.

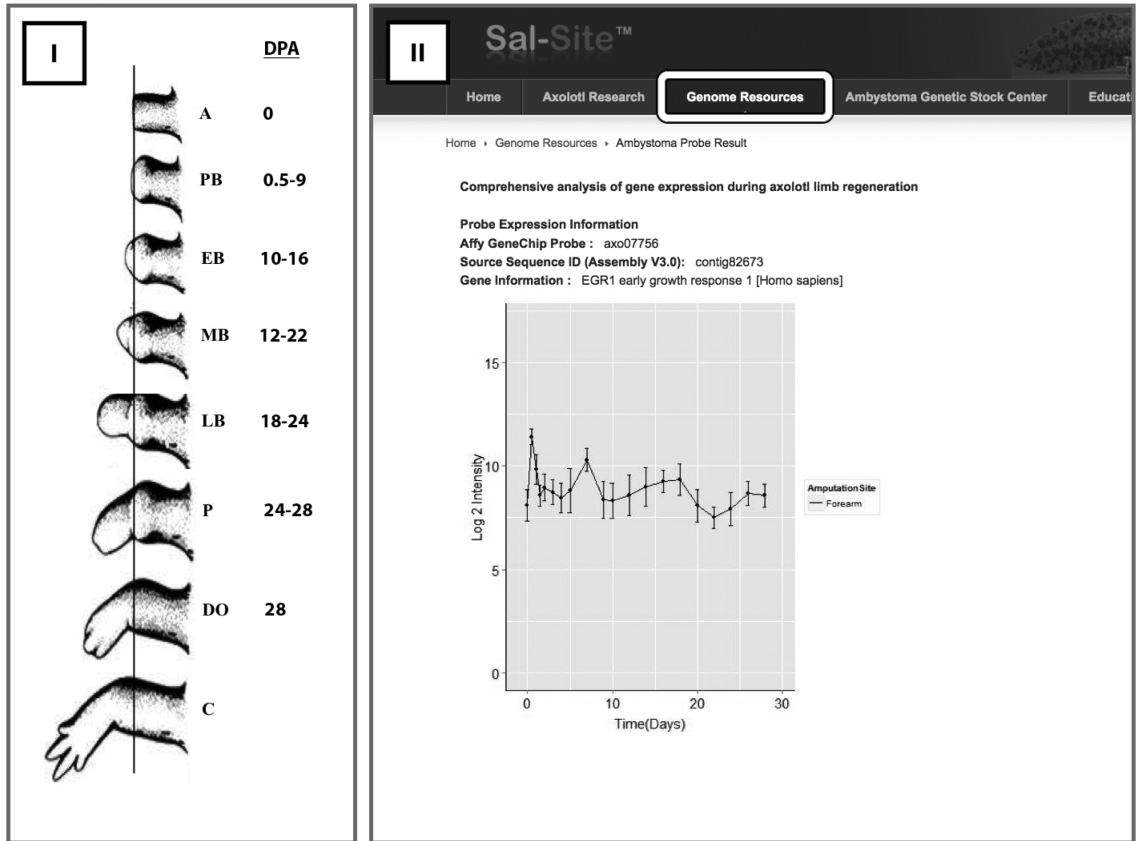


Figure. 2.13. Comprehensive microarray analysis of gene expression during axolotl limb regeneration is available on the Sal-Site genome resources page. (I) The cartoon shows regeneration stages after axolotl limb amputation (A). The stages include prebud (PB), early bud (EB), medium bud (MB), late bud (LB), palette (P), digital outgrowth (DO), and completed (C). The red horizontal line shows the plane of amputation. The DPA (days post- amputation) numbers shows when individuals were observed for each regeneration stage. (II) Temporal gene expression profile for *egr1* during the first 28 days of limb regeneration.

Sal-Site™ A A A


Home Axolotl Research Genome Resources **Ambystoma Genetic Stock Center** Education About Photo Gallery

Home » Ambystoma Genetic Stock Center

Welcome to Ambystoma Genetic Stock Center

The Ambystoma Genetic Stock Center (AGSC) maintains a breeding colony of Mexican axolotls (*Ambystoma mexicanum*) and distributes axolotl embryos, larvae, and adults to laboratories and classrooms throughout the United States and abroad. The AGSC is located in the [Department of Biology](#) at the University of Kentucky and receives financial support from the [Division of Biological Infrastructure \(DBI\)](#) at the [National Science Foundation](#).

Our mission is to serve biology research programs and educators by providing experimental material and expertise and by encouraging and facilitating the exchange of information and ideas.



[Read before you register...](#)

You must be affiliated with an IACUC-sanctioned university or other scientific program to receive animals. No animals will be sold for informal research or personal interest requests.

AGSC DOES NOT SELL PETS

Individuals interested in obtaining axolotls as pets should search for an alternative supplier.

Quick Links:

- New research customers please fill out a [registration](#) and then contact us by [email](#)
- Online Ordering now Available! [Click here](#) to place your order online.
- Hobbieist Axolotl-keepers order your supplies [here](#)
- K-12 teachers order your supplies [here](#)
- Purchasing and Accounts Payable Representatives, click [here](#) to download our W-9 form for tax purposes.

Left Sidebar:

- **Ambystoma Genetic Stock Center (AGSC)**
 - History
 - People
 - Obtaining Materials
 - Please Cite the AGSC
 - F. A. Q
 - Contact Us
- QUICK LINKS**
 - [Genetic Stock Center \(AGSC\)](#)
 - [Sal-site](#)
 - [EST Database](#)
 - [BLAST](#)
 - [Microarray Database](#)

Right Sidebar: LATEST NEWS

- **REARING FEES**
 - [Limited Quantities of larvae/juveniles/adults](#)
 - [Online Ordering now available...](#)
 - [Ordering Embryos...](#)

Figure. 2.14. The Ambystoma Genetic Stock Center (AGSC). Sal-Site provides a portal to the AGSC, where researchers and educators can purchase axolotls and supplies.

The screenshot shows the Sal-Site website interface. At the top, there is a dark header with the 'Sal-Site' logo and a navigation menu. The 'Education' link in the menu is highlighted with a white box. Below the header, the page content is organized into several sections:

- Navigation Menu:** Home, Axolotl Research, Genome Resources, Ambystoma Genetic Stock Center, **Education** (highlighted), About, Photo Gallery.
- Left Sidebar:** A list of links under the heading 'Education':
 - Guide to Axolotl Husbandry
 - Simple Brine Shrimp Hatchery
 - Embryo Staging Series
 - Limb Staging Series
 - Mutants and Strains
- Main Content Area:**

Home • Education

What is an Axolotl?

The axolotl (*Ambystoma mexicanum*) is a large salamander native to Lake Xochimilco, Mexico. It belongs to the group of salamanders known as mole salamanders. Other members of this group include the axolotl's close relative, the tiger salamander (*Ambystoma tigrinum*), and the spotted salamander (*Ambystoma maculatum*).

The wild-type axolotl is dark colored with greenish mottling. Sometimes there are silvery patches on the skin. The eyes have yellow, iridescent irises. Adult axolotls can reach 30 cm (about 12 inches) or more in length from nose to tail-tip, and they can weigh as much as 300 grams. They are known for their blunt snouts and large mouths.

Axolotls are neotenic. They keep their feathery external gills and tail fin their entire lives and maintain their aquatic lifestyle.

The first laboratory axolotls were living specimens brought to Paris in the 1860s and given to the Jardin des Plantes. Many of the axolotls raised in laboratories today, including most of those in the Axolotl Colony, are descendants of those animals.
- Right Sidebar:**

FUN FACTS

Why are axolotls the most studied salamander model?

Axolotls are used because they provide a vertebrate model organism that is easy to rear and breed in the lab.

[Read more...](#)

MOST POPULAR

 - [Gene and EST Database](#)
 - [BLAST](#)
 - [Guide to Axolotl Husbandry](#)
 - [Simple Brine Shrimp Hatchery](#)

At the bottom of the page, there is a footer with copyright information: 'Copyright © 2014 Ambystoma.org. All Rights Reserved. www.ambystoma.org' and icons for CSS and HTML.

Figure. 2.15. The Education hyperlink. Sal-Site provides useful information for working with axolotls, including information about axolotl care, use, and development.

Chapter 3: Identification of Presumptive Lineage-Specific paralogs in The Mexican Axolotl (*Ambystoma Mexicanum*)

Nour Al Haj Baddar^{a,b}

^aDepartment of Biology, University of Kentucky, Lexington, KY, 40506

^bDepartment of Neuroscience and Spinal Cord and Brain Injury Research Center (SCoBIRC), University of Kentucky, Lexington, Kentucky, 40536

3.1 Introduction

Unlike mammals, urodele amphibia have an innate ability to regenerate appendages after loss or damage. What accounts for variation in regenerative ability is a long-standing question in developmental biology. One possibility is that regeneration is associated with the evolution of genes that are unique to salamanders. Gene duplication is considered a major force in gene family expansion and the evolution of species-specific adaptations (Ohno, 1970; Hurles et al., 2004). The evolutionary retention of duplicated genes is known to be associated with changes in genetic pathways, developmental programs, physiological systems, and the origin of novel phenotypes (Han et al., 2009, Shukla et al., 2014).

Mounting evidence suggests that novel salamander genes orchestrate important regeneration-specific molecular mechanisms that are lacking in non-regenerative organisms. For example, the *prod1* gene is member of the three-finger protein family, as it has conserved cysteine residues that allow folding to create a characteristic three-pronged protein structure (da Silva et al., 2002; Graza-Garcia et al., 2009). *Prod1* encodes a cell surface protein that mediates proximal-distal patterning and neurotrophic signaling to the regenerating blastema (Echeverri and Tanaka, 2005; Blassberg et al., 2011).

Notophthalmus viridescens (*Nv*) PROD1 binds nAG (newt-anterior gradient protein), which is secreted initially by Schwann cells around nerves in the amputated limb stump, and later during regeneration in the wound epidermis (Kumar et al., 2007). Another example is the recent identification of a new member of the CCN (Connective Tissue Growth Factors) gene family in *N. viridescens* (Looso et al., 2012). Expression of these proteins is stimulated by growth factors (e.g. TGF- β) and changes in their expression correlate with cell proliferation, adhesion, migration, and angiogenesis (Leask and Abraham, 2003). Among CCN gene members, *Nv-ccn* expression is dramatically induced a few hours after injury to the heart, exclusively in damaged tissue during regeneration, while other CCN members are not expressed (Looso et al., 2012). This suggests that *Nv-ccn* diverged in a way that allowed it to be functionally integrated in a regeneration-specific gene network induced by injury in the heart. Importantly, these few salamander-specific proteins have revealed novel molecular mechanisms of regeneration. Thus, the search and identification of additional salamander-specific genes presents a promising strategy to gain new perspectives about tissue regeneration.

In this study I utilized a bioinformatics approach to identify previously unknown lineage-specific duplications in a highly regenerative salamander, the Mexican axolotl (*Ambystoma mexicanum*). I provide an initial characterization of these paralogs and their potential functions.

3.2 Materials and Methods

3.2.1 Identification of putative lineage-specific duplicates in the axolotl using Sal-Site transcriptome resources

Presumptive orthologous gene pairs were identified between humans and axolotl by reciprocally searching (tBlastx) the *Homo sapiens* RefSeq database and axolotl transcriptomic sequences available at Sal-Site (www.ambystoma.org) (Putta et al., 2004; Smith et al., 2005; Baddar et al., 2015). Reciprocal best match alignments between the human and axolotl databases were filtered for their query coverage; results were restricted to axolotl sequences that covered at least 80% of their presumptive human orthologous coding sequence (CDS). Gene pairs were required to have >30% identity and a bit score above 100 to be considered orthologs.

To identify presumptive lineage specific gene duplicates (paralogs) in the axolotl, orthologous axolotl sequences were self-searched (tBALSTx) against the Sal-Site axolotl transcriptome database. The vast majority of transcripts in this database were sampled from tissue collected during limb regeneration, however other tissues were sampled including the spleen and liver (Putta et al., 2004; Smith et al., 2005). Preliminary examinations of sequence alignments were used to identify filtering criteria. Redundant protein sequence alignments with high identity scores (99% and above) were considered potential splice variants and thus removed from further analysis. The remainder of the hits were further filtered to remove low identity alignments, which may have excluded deeply divergent paralogs. Essentially, hits with identity scores below 50% and/ or query coverage values below 50% were removed from the analysis. The approach of Smith et al. (2009) was used to identify presumptive axolotl paralogs. Briefly, if an axolotl orthologous sequence returned a higher bit score value for an alignment to an axolotl sequence than an alignment to the corresponding orthologous human sequence, it was considered a paralog. The hits

were carefully screened and alignments were manually curated to distinguish novel amino acid substitutions from sequencing errors.

3.2.2. Identification of putative lineage-specific duplicates in the axolotl based on recently published axolotl transcriptome and genomic resources

I used the recently published axolotl transcriptome (Nowoshilow et al., 2018) to generate all protein-coding genes in the axolotl genome using transdecoder (Hass et al., 2013). I then performed an all vs all BLASTP search and removed sequence alignments with identity scores below 70% to eliminate genes with deeply divergent paralogs from the list. I used the gene annotations and genomic location of the remaining genes to filter out transcript variants (Nowoshilow et al., 2018; Smith et al., 2019). All duplicated genes that were retained, were manually searched (BLASTP) against the NCBI protein database to ensure query coverage of at least 80% of subject sequences. Finally, to avoid including false positive hits, candidate gene paralogs lacking chromosomal mapping information were removed from the results.

3.2.3. Gene ontology enrichment analysis

The GO annotations for the identified presumptive lineage-specific gene paralogs were obtained using Panther tools (Thomas et al., 2003). The three GO categories: molecular function, biological process, and cellular component were analyzed. The *P*-values used to evaluate the significant enrichment of GO terms were calculated based on Fisher's exact test and corrected using the false discovery rate (FDR) test correction for multiple testing. I used a corrected *P* value < 0.05 as the significant cut off to determine significantly enriched GO terms. Redundant GO terms were removed.

3.3 Results

3.3.1 Identification of orthologs and candidate lineage-specific duplicates in the axolotl

I identified 3227 axolotl-human orthologous genes using the Sal-Site gene/EST database (Baddar et al., 2015) (Supplementary Table 3.1). Thirty-seven of the alignments identified from Sal-Site yielded 49 presumptive lineage-specific gene duplicates (paralogs) in the axolotl (Supplementary Table 3.2). In other words, these 49 presumptive paralogs showed higher sequence similarity to an axolotl sequence of an axolotl-human orthologous pair. That so few paralogs were found in common from searches of Sal-Site database likely reflects stringent filtering criteria that were used to identify paralogs.

On the other hand, analyses using axolotl transcriptome/genomic resources (Nowoshilow et al., 2018; Smith et al., 2019) identified 1574 presumptive lineage-specific duplicates from 990 orthology pairs (Supplementary Table 3.3). Information regarding their paralogs genome location and coordinate annotation are also shown (Supplementary Table 3.3). The increase in the number of the presumptive lineage specific paralogs is due to the completion of the transcriptome (Nowoshilow et al., 2018) and availability of chromosomal mapping (Smith et al., 2019).

3.3.2 Gene ontology analysis of presumptive axolotl paralogs

The retention of duplicated genes post duplication is a low probability event. However, when a duplicated gene is retained, it may contribute to organismal adaptation (Zhang et al., 2003). I used Panther tools (Thomas et al., 2003) to annotate Gene Ontology (GO) biological processes, molecular function, and cellular component (Supplementary Table 3.3) information to genes that yielded paralogous axolotl gene candidates.

The presumptive lineage specific paralogs significantly enriched general GO biological processes associated with gene expression (N = 187) involving genes encoding transcription factors and repressors (*Tead1, sp4, sp8, tcf20, tcf15, bclaf1, tbx18*), and ribosomal proteins (*Rpl27a, rpl17, rrp1b, rps8, rps13, rps10*). GO terms associated with response to stimulus (N = 181) were also enriched. Interestingly this group included genes involved in immune response and inflammation (*C6, il1b, cxcl14, cat, epx, crp, selp, pecam*), and cellular stress responsive genes encoding serine-threonine kinases that control cell signaling and cell fate (*Mapk8, mapkapk5, nlk, ulk4, wnk1, tyro3*). It also included genes encoding chaperones (*Anxa2, cul4, cul5, hspa9, hspa70*), and members of conserved signaling pathways activated by a variety of intra- and extracellular stimuli (*Fzd2, csnk1g1, tle1*). A high number of the genes involved in the aforementioned terms also enriched cellular metabolism (N = 106) and enzymatic activity including GTPases (N = 36) and hydrolases (N = 45).

Several other presumptive lineage specific paralogs enriched GO terms associated with chromatin and DNA geometry. These terms included chromosome organization (N = 67) and chromatin organization (N = 41, including *Pold3, polq, cenpc, cenph, chd2, hlcs, baz1a, bahd1*), histone modification (N = 26) comprising several histone lysine methyl transferases (*Nsd3, kdm1a, kdm6a, kdm4b, phf20*), and histone deacetylase (*Hdac11*). Several other genes enriched cell cycle, cell division, and DNA duplex unwinding GO terms (*skal, tpr, clasp2, ist1, ank3, senp5, birc6, pkn2, numa1, ubxn2b, ccnjl, mcm2, dync1h1*). Further, cellular motility, cytoskeletal organization, and cell polarity establishment were also enriched (N = 50, N = 27, N = 6). These lists contain many genes known to be important for cell motility, basement membrane organization,

and cell-matrix interaction (*lama2, epha2, tiam1, tissue factor, thrombospondin4, afdn, fer, nfl, acrt2, flna, rock1, gsn, ilk, zp3, sptb, rufy3*). A number of genes also enriched neurogenesis and neuron projection development. Some of these genes were linked to nervous system disorders like intellectual disability (*dlg2*) or associated with dendrite formation (*rasall*). A group of genes enriched animal organ morphogenesis (N = 55) that included genes that encode enzymes that constitute major proteins in vertebrate eye lense and required for its transparency (*crygb, tdrd7*) or photoreceptor development (*ift140*). Others were involved in heart muscle development (*myl, tnnc1*) and skeletal muscle organization (*tcap, mybpc1*) and melanocortin signaling (*atrn, hps4*).

A substantial number of genes enriched intracellular transport (N = 60) and exocytosis (N = 48). These lists included genes coding for enzymes essential for intracellular vesicular transport (*uso1, vps18, sec24c, copb2, tsg101, ncstn, exoc4*) and mediating trafficking across the nuclear membrane (*tpr, xop5, ndc1, kpna6, nup85*). Clearly, lineage specific paralogs in the axolotl function in diverse biological processes. Interestingly, some of these genes are predicted to function in chromatin packaging and DNA unwinding, processes that might require additional gene functions in the large axolotl genome (Keinath et al., 2015; Nowoshilow et al., 2018; Smith et al., 2019).

The list of lineage specific paralogs also enriched GO molecular function terms and cellular component (Supplementary Table 3.4). The enriched molecular terms are associated with enzymatic activity (guanyl-nucleotide exchange factor activity (N = 19), GTPase activity and GTPase binding (N = 24, N = 42), drug binding (N = 94), cytoskeletal protein binding (N = 60), cell adhesion molecule binding (N = 34) and cadherin binding (N = 27). Among enriched GO cellular compartment terms, the most

interesting where those related to lamellipodium (N = 18) and leading edge (N = 33), and also cellular compartments associated with cell division (N = 12) and chromosomes (N = 65). Overall, the GO enrichment results suggest hypotheses for the retention of lineage specific paralogs in the axolotl (Fig. 3.3).

It is noteworthy to mention that a subset of the lineage specific paralogs has no known functions. These genes constitute 15% of the total identified genes in the list (N = 278). The functions of these genes await further study.

3.4 Discussion

The process of gene duplication is widely recognized as contributing to phenotypic diversity and adaptation (Ohno, 1970). In this study, I identified paralogs that likely arose via gene duplication in the axolotl using existing and recent axolotl transcriptomic and genomics datasets. Our analyses identified a total of 1574 presumptive lineage specific paralogs in the axolotl and initially characterized their potential functional contribution. I present the first systematic analysis of presumptive lineage specific gene duplication in the axolotl and in salamanders generally.

Lineage specific gene duplication is an important component of genome evolution. (Smith et al., 2009; Church et al., 2009; Shiu et al., 2006; Wang et al., 2017). Based on our analysis, axolotl paralogs represent 8.3% of the total protein coding genes in the Nowoshilow et al (2018) genome assembly. Although this percentage is likely to change with improvements to the genome assembly, it is very close to that reported for mouse (6.2%) (Church et al., 2009) and human (6.5%) (Shiu et al., 2006). Differences in percentages obtained could be due to various analysis methods and filtering criteria. However, it was reported previously that the axolotl genome has more lineage specific paralogs compared to the human genome (Smith et al., 2009). Perhaps future studies will

document an even higher percentage of lineage specific genes in the axolotl genome than was estimated here.

Generally, duplicated genes that become fixed in populations are thought to assume three different fates: neofunctionalization, subfunctionalization, and conservation of function (Hurles et al., 2004). Neofunctionalization occurs when one duplicated gene copy undergoes an accelerated rate of amino acid changes following duplication that could lead to a new function (Hurles et al., 2004). Duplicated genes can also evolve via subfunctionalization, where the parental gene function is partitioned between them, temporally and/or spatially. Duplicated genes can also maintain a high degree of functional similarity (redundancy) with potential reduction in gene expression of both as a result of mutation in regulatory sequences (Greer et al., 2000). Further analyses are required to classify the fates and evolutionary significance of the identified paralogs in this study.

Following gene duplication, genes belonging to some functional categories seem to have been preferentially retained. Indeed, the results of enrichment analysis I performed show that these genes are central to various biological processes associated with response to stress, cell signaling, chromatin packaging, immune response, cell migration, neurogenesis, transport, in addition to heart and eye/lens specific morphogenesis. The results of the molecular function enrichment show that these duplicated genes encode enzymes with various activities (GTPases, hydrolases, transferases, ion binding, drug binding) and an array of structural proteins with established cytoskeletal activity. These findings suggest that duplicates are involved in a wide spectrum of biological processes, which points to the potential expansion and layered complexity in gene/protein networks mediating these biological processes.

My results here represent the first systematic approach performed to identify lineage specific paralogs in a highly regenerative salamander. Salamanders are known for their large genomes and unsurpassed regenerative abilities. I identified previously unknown lineage specific paralogs that may function to regulate chromatin structure and function, and regeneration. In regards to regeneration, duplicated genes are predicted to function in immune responses required for salamander limb and heart regeneration (Goodwin et al., 2013; Goodwin et al 2017). Others paralogs that were identified (e.g. MMPs) mediate tissue degradation and hydrolysis required for blastema formation (MMPs) (Vinarsky et al., 2005; Stocum et al., 2017). The exact roles that axolotl paralogs perform in the context of tissue regeneration will need further investigation.

3.5 Acknowledgements

I wish to thank Maria Torres-Sánchez and Ryan Woodcock for their help with bioinformatic analyses in this chapter.

Chapter 4: Identification of Axolotl MMP Gene Family Members, Including Novel Salamander-Specific MMP Paralogs

Nour Al Haj Baddar^{a,b}

^aDepartment of Biology, University of Kentucky, Lexington, KY, 40506

^bDepartment of Neuroscience and Spinal Cord and Brain Injury Research Center (SCoBIRC), University of Kentucky, Lexington, Kentucky, 40536

4.1 Introduction

Urodele amphibians possess a surprising ability to regenerate damaged appendages. When an appendage is amputated, the injury triggers histolysis, a process that breaks down ECM components and damaged tissue to facilitate wound healing and regeneration (Grillo et al. 1968, Dredsen and Gross, 1970, Yang and Bryant, 1994; Yang et al., 1999; Vinarsky et al., 2005; Bellayr et al., 2009). Matrix metalloproteases (MMPs), also known as matrixins, are the major degrading enzymes that mediate histolysis during limb regeneration. MMPs are highly conserved Zn^{+2} dependent proteinases that can cleave various extracellular matrix (ECM) components. During regeneration, collagenases and stromelysins release progenitor cells from the ECM and tissue niches, thus facilitating their migration below the wound epidermis to form a regeneration blastema, which is absolutely required for limb regeneration (Grillo et al. 1968, Dredsen and Gross, 1970, Yang and Bryant, 1994; Yang et al., 1999; Vinarsky et al., 2005). Thus, the actions of MMPs are critically important for successful limb regeneration.

Structurally, MMP proteins share many of the same domains (summarized in Fig. 4.1). These domains include: a signaling peptide, a pro-peptide domain that contains a cysteine switch (PCRGVPD) required for enzyme latency, a catalytic domain with a highly conserved motif containing three histidine residues (HEXXHXXGXXH) that bind Zn^{+2} ions, a linker or hinge domain that varies in length among isoforms, and a hemopexin domain (Huxley-Jones et al., 2007). Almost all MMPs share the aforementioned domains, including collagenases (MMP1, MMP8, MMP13) and stromelysins (MMP3 and MMP10). However, some of the shared domains are not present in a few MMPs, and other MMPs acquired new domains. For instance, gelatinases (MMP2 and MMP9) have fibronectin domains nested within the catalytic domain that enable attachment to gelatin, and other MMPs have a short, recognition motif (RXXR) that allows binding and activation by furin (Huxley-Jones et al., 2007). Furin-activated MMPs can be further sub-categorized into three groups; secreted (MMP11, MMP21, MMP28), transmembrane domain containing (MMP14, MMP15, MMP16, MMP23A, MMP23B, MMP24), and GPI anchored (MMP17, MMP25). On the other hand, other MMPs (MMP7 and MMP26), also called matrilysins, lack the carboxy-terminal hemopexin domain (Nagase et al., 2006; Itoh, 2015).

MMPs constitute a relatively large gene family in mammals; 23 MMPs are found in human and mouse (Jackson et al., 2010). While it seems likely that salamanders have a similar number of MMP genes, only a few MMP genes have been characterized (Yang and Bryant, 1994; Yang et al., 1999; Miyazakai et al., 1996, Chernoff et al., 2000; Kato et al., 2003, Vinarsky et al., 2005; Monaghan, 2009). Here, I searched newly available transcriptome datasets to identify 24 MMP gene members including previously uncharacterized salamander-specific paralogs. I provide the first comprehensive list of

axolotls' MMPs, thus providing a valuable resource for studies of MMP gene functions during regeneration and other axolotl developmental processes.

4.2 Materials and Methods

4.2.1 Bioinformatics search for axolotl MMPs

I used several strategies to identify and annotate axolotl MMP gene sequences. I extracted available axolotl *mmp* transcript sequences from Sal-Site (RRID: SCR_002850) (Baddar et al., 2015) and used these as queries for tBLASTx searches of axolotl transcriptome resources (Bryant et al, 2017, Nowoshilow et al., 2018). I also used human *mmp* sequences as queries for tBLASTx searches of these same axolotl transcriptome resources. The resulting MMP hits were then used as queries to search the Sal-Site database in attempt to obtain gene name and Affymetrix microarray probe information (Huggins et al., 2012). Finally, I downloaded partial and full-length MMP sequences previously identified from newts and the axolotl (Yang and Bryant, 1994, Yang et al., 1999; Miyazaki et al., 1996, Kato et al., 2003, Vinarsky et al., 2005; Monaghan, 2009).

4.2.2 Phylogenetic analyses

To investigate MMP homology relationships, I constructed a phylogenetic tree using putative axolotl MMP transcript contigs and 354 full-length *mmp* gene sequences from 19 vertebrate species. Specifically, I used axolotl contigs as queries for tBlastx searches of salamander transcriptomes (*Ambystoma andersoni*, *Ambystoma maculatum*, *Ambystoma texanum*, *Ambystoma laterale*, *Cynops pyrrhogaster*, *Hynobius chinensis*, *Bolitoglossa ramosa*, *Notophthalmus viridescens*, and *Pleurodeles waltl*), *ceacilians* (*Typhlonectes compressicauda*, *Microcaecilia*, and *Rhinatrema bivittatum*) and anuran

amphibians (*Leptobrachium boringii*, *Nanorana parkeri*). I also used NCBI resources to obtain annotated *mmp* coding sequences for *Homo sapiens*, *Danio rerio*, *Xenopus tropicalis*, and *Gallus gallus*. The transcriptomic resources that were searched are shown in Table 4.1. The accession numbers and sequences used for these analyses can be found in Supplementary files 4.1 and 4.2, respectively.

Candidate *mmps* and an outgroup sequence (PKG1) were aligned using MAFFT v7 (Kato et al., 2013) with the iterative refinement method: FFT-NS-i. Subsequently, statistical selection of the best-fit model of nucleotide substitution was computed with jModelTest2 (Darriba et al., 2012) using different selection strategies: a decision theory method (DT), Akaike, Akaike corrected, and Bayesian information criteria (AIC, AICc, and BIC). All strategies suggested the model TVM+I+G as the best model of nucleotide substitution for the alignment. Using the best-fit model, tree inference under the maximum likelihood (ML) criterion was performed with RAxML-NG (Kozlov et al., 2019). The optimal tree was inferred using 50 starting trees (25 random trees and 25 parsimonious trees). Clustal was used to analyze and compare MMP sequences, including peptide domains that characterize MMP subclasses.

4.2.3 Temporal and Spatial gene expression of axolotl MMPs

Gene expression information during limb regeneration was extracted for *mmps* that have probes on a custom axolotl affymetrix gene chip. Expression estimates for *mmps* that were not represented on the gene chip were extracted from a transcriptomic study of different axolotl tissues (Bryant et al., 2017). Axolotl tissues that were sampled to build this transcriptome included: unamputated segmented limbs (hand, forearm, elbow, and

upper arm), post limb amputation tissues sampled from regenerating limb (proximal and distal blastema, skeletal muscles, cartilage, bone, blood vessels, cartilage, bone), reproductive and embryonic tissues (testes, ovaries, and embryos-one cell to pre-hatch), heart, and gill filaments (Bryant et al., 2017). Most samples were collected from three biological replicates excepting blastema (proximal and distal), which were collected from two replicates (Bryant et al., 2017).

4.3 Results and Discussion:

4.3.1 Identification of axolotl MMP gene family members

Previous studies identified and characterized partial or complete coding sequences of a few salamander MMP (Yang et al., 1999; Yang and Bryant, 1994, Miyazakai et al., 1996, Kato et al., 2003, Monaghan, 2009). I mined transcript sequences from Sal-Site and other sources (Bryant et al., 2017, Nowoshilow et al., 2018) and identified 24 total axolotl MMP sequences.

We performed a phylogenetic analysis to reconstruct evolutionary relationships among *mmp* family members (Fig. 4.2). Twelve sub-clades within the overall phylogenetic tree were annotated as: MMP7, MMP2, MMP9, MMP16, MMP24, MMP25, MMP14, MMP15, MMP11, MMP28, MMP19, MMP23B. Each of these clades contains a presumptive ortholog from *H. sapiens*, *X. tropicalis*, *D. rerio*, *G. gallus*, and putative homologs from other amphibian species. For each of the above clades, an axolotl putative ortholog was identified and assigned the defining MMP gene name (Supplementary Table 4.1).

The remainder of the axolotl MMP sequences that were not clustered with the previous 12 clades (excepting MMP13) were grouped into salamander-specific clades, a

pattern that suggests the evolution of novel MMP paralogs. These clades include: collagenases, salamanders MMP3 and MMP13 paralogs, and salamander-specific MMPE. I discuss these clades below.

4.3.2 Salamander-specific MMP3 duplicates

Stromelysin 1, 2 are also known as MMP3 and MMP10, respectively. In salamanders, two stromelysins were identified for *N. viridescens* and designated (*NvMmp3/10a* and *NvMmp3/10b*) (Vinarsky et al., 2005). These two genes were shown to have homologs in *C. pyrrhogaster* (*CpMmp3/10a* and *CpMmp3/10b*) (Kato et al., 2003). Axolotls were shown to have three different *mmp3* that share high sequence identity to these genes (Monaghan, 2009). My analysis revealed a previously uncharacterized fourth stromelysin in the axolotl (Supplementary Table 4.1). I denote the axolotl putative MMP3 paralogs as *mmp3a*, *mmp3b*, *mmp3c*, and *mmp3d*. All of these axolotl paralogs cluster with Nv- and Cp MMP3/10 a and b in the phylogenetic tree, along with putative stromelysin homologs in other salamander species. Surprisingly, stromelysins from other vertebrates (human, zebrafish, chicken, and frogs) were not included within this clade, suggesting significant stromelysin sequence divergence in salamanders (Fig. 4.3).

4.3.3 Salamander-specific Collagenases

Three collagenase paralogs identified previously in the axolotl were designated *mmp1a*, *mmp1b*, and *mmp1c* (Monaghan, 2009) to reflect their homology to newt collagenase (*Nv* collagenase) (Vinarsky et al., 2005). These three axolotl collagenases are found in the same sub-clade in the phylogenetic tree (Supplementary Table 4.2, Fig. 4.2 and enlarged in Fig. 4.4). The collagenase clade, is subdivided into three subclades as annotated in Fig. 4.2 and Fig. 4.4 (*mmp1a*, *mmp1b*, and *mmp1c*). Each of these subclades

includes presumptive MMP orthologs from other salamander species. The collagenase clade excludes non-urodele vertebrate MMPs, with one exception. Presumptive collagenase orthologs from three caecilian species grouped with the salamander. These data may suggest an ancient gene duplication of collagenases in the urodele lineage, or less parsimoniously, gene duplication in the amphibian ancestor with sequential losses in both caecilian and anuran lineages.

4.3.4 Salamander MMP13 duplication

Two different *mmp13* transcripts were identified from Sal-Site (Baddar et al., 2015) (Supplementary Table 4.1) that encode different protein-coding sequences. We denote these as *mmp13a* and *mmp13b*; the former matches sequence “*ammp13*” identified previously by Monaghan (2009) and *mmp13b* is the homolog of *C. pyrrhogaster mmp13* identified by Yang et al. (1999). Both axolotl *mmp13* sequences cluster within the MMP13 clade that includes MMP13 orthologs from *H. sapiens*, *G. gallus*, *X. tropicalis*, and *N. parkeri*. Two salamanders (*A. andersoni* and *B. ramose*) were found to have homologs for both MMP13 sequences, while other salamander species (*A. maculatum*, *H. chinensis*, *N. viridescens*, and *P. waltl*) had only one *mmp13* homolog (Supplementary Table 4.2, Fig. 4.4). This suggests that the *mmp13* duplication occurred in an ancestor of ambystomatid and plethodontid salamanders. However, most family-level reconstructions of urodeles suggest that salamanadrids are more closely related to ambystomatids. If this is true, newt species would also be expected to have two *mmp13* genes. Additional data are needed to reconstruct the evolution of *mmp13* paralogs.

4.3.5 Salamander-specific MMPE

Kato et al. (2003) identified a novel MMP (designated as nMMPe) from *C. pyrrhogaster* that showed low sequence similarity to other vertebrate MMPs (Kato et al., 2003). The cloned gene was shown to have a threonine-rich 42 amino acid insertion in the hinge domain. Another distinctive feature of this novel MMP was a proline to serine amino acid substitution in the conserved cysteine switch motif PRCG(V/N)PD. I identified presumptive orthologs for *nmmpe* in the axolotl, *A. maculatum*, *A. andersoni*, *N. viridescens*, and *P. waltl* (Fig. 4.2 and Fig. 4.4). However, I note that some of these genes did not cluster together as would be expected if they shared a common evolutionary history.

4.3.6 Gene Expression profiles of *Mmps* in the axolotl

Only a few MMPs have been characterized and studied during regeneration in salamanders. As we identified the entire axolotl MMP gene family in the axolotl in this report, we sought next to gain biological insights regarding their gene expression during regeneration. To accomplish this, I extracted gene expression data during limb regeneration from Sal-Site and an axolotl tissue transcriptome catalog (Bryant et al., 2017).

The Ambystoma microarray gene chip (Huggins et al., 2012) has probes for axolotl gelatinases (*mmp2* and *Mmp9*), collagenases (*mmp1a*, *mmp1b*, and *mmp1c*), *mmp13 b*, and *mmp3* paralogs (*mmp3a*, *mmp3b*, *mmp3c*, *mmp3d*). The gene expression levels of these genes during limb regeneration are shown in (Fig. 4.5) (Voss et al., 2015). *Mmp9* (a gelatinase) is upregulated in a biphasic manner after limb amputation; the first phase around 2 hpa (hours post amputation) in the wound epidermis and then later when the blastema starts forming (Yang and Bryant, 1994; Yang et al., 1999; Kato et al., 2005). The expression profile for axolotl *mmp9* (Fig. 4.5 A) confirms these reports. Gene expression data for the three collagenases during axolotl limb regeneration shows that they all are

dramatically upregulated after injury up to 5 dpa (Fig. 4.5 B), Voss et al., 2015; Sal-Site). The results agree with Vinarsky et al. (2005) who observed that the expression of *Nv* collagenase, the presumptive axolotl *mmp1a* homolog, peaks at 1dpa in wound epidermis, and the apical epidermal cap, and later in the blastema. This suggests a conserved role for these collagenases in salamanders and highlights the importance of collagenase activity early during regeneration to prevent basal lamina formation, thus ensuring communication between the wound epidermis and mesenchyme (Yang et al., 1999). The gene expression profile of axolotl *mmp13b* during axolotl limb regeneration is shown in Fig. 4.5 B. Unlike collagenases, *mmp13b* expression only gradually increases after amputation and peak later around the time the blastema forms.

The abundance of all axolotl *mmp3* transcripts peaked early after limb amputation (~12 hpa-5 dpa) (Fig 4.5C). Similarly, newt *mmp3* paralogs *NvMmp3/10a* and *NvMmp3/10b* and *CpMmp3/10a* and *CpMmp3/10b* were upregulated between 18-24 hpa (Vinarsky et al., 2005; Kato et al., 2003). These genes were found to be expressed in the basal layer of the wound epidermis. Together, the data indicates that amputation triggers the dramatic upregulation of *mmp3* transcripts in salamanders, perhaps by a shared mechanism.

During regeneration, nMMPe protein levels seem to specifically intensify in wound epidermis and the apical epithelial cap during salamander limb regeneration (Kato et al., 2003). Figure 4.6 A shows that the axolotl homolog of the newt (*nMmpe*) is only expressed in the limb blastema, with almost no expression in any of the other axolotl tissues sampled (Fig 4.5 A). This suggests that this unique salamander specific MMP may have evolved exclusively in salamander lineages to facilitate regeneration-specific ECM remodeling

processes required for regeneration and wound healing. Other axolotl MMP (*Mmp13a*, *mmp11*, *mmp19*, *mmp14*, *mmp25*) showed similar upregulation during regeneration with relatively low to basal expression in non-regenerating tissues (Fig. 4.6). Still other Mmps showed higher abundance in other tissues relative to blastema. *Mmp28* and *mmp25* transcripts were relatively highly abundant in ovaries and circulatory tissues, respectively (Fig. 4.5 C and D). Although these data were generated from low number of samples, they suggest the involvement of the majority of axolotl *mmps* in blastema formation/maintenance. Future research will be needed to shed more light on the function of these previously uncharacterized axolotl's *mmps* during regeneration. For example, CRISPR gene knockout may identify their exact functions during regeneration.

4.3.7. Salamander-specific molecular sequence signatures in MMP3 paralogs

It has been proposed that salamander MMPs have a unique sequence modification in their hinge domain that distinguishes them from homologs in mammals and frogs (Yang and Bryant et al., 1999; Kato et al, 2003). Specifically, NvMMP/10a and its homolog in *C. pyrrhogaster* (CpMMP3/10 a) have an insertion of 12 amino acids (mostly threonine residues) in their hinge domain compared to mammalian stromelysin. This contrasts with Nv- and CpMMP3/10b, which is relatively shorter than the human ortholog and lacks the inserted amino acids (Bryant et al., 1999; Kato et al, 2003). Focusing on the hinge domain sequence modification shown in Fig. 4.7, salamander MMP3 sequences form three major groups; MMP3s with no threonine-rich insertion (AmMMP3a, NvMMP3/10b, CpMMP3/10b), MMP3s with a long threonine-rich insertion of 23 amino acids (AmMMP3c and AmacTR175981_c0_g1_i1), and MMP3s with relatively short threonine insertions (AmMMP3b and d, NvMMP3/10a, CpMMP3/10a). Combining the above

sequence alignment information with data obtained from tBlast_x of axolotl's MMP3 proteins in Table 3, shows that axolotl, *P. waltl*, *N. viridescens*, and *P. C. pyrrhogaster* have all three MMP3 paralogs (Table 4. 4). It is possible that other salamander species in this study also have orthologs for these MMP3 genes, however, their short/partial sequences failed to enable specific MMP assignments; better transcriptome assemblies are needed to address this question. A presumptive ortholog for the axolotl MMP3c homolog was identified in *A. maculatum* but not in any other salamander species. This suggests that the MMP3c gene arose specifically within Ambystomatidae.

4.4 Conclusions

The activities of MMPs are critical for limb regeneration, especially in remodeling the stump tissues to facilitate wound healing and blastema formation. Over the last 40 years, very few MMPs have been studied within the context of salamander regeneration (Grillo et al. 1986; Dredsen and Gross, 1970, Yang and Bryant, 1994; Miyazakai et al., 1996; Yang et al., 1999; Vinarsky et al., 2005; Kato et al., 2003; Monaghan, 2009). Using bioinformatic analyses coupled with phylogenetics, we robustly identified 24 MMPs in the axolotl genome. Many of the MMPs showed high similarity to other vertebrates MMPs, however others appear to have arisen by duplication within urodeles. Specifically, salamanders have three collagenases, 3-4 MMP3 *genes*, and two MMP13 genes. I also identified homologs for newt MMPE in other salamanders. My analysis allowed us to correctly assign MMP gene names to microarray probesets (Fig. 4.5*). The expression profiles of the axolotl collagenases, stromelysin *and* MMP9 during limb regeneration corroborate previous reports (Yang and Bryant, 1994; Miyazakai et al., 1996; Yang et al.,

1999; Vinarsky et al., 2005; Kato et al., 2003. It will be important to detail expression profiles for the newly identified MMPs.

Salamander MMP3s have various threonine insertions in their hinge domains. Also, all nMMPe homologs have a 43 amino acid, threonine-rich insertion in their hinge domain. Kato et al (2003) suggested that this insertion is salamander-specific and our data strongly corroborate this assertion. Since the hinge domain is implicated in MMP catalytic activity and substrate specificity (Fasciglione et al., 2012), the threonine insertion may perform a unique function in salamanders that could be addressed in the future.

4.5 Acknowledgements

I wish to thank Maria Torres-Sánchez and Ryan Woodcock for their help with bioinformatic and phylogenetic analyses in this chapter.

Table 4.1. Resources of the transcriptomes used to extract MMP sequences in the organisms listed.

Organism	Resource Reference
<i>A. maculatum</i>	Dwaraka et al., 2018
<i>A. andersoni</i>	Dwaraka et al., 2018
<i>A. texanum</i>	McElroy et al., 2017
<i>A. laterale</i>	McElroy et al., 2017
<i>C. pyrrhogaster</i>	Casco Robles et al., 2018
<i>H. chinensis</i>	Che et al., 2014
<i>B. ramosi</i>	Arenas Gomez et al., 2018
<i>N. viridescens</i>	Abduallyev et al., 2013
<i>P. waltl</i>	Elewa et al., 2017
<i>T. compressicauda</i>	Torres-Sánchez et al., 2019
<i>M. unicolor</i>	Torres-Sánchez et al., 2019
<i>R. bivittatum</i>	Torres-Sánchez et al., 2019
<i>L. boringii</i>	Zhang et al., 2016
<i>N. parkeri</i>	Sun et al., 2015

Table 4.2. Refined analysis showing the best candidate sequences for salamander MMP3 genes. We only include sequences that have been identified as high confidence best Blast hits to axolotl MMP3. (-) indicates transcript is missing or fragmented/very short. T denotes threonine.

Salamander species	AmMMP3a No T insertion	AmMMP3b and AmMMP3d Short T insertion	AmMmp3c Long T insertion
<i>A.maculatum</i>	TR71476_c3_g5_i1	-	TR175981_c0_g1_i1
<i>A.laterale</i>	Alat_GFLO01004241.1	-	-
<i>A.andersoni</i>	-	-	-
<i>A.texanum</i>	-	-	-
<i>N. viridescens</i>	NvMMP3/10b	Nv_117895 and NvMMP3/10a	-
<i>C.pyrrhogaster</i>	CpMMP3/10b	CpMMP3/10a and comp511371_c0_seq2	-
<i>B. ramosi</i>	Bram_TR122436_c0_g1_i1	-	-
<i>H. chinensis</i>	Hchi_GAQK01002038.1	-	-
<i>P. waltl</i>	Pwaltl_36235	Pwaltl_389547 and Pwaltl_99975	-

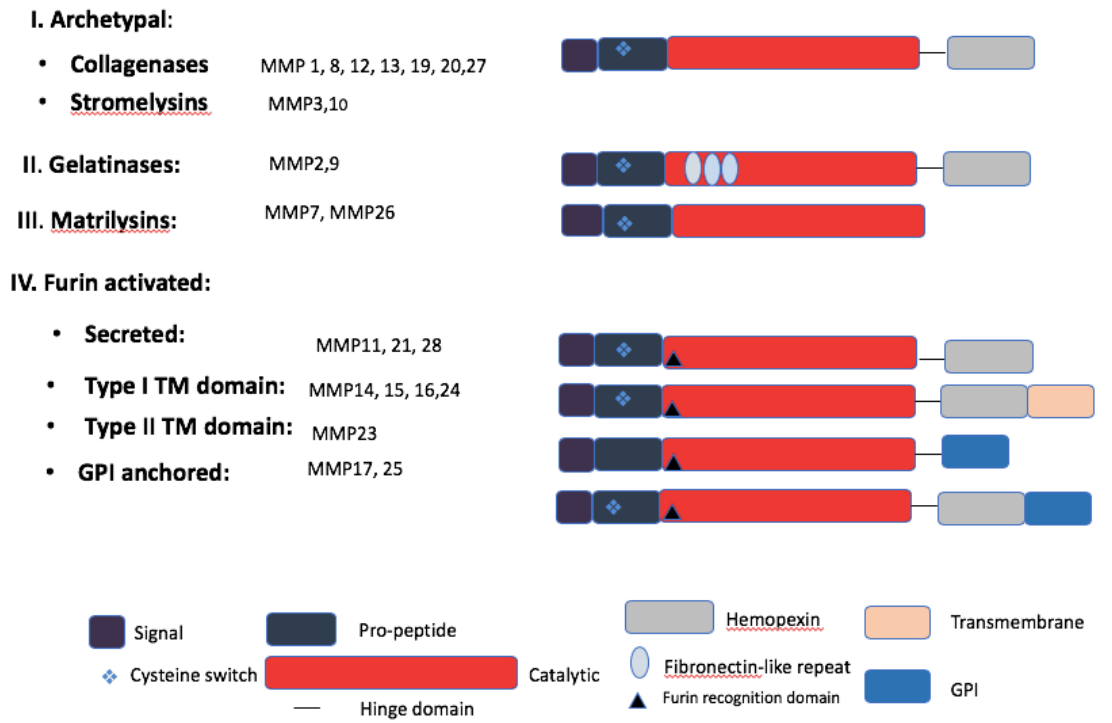


Figure 4.1. The MMP gene family is typically categorized based on domain structure into 4 main groups; archetypal, gelatinases, matrilysins and furin-activated MMPs.

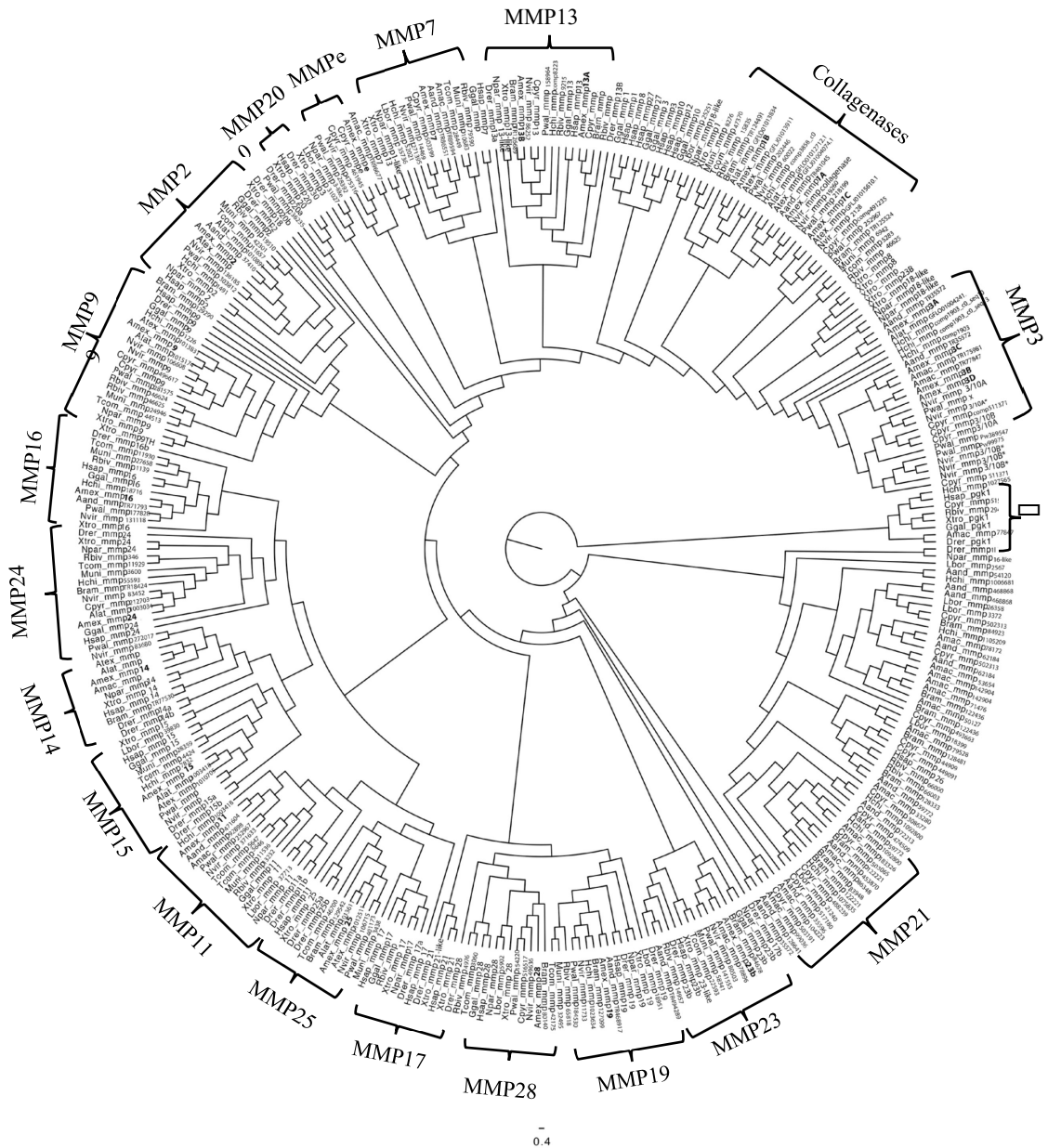


Figure 4.2. Cladogram representing MMPs in axolotl and other vertebrates. Axolotl MMPs are highlighted in bold. * indicates splice variants. □ indicates outgroup.

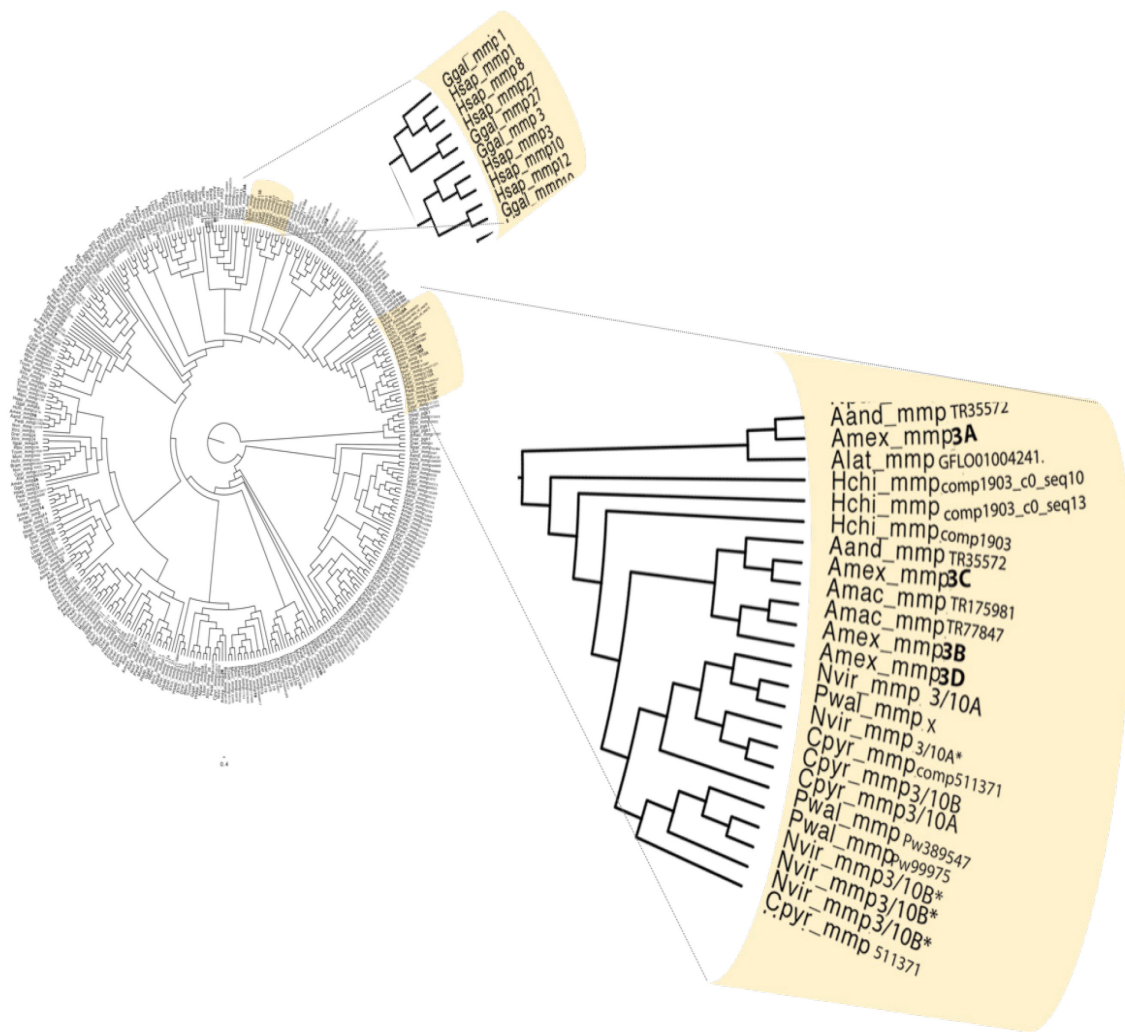


Figure 4.3. A magnified salamander MMP3 clade and human collagenase and stromelysin clade shown in Fig 4.2.

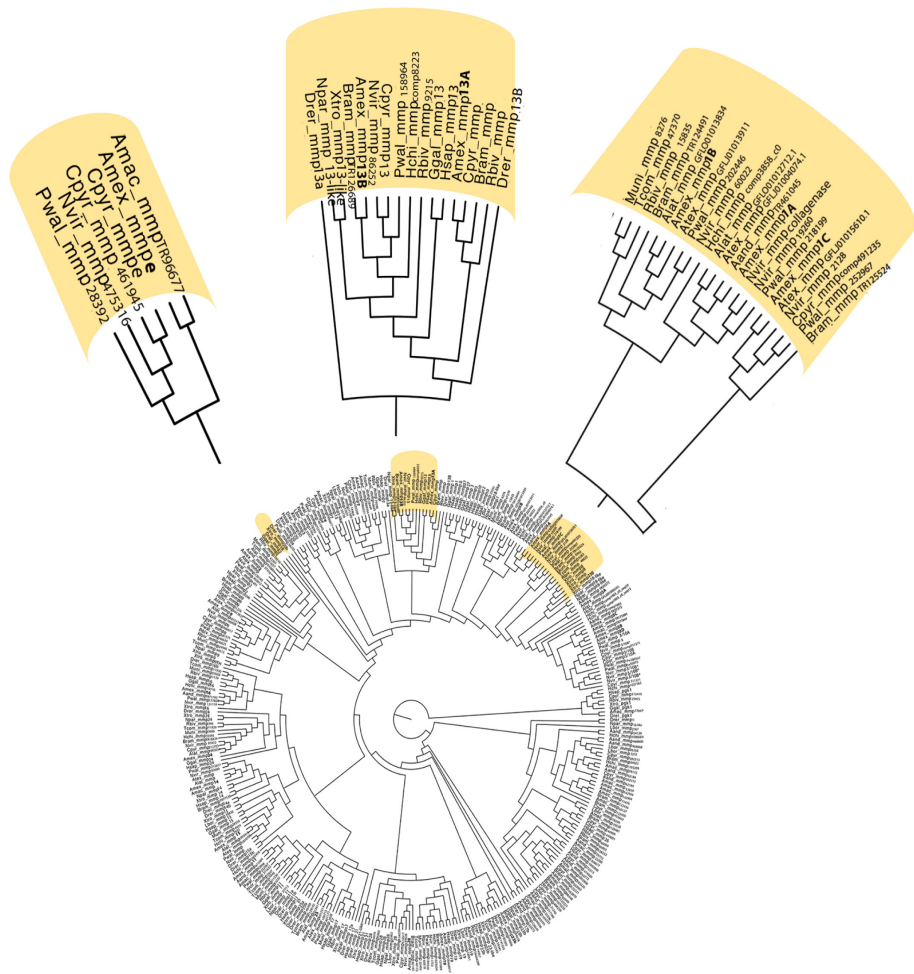


Figure 4.4. Magnified view of salamander specific clades collagenase, MMPE clades, and the MMP13 clade shown in Fig 4.2.

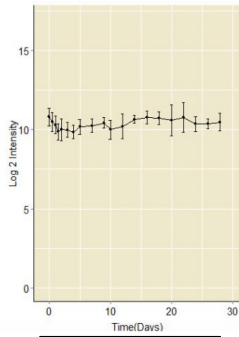
A. Gelatinases

Probe Expression Information

Affy GeneChip Probe : axo10176

Source Sequence ID (Assembly V3.0): contig86041

Gene Information : MMP2 matrix metalloproteinase 2

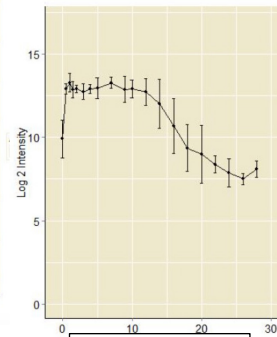


Mmp2

Affy GeneChip Probe : axo05645

Source Sequence ID (Assembly V3.0): contig67644

Gene Information : MMP2 matrix metalloproteinase 2



Mmp9*

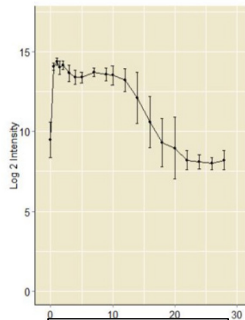
B. Collagenases

Probe Expression Information

Affy GeneChip Probe : axo08175

Source Sequence ID (Assembly V3.0): contig67637

Gene Information : MMP1 matrix metalloproteinase 1

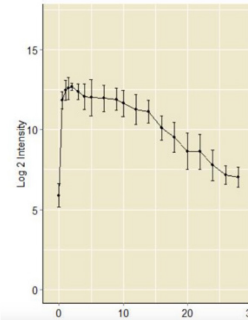


Mmp1a

Affy GeneChip Probe : axo08174

Source Sequence ID (Assembly V3.0): contig60497

Gene Information : MMP1 matrix metalloproteinase 1

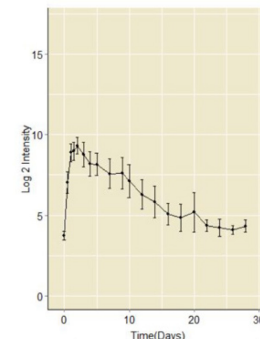


Mmp1b

Affy GeneChip Probe : axo08186

Source Sequence ID (Assembly V3.0): contig66932

Gene Information : MMP13 matrix metalloproteinase 13

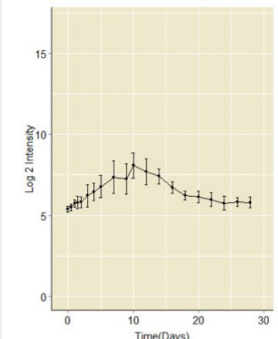


Mmp1c*

Affy GeneChip Probe : axo08185

Source Sequence ID (Assembly V3.0): contig85410

Gene Information : MMP13 matrix metalloproteinase 13



MMp13b

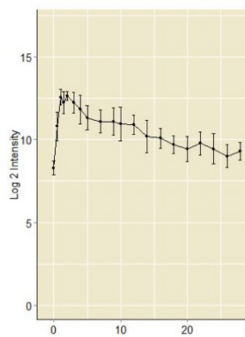
C. Stromelysins

Probe Expression Information

Affy GeneChip Probe : axo08179

Source Sequence ID (Assembly V3.0): contig65376

Gene Information : MMP3 matrix metalloproteinase 3



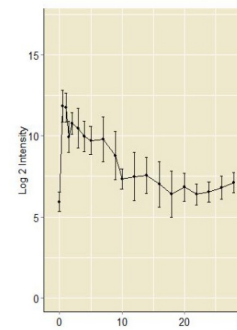
Mmp3a

Probe Expression Information

Affy GeneChip Probe : axo08181

Source Sequence ID (Assembly V3.0): contig65563

Gene Information : MMP3 matrix metalloproteinase 3



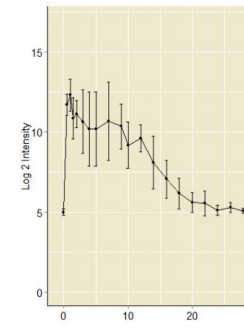
Mmp3b

Probe Expression Information

Affy GeneChip Probe : axo08180

Source Sequence ID (Assembly V3.0): contig65483

Gene Information : MMP3 matrix metalloproteinase 3



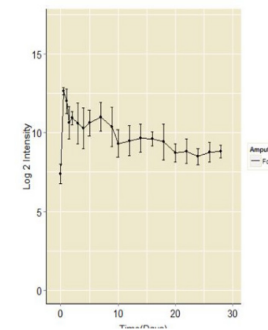
Mmp3c*

Probe Expression Information

Affy GeneChip Probe : axo08178

Source Sequence ID (Assembly V3.0): contig65265

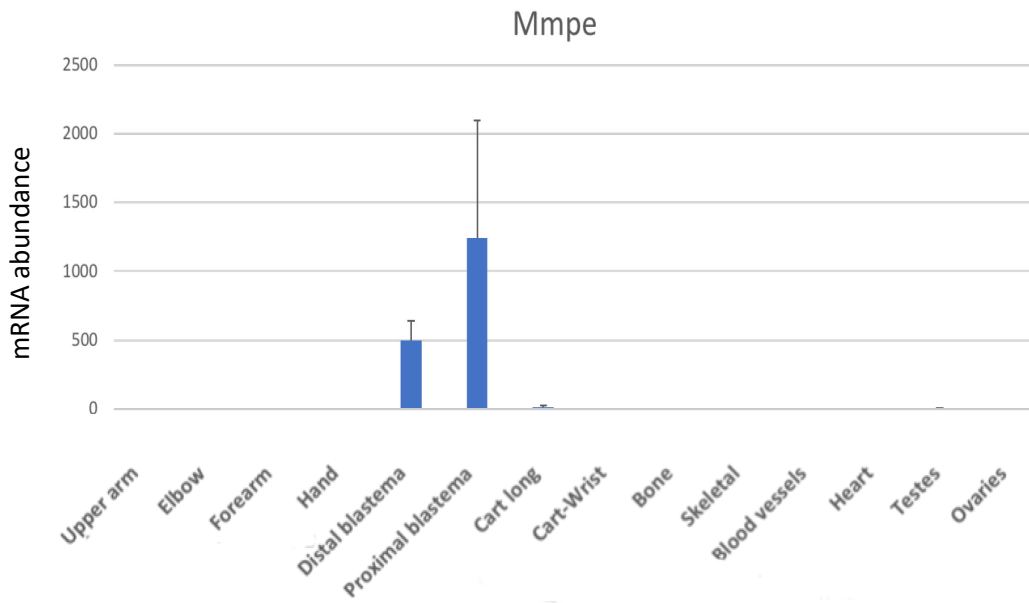
Gene Information : MMP3 matrix metalloproteinase 3 preprope



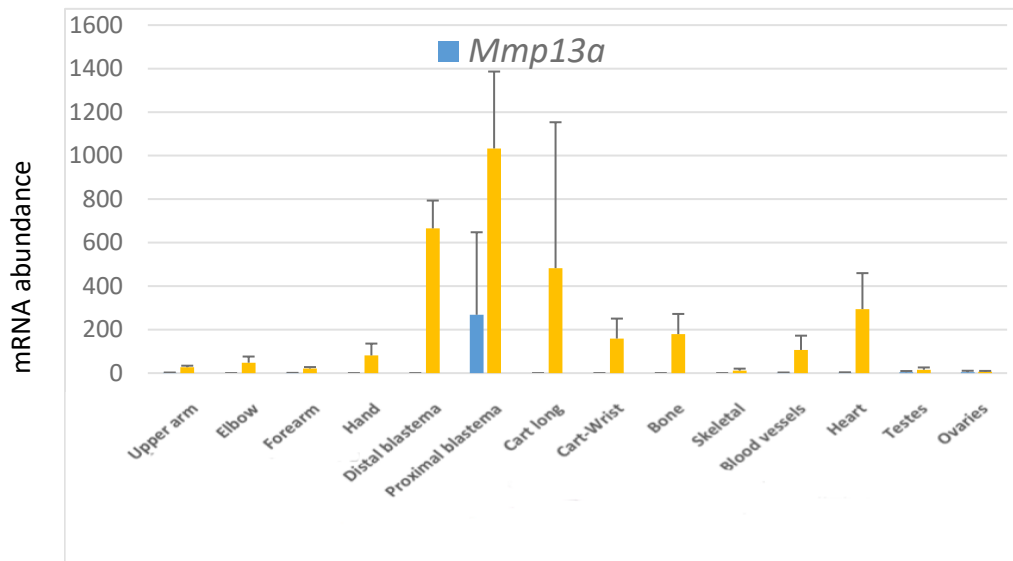
Mmp3d

Figure 4.5. Gene expression of salamander specific *mmps* during limb regeneration. (A) Gelatinases including *mmp2* and *mmp9*, (B) Collagenases including *mmp1a*, *mmp1b*, *mmp1c* and *mmp13b*, and (C) Stromelysins including *mmp3a*, *mmp3b*, *mmp3c*, *mmp3d*. *: indicates the *mmps* whose annotation was corrected as a result of our analysis.

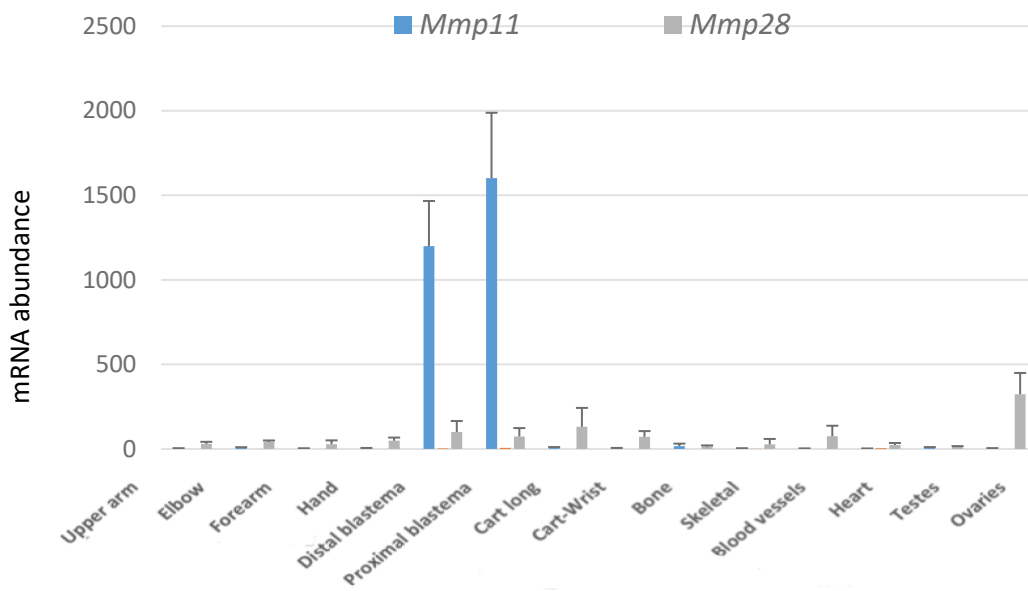
A



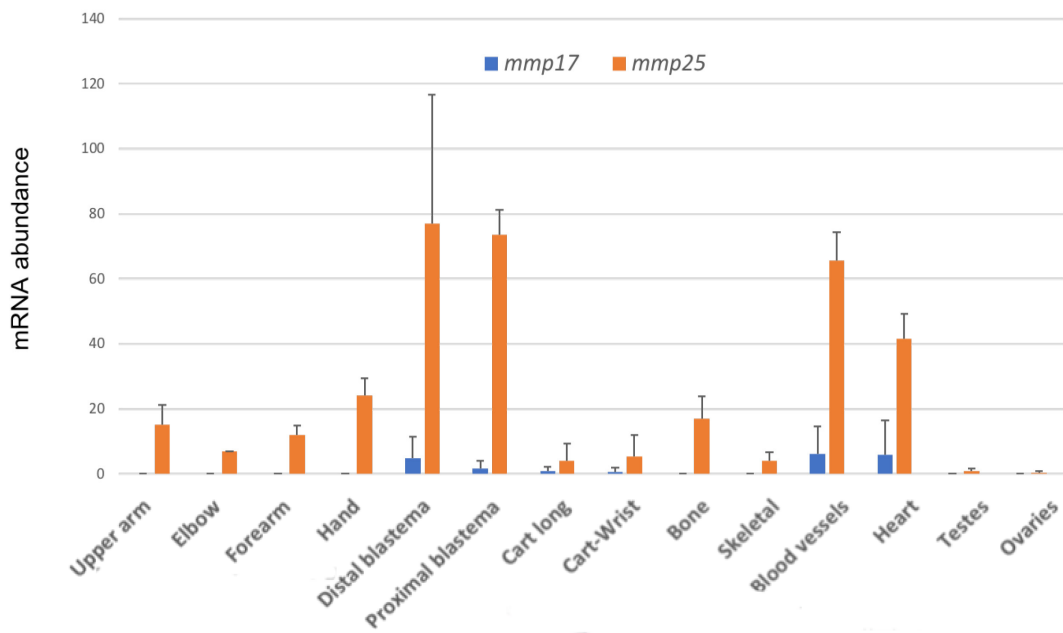
B



C



D



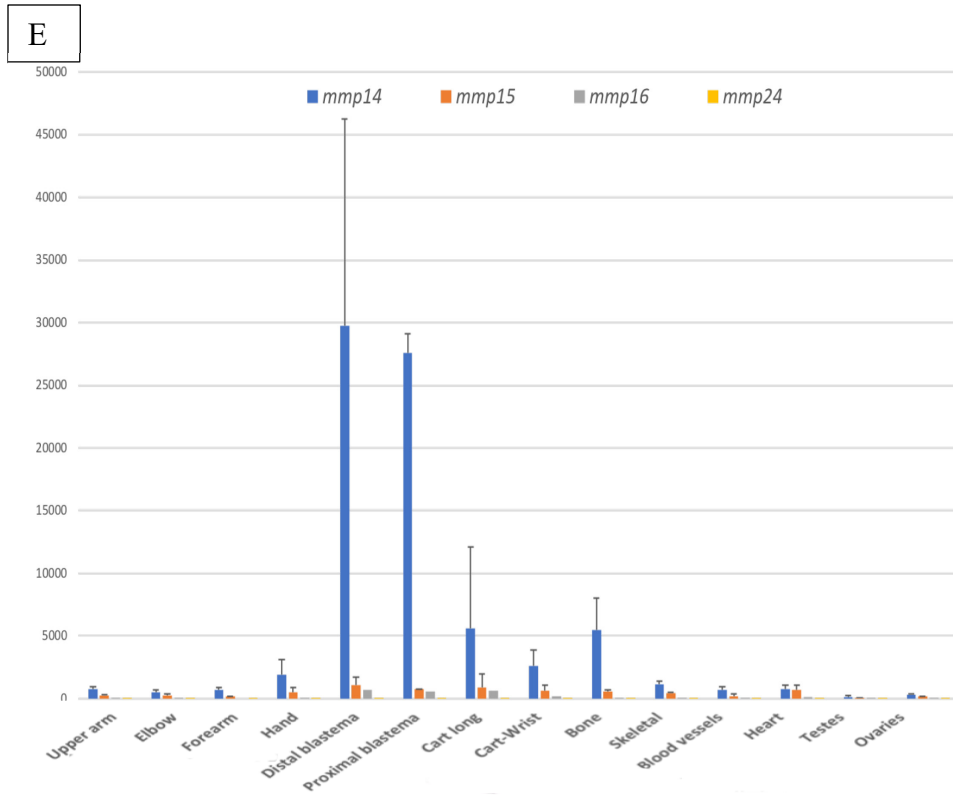


Figure 4.6. Gene expression analysis of MMPs across different tissues in the axolotl. A) Salamander specific MMPs, B) Mmp13a, and Mmp19, and furin-activated MMPs: C) MMP11, MMP28, D) MMP17, MMP25, E) MMP14, MMP15, MMP16, MMP24. Error bars represent standard deviation of the means.

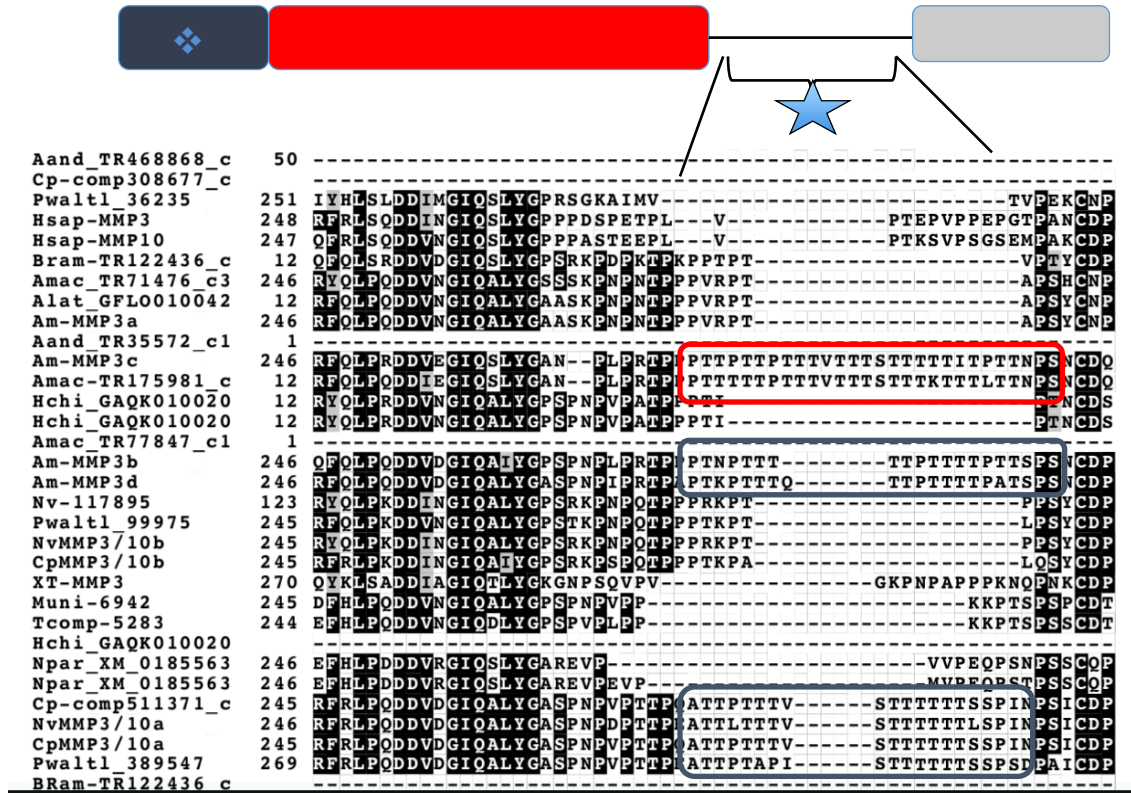


Figure 4.7. Hinge domain sequence variation within salamanders MMP3s. (The sequences in the figure are shown in Table 2). A cartoon of a typical MMP is shown to point to the hinge region (star). MMP3s either have no threonine insertion (e.g. AmMMP3a), a long insertion containing 23 residues (mostly threonine, e.g. Am MMP3c, red box), or a relatively short insertion (AmMMP3b and d; blue boxes).

Chapter 5: Role of JNK Signaling During Axolotl Embryo Tail Regeneration: A Microarray Study to Identify Downstream Targets

Nour W. Al Haj Baddar^{a,b}

^aDepartment of Biology, University of Kentucky, Lexington, KY, 40506

^bDepartment of Neuroscience and Spinal Cord and Brain Injury Research Center (SCoBIRC), University of Kentucky, Lexington, Kentucky, 40536

5.1 Introduction

Tissue regeneration is orchestrated by highly conserved signaling pathways and genetic programs (Stoick-Cooper *et al.* 2007; Herman *et al.*, 2018). Studies have established that the stress-induced MAPK signaling pathway (JNK) is necessary for regeneration of the planarian body (Tasaki *et al.*, 2011) zebrafish fin (Gauron *et al.*, 2013), tadpole tail (Sugiura *et al.*, 2009), and salamander spinal cord (Sabin *et al.*, 2015). JNK signaling is activated by extracellular stimuli that are generated at the time of tissue injury and during early phases of the wound healing response (Chen *et al.*, 2012; Sader *et al.*, 2019). These stimuli activate intracellular signal transduction cascades that ultimately alter gene transcription (Zeke *et al.*, 2016; Nadal-Ribelles, 2018). The discovery of genes that are activated by JNK signaling could provide novel insights and new targets for studies of tissue regeneration.

Signaling pathways can be perturbed using genetic and pharmacological approaches. For example, small molecules can be used to inhibit membrane proteins that initiate signal transduction cascades (Ponomareva *et al.*, 2015). In this Chapter, I used a

small molecule (SP600125) (Bennette et al., 2011) to inhibit JNK signaling during axolotl embryo tail regeneration. By comparing transcription between SP600125 and non-treated embryos at 24 hours post-amputation, I discovered gene targets and used these to infer protein functions and biological processes associated with JNK signaling and tissue regeneration.

5.2 Materials and Methods

5.2.1 Chemical treatment with JNK inhibitor and regeneration assays

The axolotl embryo tail regeneration model was described by Ponomareva et al (2015). JNK inhibitor, SP600125 was dissolved in DMSO and used at 5 μ M. To investigate the requirement of JNK signaling during regeneration, embryos were treated with SP600125 from 0-7 days post-amputation. Tail length was measured after tail amputation to quantify tissue regeneration and images of embryos were taken at 7 dpa. Students't-test was used to test for differences in tail length and t-statistics that yielded probability values < 0.05 were considered statistically significant.

5.2.2 Microarray gene expression analysis

A total of 96 axolotl embryos were administered tail amputations (Ponomareva et al. 2015). Forty-eight embryos (control) were treated with 0.1% DMSO and forty-eight embryos (treatment) were treated with 5 μ M SP600125 from 0-24 hpa. At 24 hpa, exactly 1mm of the distal tip was removed from embryos and tail tissues from 12 embryos were pooled into a 1.5 ml tube with 0.5 ml RNA-Later (Qiagen) yielding 4 control and 4 treatment replicates. The harvested tails were preserved at 4 C° in RNA later for < 7 days. RNA isolation followed the Trizol method, and then a Qiagen minikit with on-the-column DNase treatment of contaminating DNA. Microarray hybridization using an *Ambystoma*

Affymetrix array (Huggins et al., 2010) was performed by the University of Kentucky Genomic lab facility. Differentially expressed genes were analyzed for enriched gene ontology (GO) terms and further evaluated for gene functions using results from the scientific literature.

5.2.3 Statistical analyses

All of the Gene Chips were normalized using Affymetrix Expression Console software to accomplish robust multichip averaging (RMA) (Irizarry et al., 2003). Student's t-test with false discovery rate correction (Benjamini-Hochberg procedure, $p < 0.05$) was performed between control and SP600125-treated embryos to identify probe sets that yielded significantly different average expression values as a function of treatment. These lists were further filtered using a minimum 1.5-fold difference between treatment and control means.

5.2.4 Nanostring nCounter® SPRINT Profiler development and analysis

To validate the microarray data, a new set of biological samples was prepared for gene expression analysis using a custom Nanostring codeset. This codeset was designed to validate 100 gene targets and included the most highly differentially expressed genes from the SP600125 microarray analysis (*hebp2*, *wdr76*, *xpc*, and *ese3*). Ninety-six embryos were administered amputations and an equal number were randomly assigned to DMSO control and 5 uM SP600125 treatments. At 24 hpa, exactly 1 mm of tissue was sampled from the distal tail tip of each embryo. Tail tips from 12 embryos were pooled to create 4 replicate and 4 treatment samples for RNA isolation. Sample processing was performed on a nCounter® SPRINT Profiler by the University of Kentucky Health Care Genomics Core. Manufacturer internal negative and positive control probes, as well as probes designed for

axolotl reference genes, were used to normalize the raw data. One of the treatment samples yielded off scale data as a result of a channel failure in the Nanostring cartridge. This sample was removed from subsequent analyses. The resulting normalized data were log₂ transformed and analyzed using t-tests. Significance was evaluated using the Benjamini-Hochberg procedure and a 0.1 FDR.

5.3 Results and Discussion

5.3.1 JNK activity is essential for axolotl embryo tail regeneration

To directly test the requirement of JNK signaling during axolotl embryo tail regeneration, embryos were treated with JNK inhibitor SP600125 (Bennette et al., 2011). This compound acts as an ATP-competitive inhibitor that blocks activity of jnk1, jnk2, and jnk3 by binding the ATP binding site in these enzymes (Bennette et al., 2011). Sader et al. (2019) experimentally confirmed that 5 μ M SP600125 inhibited levels of phosphorylated JNK during limb regeneration in the axolotl. Embryos treated with 5 μ M of SP600125 from 0-7 dpa regenerated less tissue than control embryos that were reared in 0.1% DMSO (Fig. 5.1), and this difference was statistically significant. Thus, JNK signaling is required for axolotl tail regeneration, a result that further corroborates JNK signaling as a phylogenetically conserved pathway required for successful tissue regeneration.

5.3.2 Identification of transcripts that changed as a result of JNK inhibition at 1 dpa

It has been established that active JNK signaling is required for tissue and organ regeneration, however, down-stream gene targets remain largely uncharacterized. To identify downstream transcriptional targets of JNK signaling during axolotl tail regeneration, we used custom Affymetrix GeneChips and performed a microarray analysis (Fig. 5.2). Embryos were either treated with 0.1%DMSO or 5 μ M SP600125 from 0-24

hpa. At 24 hpa, exactly 1 mm of the distal tail tip was removed for RNA isolation and gene expression analysis. A total of 220 probesets were identified as differentially expressed between the control DMSO and SP600125 treatment groups. Of these probesets, 77 were significantly downregulated in the treatment group while 142 were upregulated (Supplementary Table 5.1). Log₂ fold differences (control vs treatment) for 100 probesets on the microarray were highly concordant with the log₂ fold differences obtained for these same 100 gene targets using the Nanostring platform ($r = 0.87$, Fig 5.3). This included validation of the most differentially expressed genes, including *hebp2*, *wdr76*, *xpc*, *hsp90AA1*, *gpihbp1*, *cyp26a1*, and *ese3*.

5.3.3 GO enrichment analysis of genes that were upregulated in the JNK inhibitor treatment group

The probe sets that were upregulated in SP600125 embryos at 24 hpa enriched Gene Ontology (GO) terms corresponding to circadian regulation of gene expression, glucocorticoid receptor regulation, and oxidation reduction processes (Table 5.1, A). The genes that enriched circadian rhythm (*arntl*, *cry1*, *cry2*, *csnk1d*, *csnk1e*) are core components of the clock molecular machinery. The vertebrate circadian clock molecular machinery is established via multiple negative feedback loops of transcription, translation, and degradation of core clock gene transcripts. These core components are classified into transcriptional activators (*arntl*, *clock*) and transcriptional repressors (*per1*, *per2*, *per3*, *cry1*, *cry2*) (Takahashi, 2107). The heterodimerization and binding of the transcription factors *arntl* and *clock* to regulatory element E-boxes drives the rhythmic expression of their repressors (*per1*, *per2*, *per3*, *cry1*, *cry2*). The encoded repressors accumulate, translocate to the nucleus and perturb ARNTL and CLOCK heterodimerization and

suppress their own expression. The phosphorylation of PER proteins by the serine threonine kinases CSNK1D and CSNK1E target them for ubiquitylation and proteasomal degradation. CRY1 and CRY2 are phosphorylated by different enzymes - AMPK and GSK3B - prior to their ubiquitylation and proteasomal degradation (Takahashi, 2107). This allows clearing of their inhibitory effects on ARNTL and CLOCK heterodimer formation, therefore, they can activate the cycle again.

Phosphorylation of specific clock core protein components differentially impacts their stability and subsequently the timing of the activation and repression of the positive and negative limbs of the circadian clock (Vanselow and Kramer, 2007). For example, *in vitro* experiments using mammalian cells in culture have shown that ARNTL phosphorylation following JNK activation leads to ARNTL destabilization and degradation, while ARNTL phosphorylation by CSNK1E enhances stability (Uchida et al., 2012). Our data show that JNK inhibition upregulated *csk1e* and *csk1d*. In response to inhibition of JNK signaling, *csk1e* upregulation would be expected to stabilize ARNTL. Given that ARNTL and CLOCK activate *arntl* gene expression, via a different feedback loop (Takahashi, 2017), increased stability of ARNTL by JNK pathway inactivation is expected to upregulate *arntl*, and indeed this was observed in our experiment. If ARNTL and CLOCK remain stable for extended periods of time under JNK inhibition, this would be expected to upregulate their gene targets. Indeed, *cry1* and *cry2* were expressed more highly in the JNK inhibitor treatment group. We note that *per1* and *per2* were also upregulated in the JNK inhibitor treatment group but the difference relative to controls was not statistically significant. Taken together and consistent with the mammalian circadian clock literature (Goldsmith and Bell-Pedersen, 2013), our results suggest a role for JNK

signaling in influencing activity and degradation of positive and negative components that are essential for circadian clock function. Further studies are needed to determine if clock gene dysregulation inhibits axolotl tail regeneration.

JNK signaling inhibition enriched glucocorticoid receptor signaling GO terms. Some of the genes in this group also included clock core proteins (*Arntl*, *cry1*, *cry2*). We additionally identified upregulation of *gfpt2*, which is known to drive cellular uptake of glucose and is associated with metabolic changes during cancer (Zhang et al., 2018). The upregulation of glucocorticoid receptors during zebrafish fin regeneration, specifically at early time points encompassing wound healing and blastema formation, blocked regeneration (Mathew et al., 2007). This may suggest that glucocorticoid receptor signaling is a conserved early component of regeneration in zebrafish and axolotl.

Other genes upregulated as a result of JNK inhibition are associated with muscle tissue function. For instance, genes involved in muscle contraction, including *ttn*, *mylh2*, *mylh4*, *mylh10*, *neb*, *acta2*, were upregulated in the JNK inhibitor treatment group relative to controls. The majority of these genes are characteristically downregulated during axolotl limb regeneration (Voss et al., 2015). This suggests that amputation-induced myofiber fragmentation and remodeling was inhibited in embryos treated with the JNK inhibitor. Similarly, some of these muscle genes were also upregulated when the Wnt pathway was pharmacologically inhibited using this same axolotl embryo tail regeneration model (Ponomareva et al., 2015). Noncanonical Wnt signaling maybe an upstream activator of JNK signaling (Saadeddin et al., 2007).

Our data also show that JNK inhibition is associated with the upregulation of genes typically known to be induced under cellular stress conditions, like genes associated with

DNA damage and repair (*xpc, nil3, nabp2, ddit3, rad 50, dclrea, rrm2, rrm1*) and genes promoting apoptosis under stress conditions (*ghitm, higd1a, ptrh2, hebp2*). Genes that encode proteins that metabolize drugs or have functions that associate with the electron transport chain were also upregulated (*gstp1, cbr1, cyp2d6, cyp2d6, cyp4f22, hccs, sdha*). Cellular stress specifically induces *hsp90aa* expression to encode chaperones that promote protein proper folding and structural integrity. Further, oxidative stress can convert methionine in peptides into methionine sulfoxides and genes like *mrsa* and *sepx1* repair these oxidatively damaged proteins (Sreekumar et al., 2011). These results could suggest that in the absence of JNK activity, cells upregulate genes to mitigate and adapt to stressful conditions (Zuehelke et al., 2015).

5.3.4 GO enrichment analysis of genes that were downregulated in the JNK inhibitor treatment group

Some of the genes that were downregulated as a result of JNK inhibition are known to affect biological processes critical for regeneration (Table 5.1B). Others, although not specifically implicated in regeneration studies, are known to function in cellular processes that are almost certainly critical for successful regeneration, including the immune response, extracellular matrix dynamics, cell signaling, and cellular proliferation.

Generally, JNK signaling pathways are implicated in activating innate and adaptive immune responses in vertebrates (Dong et al., 2002). The immune response is critical to regeneration, specifically, in inflammation, wound healing (Godwin et al., 2013; Franklin et al., 2017, Godwin et al., 2017) and, interestingly, in removal of senescent cells produced in the axolotl limb blastema (Yun et al., 2015). Genes expressed in phagocytic and myeloid cells responsible for generating reactive oxygen species (ROS) to combat microorganism,

like *nox2* and *mpo*, were downregulated, as were genes that mediate immune cell migration (*lglas9*, *grk5*), and the secretion of inflammatory mediators (*c9*) (Sengel and Segal, 2016; Godwin et al., 2017). At 1 dpa, Franklin et al. (2017) showed that phagocytic cell numbers increase in the axolotl embryo tail. It is possible that JNK inhibition decreased phagocyte cell recruitment and/or perturbed gene expression and signaling in these cells (Hahn et al., 2009).

Extracellular matrix (ECM) remodeling is also pivotal in regeneration (Stocum et al., 2017). We found that some genes encoding ECM components were lowly expressed in the JNK inhibitor treatment group (*adamtsl2*, *lepre1*, *pcolce2*, *thbs2*, *itgb1bp3*, *hecw2*, *frem2*, *fn*). *Frem2* is a matrix substrate that contributes to ECM rearrangement required for tissue morphogenesis and angiogenesis during development of several organs in the mouse (Timmer et al., 2005). Fibronectin is also upregulated in the blastema during salamander limb regeneration (Clave et al., 2010) and is highly deposited in the ECM of damaged zebrafish cardiac tissue after injury (Wang et al., 2013). *Thbs2* and *hecw2* are also implicated in angiogenesis during wound healing (Kyriakides and Mclauchlan, 2009; Choi et al., 2016). This suggests that JNK signaling functions to activate genes required for wound healing and ECM remodeling, and more generally to create a regeneration-permissive environment.

A relatively higher number of genes encoding components of several other signaling pathways also downregulated in the JNK inhibitor treatment group. This list of genes included *inhbb* (a TGF- β protein superfamily component), *igfbp3* (receptor insulin signaling), *hbegf* (growth factor), *synj2* (phosphoinositide 3-kinase pathways), *ngfr* (*nerve growth factor receptor*), and a group of GTPases activating proteins (*rasal2*, *arhgap29*,

arhgef4, *arhgap23*, and *rgs10*). Two downregulated genes that are involved in RA (retinoic acid) metabolism and RA signaling were also identified (*cyp26a1* and *cyp26b*). These genes encode enzymes that provide tight control of RA tissue localization (Abu-Abed et al., 2001). This suggests that several other signaling pathway components are potential down-stream transcriptional targets of JNK pathway.

Other genes that were downregulated in the JNK inhibitor group are highlighted below given their potential significance for understanding regeneration processes:

- 1) *ccne1* encodes a cell cycle protein that contributes to the regulation of G1/S transition by activating kinase CDK2 which in turn phosphorylates retinoblastoma protein (rb). This phosphorylation induces expression of S phase proteins (Caldon and Musgrove, 2010).
- 2) *rbbp6* and *ppp1r26* are known to be essential for neural development and proliferation.
- 3) Genes associated with cell migration and EMT (*flna*, *rccd1*, *vash1*) were also downregulated. EMT is a process whereby epithelial cells undergo behavioral changes that are required for migration during development, wound healing, regeneration. Recently, both JNK and TGF signaling pathways were found necessary for EMT for during axolotl limb regeneration (Sader et al., 2019).
- 4) JNK signaling inhibition affected some gene targets related to morphogenesis and patterning, for example, *hoxa13* was lowly expressed in the JNK inhibitor treatment group. *Hoxa13* is expressed in the axolotl limb stump at 24-48 hpa in the mesenchyme below the wound epidermis, suggesting a possible role in

dedifferentiation (Gardiner et al., 1995). Similarly, *hoxa13* is expressed within a few days post tail amputation of axolotl larvae (Mchedlishvili et al., 2012).

Overall, our results show that JNK signaling affects a diverse set of transcriptional targets early in regeneration, including genes that function in wound healing and the immune response, ECM and muscle remodeling, cell cycle regulation, and apoptosis. This corroborates findings from other studies that similarly inhibited JNK signaling during regeneration (Sugiura et al, 2009; Tasaki et al., 2011; Gauron et al., 2013; Sabin et al., 2015). Our results suggest that inhibition of the JNK pathway is likely to affect the activity of other signaling pathways, including retinoic acid, TGF- β , and Wnt signaling cascades. Also, we show for the first time that JNK signaling affects biological processes that have not previously been implicated in regeneration studies, including regulation of central circadian clock genes and mitigation of DNA damage and cellular stress after injury. These results suggest that JNK signaling is required for regulating the expression of target genes that encode regeneration permissive proteins.

5.4. Conclusions

Despite the fact that many studies have established a requirement for JNK signaling during regeneration, the target genes of JNK pathway activation are poorly known. Our study is the first to uncover global gene expression changes following JNK inhibition in a highly regenerative salamander, the Mexican axolotl. The genes identified in this study provide novel insights and new targets for future studies of tissue regeneration.

Table 5.1. Gene ontology enrichment terms for differentially expressed genes as a result of SP600125 treatment.

A. Upregulated genes in SP600125

GO biological process complete	Gene symbols	p-value
Regulation of glucocorticoid receptors	<i>Arntl, cry1, cry2.</i>	3.84E-02
Circadian regulation of gene expression	<i>Arntl, cry1, cry2, csnk1d, csnk1e.</i>	2.57E-02
Oxidation-reduction processes	<i>rrm2, rrm2b, cyp2d6, acat2, sdha, sepx1, zadh2, msra, higd1a, cyp27c1, pla2g7, cyp4f22, gfpt2, dhrrs12, hccs, cbr1.</i>	2.50E-02

B. Downregulated genes in SP600125

GO biological process complete	Gene symbols	P-value
Signal transduction	<i>Igfbp3, tiam2, fn1, grk5, hbegf, frem2, inhbb, ngfr, rasal2.</i>	3.91E-02
Cellular proliferation	<i>Ccne1, hbegf.</i>	4.68E-02
Cellular import	<i>Slc7a3, slc39a6.</i>	1.10E-02

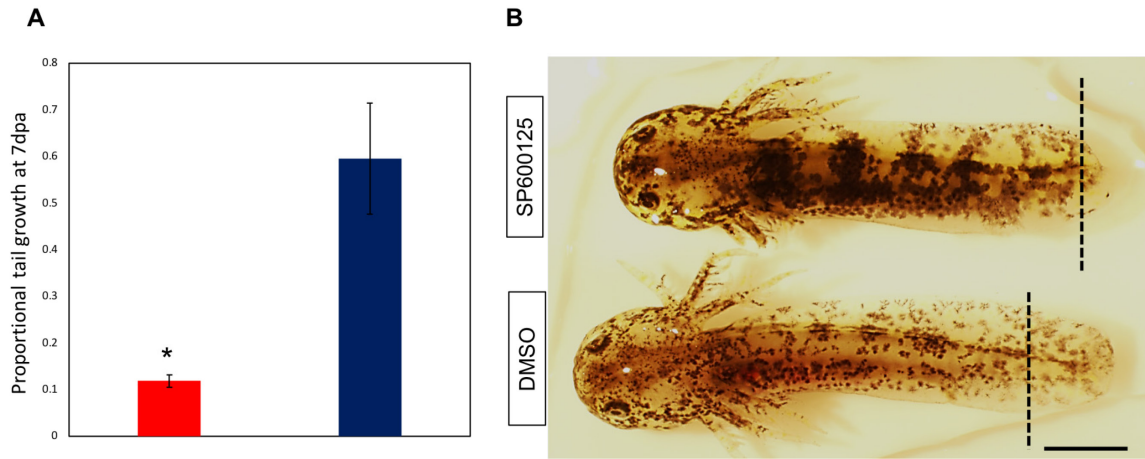


Figure 5. 1 JNK inhibitor SP600125 treatment blocks tail regeneration in axolotl embryos. B) SP600125 treated and control embryos at 7 dpa, (N = 6 each). Dotted lines represent plane of amputation. Scale bar = 1 mm.

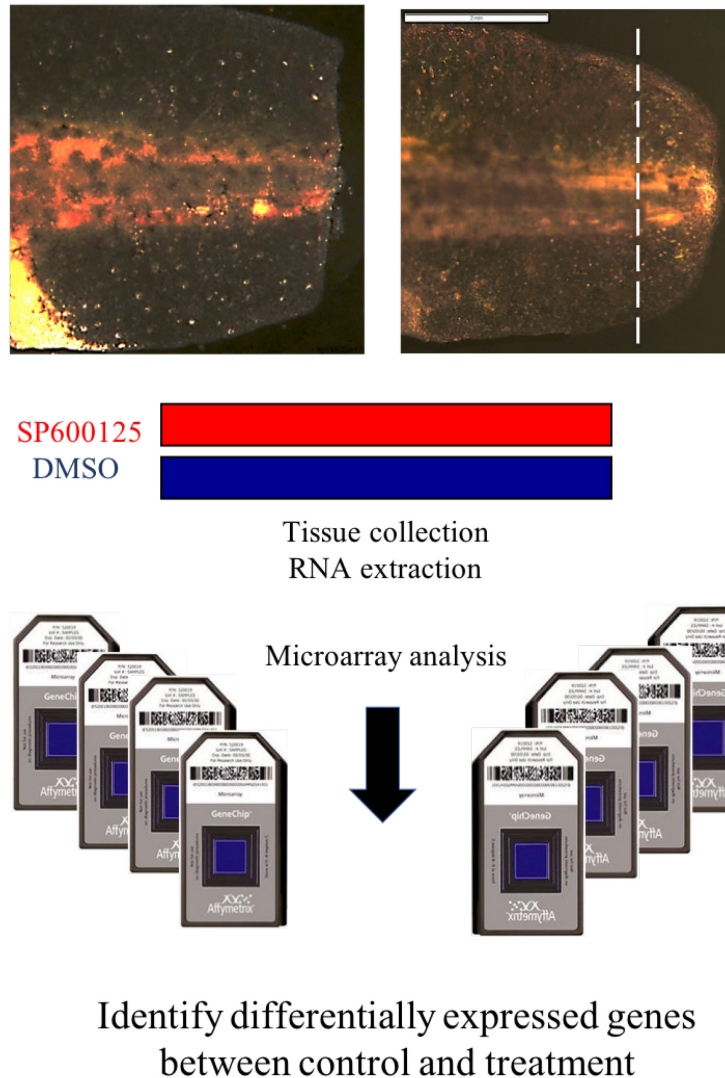


Figure 5. 2. Experimental design used to collect tissue for microarray analysis. A total of 96 embryos (N = 48 per group) embryos were treated with 5uM of SP600125 or DMSO at the time of amputation (0 dpa) till 1 dpa. At that time point, 1mm of distal tail tip tissue was collected and pooled from 5 embryos to form each biological replicate for RNA isolation. In total, four replicates per group were used for the microarray experiment.

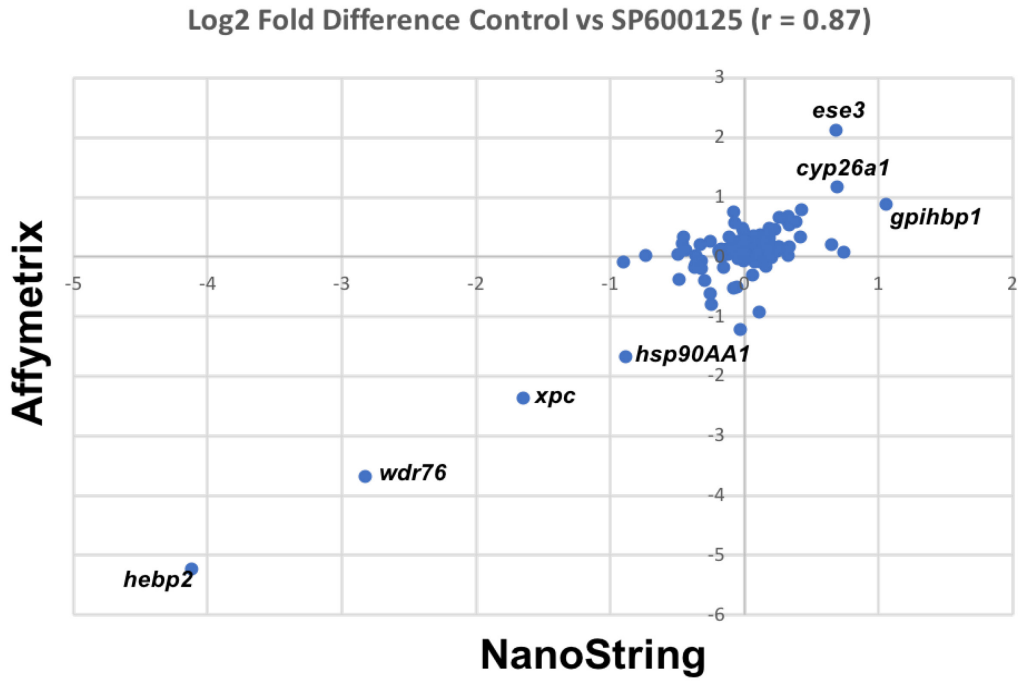


Figure 5. 3. Correlation of normalized log2 fold change estimates across gene platforms; ncounter Nanostring and Ambystoma Affymetrix. Pearson's correlation coefficients were calculated using fold change estimates for genes.

Chapter 6: Amputation-Induced ROS Signaling is Required for Axolotl Tail Regeneration

Nour W. Al Haj Baddar^{a,c}, Adarsh Chithrala^b, and S. Randal Voss^{c,d}

^aDepartment of Biology, University of Kentucky, Lexington, KY, 40506

^bPaul Laurence Dunbar High School, Lexington, KY 40513

^cDepartment of Neuroscience and Spinal Cord and Brain Injury Research Center (SCoBIRC), University of Kentucky, Lexington, KY 40536

^dAmbystoma Genetic Stock Center, University of Kentucky, Lexington, KY 40536

Previously published:

Al Haj Baddar, N. W., Chithrala, A. and Voss, S. R. (2019), Amputation-induced reactive oxygen species signaling is required for axolotl tail regeneration. *Dev. Dyn.*, 248: 189-196. doi:10.1002/dvdy.5

Grant sponsor: National Institutes of Health; Grant number: R24OD021479; Grant sponsor: the Ambystoma Genetic Stock Center at the University of Kentucky; Grant number: NIH P40OD019794.

6.1 Introduction

Urodele amphibians (i.e. salamanders) are unparalleled among vertebrates in their ability to regenerate appendages. Exactly how salamanders regenerate their limbs and tail largely remains a mystery. Many studies of salamander appendage regeneration have focused attention on the dynamics of progenitor cells that are recruited relatively late during the regeneration process (Mchedlishvili *et al.* 2007; Kragl *et al.* 2009). Earlier events that precede progenitor cell proliferation have received less attention. Several injury-associated cues affect the initiation of tissue regeneration in fish and frog tadpoles,

including ion gradients, reactive oxygen species (ROS), and hypoxia (Tseng and Levin 2012; Joplin *et al.* 2012; Love *et al.* 2013; Gauron *et al.* 2013; McLaughlin and Levin 2018). Whether these or other cues initiate appendage regeneration in highly regenerative urodeles is unknown.

ROS are chemically reactive oxygen-containing molecules generated endogenously by several cellular components, including mitochondria, lysosomes, and the plasma membrane (Di Meo *et al.* 2016). The reduction of molecular oxygen produces superoxide anion (O_2^-), a precursor of hydrogen peroxide (H_2O_2) and hydroxyl radicals (OH). ROS are well known components of metazoan innate immune responses and at moderate concentrations serve others roles in tissue injury, wound healing, cellular signaling, and gene expression (Weidinger and Kozlov, 2015). A growing number of studies highlight ROS in the regeneration of organs that span vertebrate and invertebrate taxa, thus implicating ROS as a phylogenetically conserved mechanism that initiates regeneration programs (Niethammer *et al.* 2009; Gauron *et al.* 2013; Love *et al.* 2013; Piorette *et al.* 2015; Hameed *et al.* 2015; Zhang *et al.* 2016). These and other studies (Yoo *et al.* 2012; Lisse *et al.* 2016) show that ROS recruit regeneration-permissive lymphocytes, induce mitogen signaling pathways required for progenitor cell proliferation, and modulate cell fate. Thus, ROS are not only produced to mitigate pathogens at wound sites, additionally, they provide injury cues to initiate regeneration programs. Still, because relatively few models and research paradigms have been investigated to date, there is need to further examine ROS signaling during regeneration. Here we report the requirement of ROS for appendage regeneration in the primary salamander model, *Ambystoma mexicanum* (axolotl).

6.2 Materials and Methods

6.2.1 Ethical procedures

The use of pre-feeding stage axolotls does not require a protocol approved by the Institutional Animal Care and Use Committee at University of Kentucky, however embryos used in this study were treated according to the same ethical standards that apply to feeding axolotls.

6.2.2 Regeneration assay

Mexican axolotl embryos (RRID: AGSC_100E) were obtained from the Ambystoma Genetic Stock Center (RRID: SCR_006372) at University of Kentucky. Stage 42 (Bordzilovskaya *et al.* 1989) embryos were used for all experiments reported in this paper. The embryos were manually hatched, administered benzocaine anesthesia (0.2 g in 10 ml ethanol / liter water) and photographed. Embryos with tail amputations were reared in artificial pond water (43.25 g NaCl, 0.625 g KCl, 1.25 g MgSO₄, 2.5 g NaHCO₃, and 1.25 g CaCl₂ per 50 liters RO water). In administering amputations, the distal most 2 mm of tail tissue was removed with a sterile razor blade. Whole embryo images were captured using an Olympus SZX16 microscope with a 0.5x objective lens and DP400 camera. Embryos were reared at 18-19 C in 12-well microtiter plates, one embryo per well. The effect of 4 μ M diphenyleneidonium chloride (DPI) on tail regeneration was assessed by measuring the distance between the distal tail tip and notochord, as the latter does not regenerate leaving a clear mark of the amputation plane. Experiments were performed three times; similar results were obtained and are combined for the analyses. Post amputation measurements were compared between chemically treated embryos (n = 15) and controls (n = 14) using Student's t-test, and P < 0.05 was considered statistically significant.

6.2.3 Histology and immunohistochemistry

Embryos were euthanized in benzocaine and fixed in 4% PFA overnight at 4 C°, washed three times with 1X PBS (pH=7.4) and cryopreserved in 30% sucrose overnight at 4 C°. Embryos were embedded in OCT and sectioned longitudinally at 10-15 µm. Tissue sections were mounted on slides and stained using hematoxylin and eosin (Fischer *et al.* 2008) or stored at -80 C° for immunohistochemistry.

For immunohistochemistry, slides were rehydrated with 1X PBS, incubated with blocking buffer (1X PBS with 5% Bovine serum albumin, 1% tween 20, and 0.3% Triton X-100) for one hour at room temperature. Slides were then incubated with mouse anti-phospho-Histone H3 (Ser10) antibody (1:1000, EMD Millipore # 05-1336-S) overnight at 4 C°. Slides were washed in 1X PBS and incubated with goat anti-mouse antibody (1:200, Thermo Fisher # A32723) for one hour at room temperature. Slides were incubated with DAPI (Thermo Fisher # 62248) in 1X PBS (1:25,000) for 20 minutes, washed in 1X PBS, and mounted with fluoroshield (Sigma-Aldrich # F6937).

6.2.4 *In vivo* ROS imaging

The detection of ROS during axolotl tail regeneration was performed by incubating embryos in 5 µM dihydroethidium (DHE) in darkness for two hours prior to imaging. Embryos were then washed to remove excessive stain, anesthetized in 0.02% benzocaine, and imaged using an SZX16 Olympus microscope with 2X objective lens and DP400 camera. Fluorescence quantification at the tail tip was measured as described by Jensen (2013) and Ozkucur *et al.* (2010) using ImageJ (Schneider *et al.* 2012). Briefly, an exact region of interest was drawn around the distal tail for each embryo image and the gray pixel intensity was measured and background-subtracted. The measurements were then averaged

for embryos (n = 6 -12 embryos per time point) and results were analyzed by one-way ANOVA followed by Tukey's post hoc analysis to compare all time points to pre-amputation levels. Fluorescence quantification of embryos treated with 5 μ M VAS2870 (n = 15) and controls (n = 15), and embryos treated with 4 μ M DPI (n = 15) and controls (n = 15) was performed as described above. All experiments were performed three times yielding similar results that were combined for statistical analysis.

The resulting data were analyzed using Student's t-test, and $P < 0.05$ was considered statistically significant.

6.2.5 Cellular proliferation assay

Cellular mitosis was measured using PH3 staining, where DPI-treated embryos and controls (n = 8 each) were fixed and processed as described above. Embryo tails were sectioned at 15- 20 μ m thickness and stained for PH3 as described above. For each embryo, 3 - 8 sections were analyzed to identify anatomically matching sections between control and treated embryos. For each section, all cells staining positive for PH3 within the distal 0.5 mm² of the amputation plane were counted as well as cells staining positive for DAPI (Franklin *et al.* 2017). A mitotic index was calculated by dividing the number of PH3 positive cells by the number of DAPI positive cells in a common area for each tissue section. Student's t-test was used to assess statistical significance $P < 0.05$ was considered significant. To further study the effect of DPI treatment on individual tissue types in the tail, we divided the number of PH3 positive cells within each of the following tissues (spinal cord, epidermis, and mesenchyme) by the number of cells found in the distal 0.5 mm². Student's t-test was used to assess statistical significance, $P < 0.05$ was considered statistically significant.

To assay for cell cycle reentry, we used EdU Click-iT[®] kit to detect DNA synthesis during S phase (Salic and Mitchison, 2008). Embryos at stage 42 were amputated and treated with either 4 μ M DPI (n = 15) or 0.04% DMSO (n = 12). Embryos were microinjected with 0.5 μ l of 8 mM EdU using a picospritzer at 2 dpa. Embryos were euthanized at 3 dpa and fixed in 4% PFA overnight. Embryos were washed three times in 1X PBS and dehydrated in a series of methanol concentrations (25%, 50%, 75%, 100%). Embryos were then rehydrated by running through the methanol concentrations backwards and incubated in 1X trypsin for 30 min at room temperature. The embryos were then washed in distilled water three times and placed in acetone for 10 minutes at -20 C[°] followed by washing in 1% PBST three times. EdU cocktail reaction was prepared per manufacturer kit with minor modification; 100 mM sodium ascorbate replaced Click-iT[®] EdU buffer additive at the same recommended volume per reaction. DAPI was used to counterstain nuclei. Embryos placed in EdU reaction solution were placed in the dark and gently rocked for 30 minutes followed by washing in 1X PBS prior to imaging.

Cell proliferation measurements were performed as described in (Franklin *et al.* 2017) with some modifications. We were interested in measuring cell proliferation within the regenerating tissue, distal to the amputation plane; these areas were used for quantification. All EdU labeled cells in regenerating tissue were counted as well as cells staining positive for DAPI, after normalizing for regenerate tissue area. Student's t-test was used to assess statistical significance and $P < 0.05$ was considered statistically significant.

6.3 Results and Discussion

6.3.1 Histology of axolotl embryo tail regeneration

Previously we showed that developmental stage 42 (Bordzilovskaya *et al.* 1989) axolotl embryos are capable of regenerating 2 mm of amputated, distal tail tip tissue in approximately 7 days (Ponomareva *et al.* 2015). To further advance this model and provide context for interpreting chemical perturbation of the regeneration process, we used H&E staining to detail histological changes during tail regeneration (Fig. 1). The tail amputation procedure removed the symmetrical, rounded tail tip, leaving a blunt tail stump (Fig. 1A, A'). In approximately 40 minutes post amputation (mpa), the open wound was covered by a thin epithelium (Fig. 1B, B'). By two-days post amputation (2 dpa), a few scattered erythrocytes and tissue debris were observed between the notochord and the wound epidermis (Fig. 1C, C'). Also at this time, mesenchymal tissue was observed between the wound epidermis and ependymal tube of the spinal cord, which had regenerated approximately 100 μ m beyond the amputation plane. By 5 dpa, the spinal cord had lengthened considerably into the mesenchyme of the regenerating tail (Fig. 1D, D'). Ventral to the outgrowing spinal cord and distal to the notochord was a nodule of cartilaginous tissue observed at 7 dpa (Fig. 1E) that by 12 dpa was an elongated rod comprised of chondrocyte-like cells (Fig. 1F). Overall, histological changes observed during axolotl embryo tail regeneration approximated changes previously described for adult salamanders (Globus and Liversage 1975; Iten and Bryant 1976).

6.3.2 Association of ROS with axolotl embryo tail regeneration

ROS production during tail regeneration was measured by dihydroethidium (DHE), a dye that permeates plasma membranes to report super oxide anion production (Owusu-Ansah *et al.* 2008). Upon reaction with superoxide anions, DHE forms a red fluorescent product (ethidium) that intercalates with DNA and subsequently becomes retained by cells.

After amputation of axolotl embryos, DHE staining revealed a marked increase of ROS production in midline, axial tissues (e.g. somites, spinal cord, notochord) of the tail (Fig. 2A). Elevated ROS levels remained high after wound closure and were sustained through 24 hours post amputation (hpa), but dropped to basal (unamputated) levels after that (Fig. 2B, C). This suggests that ROS production is associated with early wound healing events that precede cell proliferation and tail outgrowth.

6.3.3 NOX activity is required for amputation induced ROS production

NAPDH oxidases (NOX) generate the majority of ROS (O_2^- and H_2O_2) (Bedard and Krause 2007). These enzymes are phylogenetically conserved and expressed across many tissue types, and thus we used pharmacological inhibitors of NOX activity (diphenyleneidonium chloride - DPI and VAS2870) to test the requirement of ROS for tail regeneration. DHE staining of embryos treated with 5 μ M VAS2870 (Winger *et al.* 2012) showed a significant reduction in ROS production at 6 hpa, however embryos did not survive past 24 hpa. (Fig. 3). Lower, non-lethal doses of VAS2870 did not significantly lower ROS production or affect tail regeneration. Embryos treated with 4 μ M DPI (Bedard and Krause 2007) did not show a decrease in ROS production at 6 hpa, but levels were significantly lower at 24 hpa. Interestingly, while a 0-24 hpa DPI treatment decreased ROS levels, embryos successfully completed tail regeneration. This suggested a requirement for NOX activity after 24 hpa. To test this hypothesis, embryos were treated for progressively longer periods of time, extending the treatment window by 24 hr intervals. Embryos that were treated for 0-2 days successfully completed tail regeneration while individuals that were treated for longer than 3 days died. Only individuals that were treated for 0-3 dpa showed significant inhibition of tail and spinal cord regeneration at 7 dpa (Fig. 4A, B).

Because mesenchymal tissue did not form distal to the amputation plane in DPI-treated embryos, spinal cord regeneration was reduced and the underlying cartilaginous rod did not form (Fig. 4C). These results implicate NOX activity in amputation-induced ROS production and successful tail regeneration.

6.3.4 ROS as an early injury-induced signal and its role in cellular proliferation

ROS signaling is associated with the activation of cellular signaling pathways that regulate the proliferation of progenitor cells in planaria and frog tadpoles (Gauron *et al.* 2013; Love *et al.* 2013; Pirotte *et al.* 2015; Zhang *et al.* 2016). These findings prompted us to investigate the link between ROS production and cell proliferation during axolotl tail regeneration. The rate of distal tail outgrowth in the axolotl embryo model increases linearly between 12 and 72 hpa, and then after this time the rate increases more steeply (Ponamareva *et al.* 2015). Under the assumption that cell proliferation drives tail outgrowth, we quantified cell proliferation during the linear phase of tail outgrowth at 2 dpa. Embryos were treated with 4 μ M DPI from 0-2 dpa and the number of mitotic, phospho-Histone H3 (PH3) positive cells in the tail stump were quantified relative to untreated, control embryos (Fig. 5). Overall, relatively few mitotic cells were observed and their distribution was not localized within any particular tissue compartment. However, the number of PH3-positive cells was significantly higher in control embryos (Fig. 5A, B). Further, we found that DPI treatment significantly reduced mitosis in the spinal cord (SC) and the epidermis (EP) but not in the mesenchyme (Mes) (Fig. 5C, D). These results suggest that NOX activity affects cell mitosis in the spinal cord and the epidermis of the axolotl tail.

To further test the idea that NOX activity is required for cell proliferation, we tested DPI for an effect on cell cycle re-entry (S- phase). Embryos were treated continuously with 4 μ M DPI, microinjected with EdU at 2 dpa, and then tissue was collected at 3 dpa for quantification of Edu positive cells (Fig. 6A). EdU indices showed that cell proliferation was significantly reduced in DPI-treated embryos (Fig. 6B, C) relative to controls, which showed strong incorporation of EdU in regenerating spinal cord and tail fin (Fig. 6B, top panel). Though the area of regenerating tissue in control embryos was significantly greater than that of DPI-treated embryos at 3 dpa, EdU incorporation were still significantly greater in control embryos after normalizing for tissue area. While the regenerating tails of control embryos exhibited strong EdU incorporation in the regenerating spinal cord and the mesenchyme, DPI treated embryos failed to regenerate spinal cord and had few EdU positive cells located within the tail fin (mesenchyme) (Fig. 6C). These results are similar to the data shown in (Fig. 5) which supports the idea that NOX activity and ROS signaling are required for cell cycle reentry and the proliferation response that drives regenerate outgrowth, especially in the spinal cord.

In the context of tissue damage or injury, ROS can modulate injury-induced gene expression responses and regulate proteins involved in wound signaling and regeneration (Enyedi and Niethammer, 2015; Neithammer 2016; Lessi *et al.* 2016). Our results show that ROS signaling and NOX activity are required for axolotl spinal cord and tail regeneration. Although nothing is known about the regulatory targets of ROS signaling during axolotl tissue regeneration, studies of zebrafish and *Xenopus* suggest ROS may target essential mitogens, such as sonic hedgehog (SHH) and bone morphogenetic protein (BMP), which are required for proper cellular proliferation and blastema formation during

axolotl tail regeneration (Stoick-Cooper *et al.* 2007; Schnapp *et al.* 2005). Recently, SHH was identified as a redox target during zebrafish fin regeneration in a study that examined ROS signaling during axon regeneration and cellular proliferation (Meda *et al.* 2016; Meda *et al.* 2017). Also, *fgf20*, one of the direct targets of Wnt/ β -catenin signaling, is downregulated along with cell proliferation, when NOX-derived ROS production is inhibited during tadpole *Xenopus* tail regeneration (Love *et al.* 2013). Interestingly, Wnt signaling is essential for successful axolotl embryo tail regeneration and *Fgf9* is one of the transcriptional targets that is downregulated upon Wnt inhibition (Ponomareva *et al.* 2015). This implicates Wnt signaling as a potential candidate redox target of NOX activity and ROS production. Future studies will determine if these and other signaling pathways are regulated by ROS in the axolotl tail regeneration model.

6.4 Conclusions

Urodele amphibians are exceptional in regards to regenerating complex organs and tissues. Our results are consistent with findings from studies of planaria (Pirrotte *et al.* 2015), zebrafish fin (Gaouron *et al.* 2013), *Xenopus* tail (Love *et al.* 2013), and newt adult brain (Hameed *et al.* 2015); clearly ROS are required for successful tissue / appendage regeneration. We show that ROS are produced shortly after amputation in axial tissues and their production is sustained during the first 24 hpa. We also found that ROS signaling influences cellular proliferation during the early phase of tail regeneration. Our study is the first to show the requirement of NOX activity and ROS regulation for urodele appendage regeneration, and given similar findings in other metazoan taxa, suggest that ROS is a phylogenetically conserved mechanism of tissue regeneration.

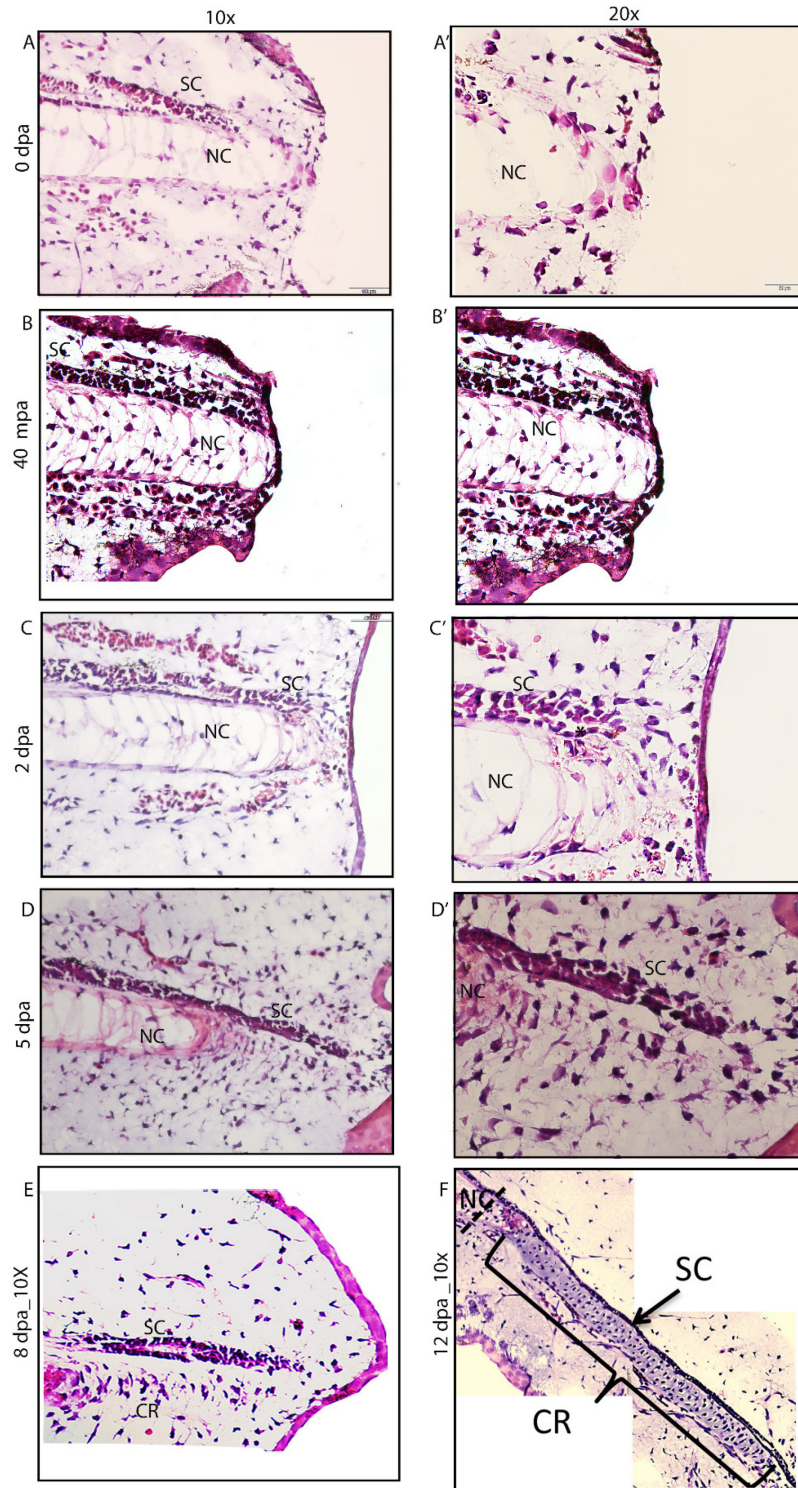


Figure 6.1. H&E stained longitudinal sections of axolotl embryo tail regeneration. A and A') At 0 dpa the wound is open at the site of amputation. B and B') A thin epithelial layers covers the amputation plane at 40 mpa. C and C') At 2 dpa, the wound is sealed and the terminal vesicle of the spinal cord is formed dorsal to the notochord (C': star). D

Figure 6.1 (Continued)

(and D') The regenerating spinal cord elongates within the regenerating mesenchyme of the tail. E) A cartilaginous rod forms ventral to the regenerating spinal cord (CR). F) At 12 dpa, the CR is comprised of chondrocyte-like cells. The black dotted line represents the plane of amputation. Scale bar = 100 μ m (10x) and 50 μ m (20x). SC: spinal cord, NC: notochord, CR: cartilaginous rod.

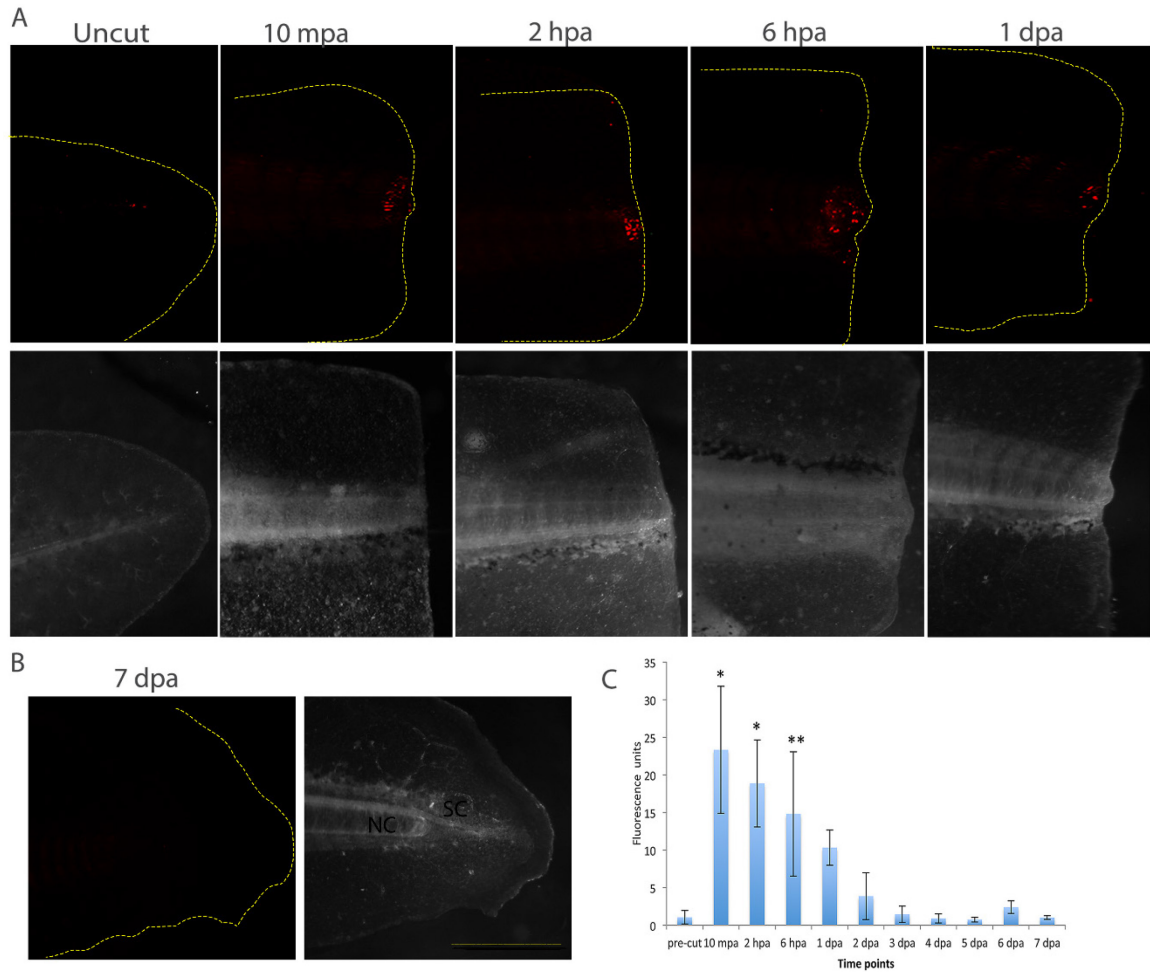


Figure 6.2. Association of ROS production with axolotl embryo tail regeneration. A) *In vivo* imaging of ROS production revealed by DHE staining over the course of 7 dpa. Top panels show fluorescent images while the bottom panels show the tail in grayscale at the representative time points. The DHE signal was observed by 10 minutes post amputation (mpa) in the medial part of the tail before returning to basal levels at 2-7 dpa (scale bar = 1 mm, n = 6 - 12 embryos per time point). B) A representative image of a tail at 7 dpa stained with DE (left) and grayscale (right). C) Quantitative analysis of ROS produced throughout the course of regeneration. Error bars represent standard deviations of the mean; n = 6 - 12 embryos per time point; * P < 0.01, ** P < 0.05). NC: notochord, SC: spinal cord⁸⁷

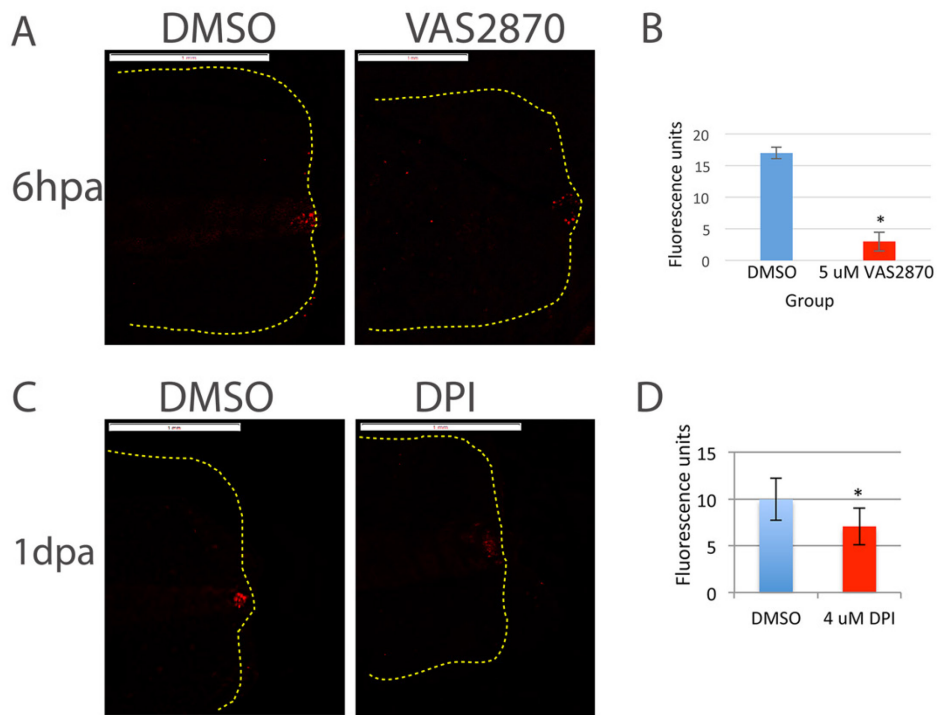


Figure 6.3. DPI and VAS2870 reduced ROS production during tail regeneration. A) Effect of 5 mM VAS2870 (n = 15) on amputation induced ROS at 6 hpa compared to controls (n = 15); scale bar = 1mm. B) Quantitative analysis of data shown in A; error bars represent standard deviations of the mean (*P < 0.05). C) Effect of 4 mM DPI (n = 15) on amputation induced ROS at 24 hpa compared to controls (n = 15), scale bar = 1 mm. D) Quantitative analysis of data shown in C; error bars represent standard deviations of the mean (*P < 0.05).

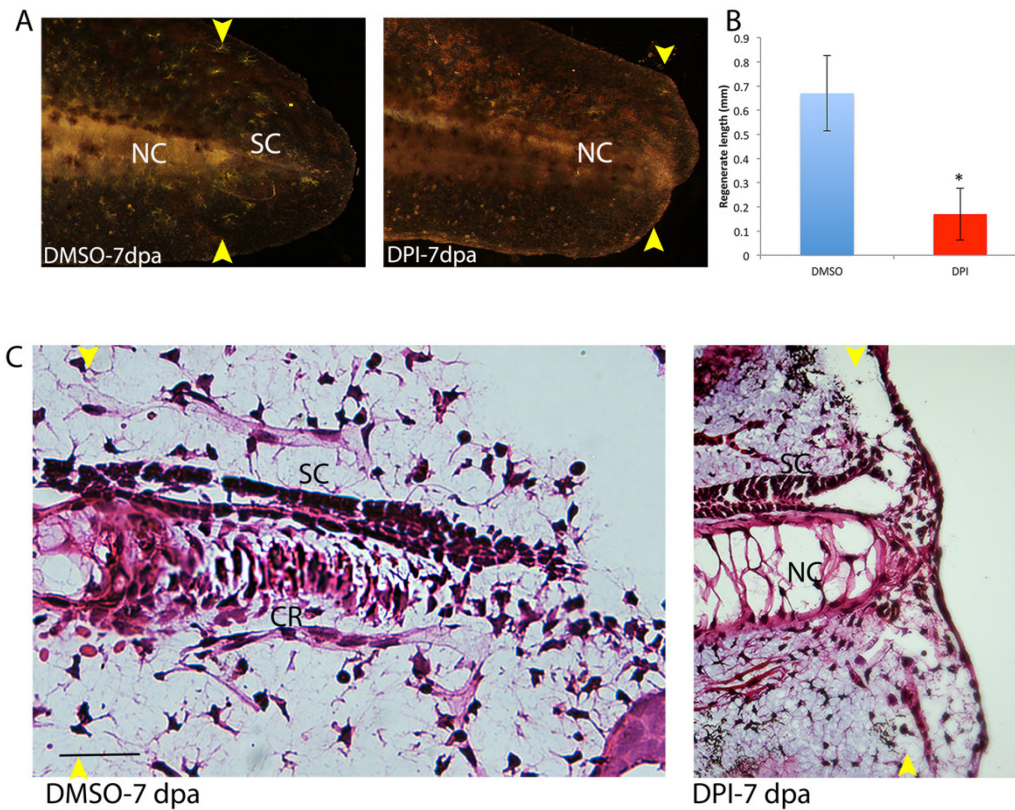


Figure 6.4. Treatment with 4 μm DPI (NOX inhibitor) significantly inhibits axolotl embryo tail regeneration. A) Representative images of the axolotl tail at 7 dpa for control embryos (left) and DPI-treated embryos (right). The yellow arrowheads represent the plane of amputation, scale bar = 1 mm. B) Quantitation of the length of tail regeneration between controls ($n = 14$) and DPI-treated embryos ($n = 15$) at 7 dpa. Error bars represent standard deviations of the mean (* $P < 0.01$). C and D) H&E staining of control (C) and DPI-treated embryos (D) at 7 dpa. The dashed lines represent the plane of amputation, SC: spinal cord, CR: cartilaginous rod, scale bar = 50 μm . In DPI-treated embryos, spinal cord regeneration was reduced and the cartilaginous rod did not form.

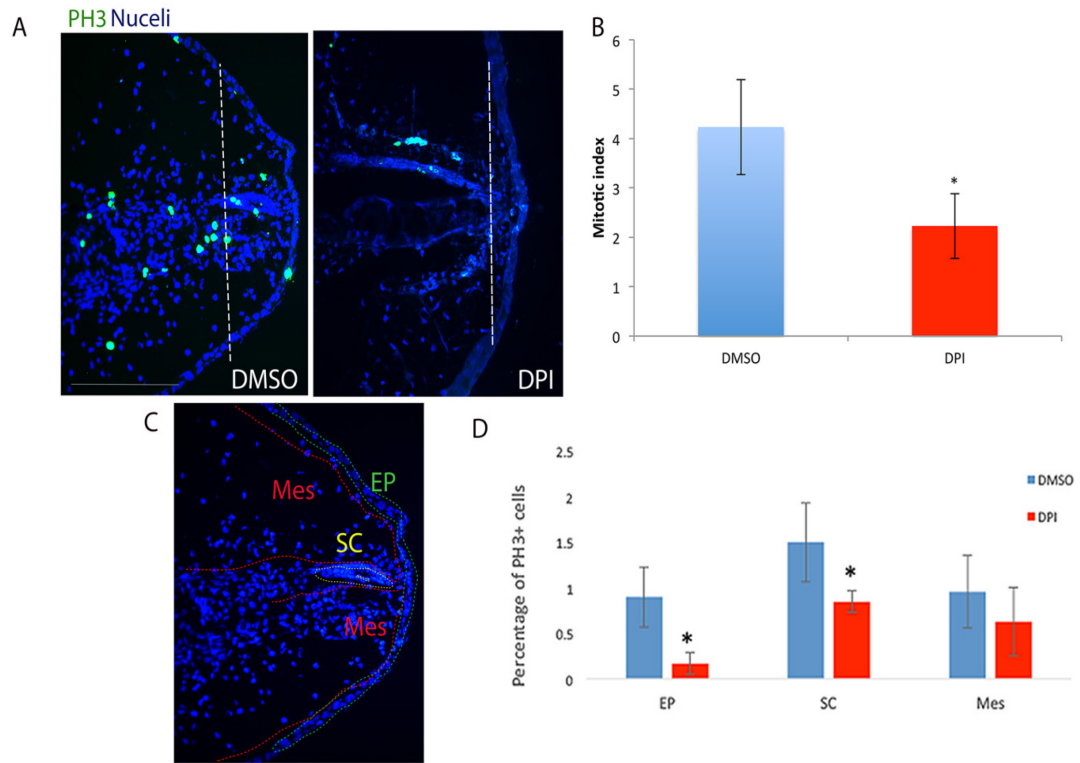


Figure 6.5 ROS signaling is important for mitosis during axolotl embryo tail regeneration. A) Treatment of embryos with 4 mM DPI (n = 8) significantly decreased the number of PH3 positive cells at 2 dpa compared to control embryos (n = 8), white dashed lines show the plane of amputation. B) Quantification of PH3 positive cells. Error bars represent standard deviations of the mean (* P < 0.05). C) ASC: spinal cord, scale bar = 500 mm. C) Colored dashed lines representing (SC: spinal cord), (Ep: epidermis), (Mes: mesenchyme) drawn on embryo tail section to outline the individual tissue types for the analysis shown in D. D) Quantitative analysis showing the effect of DPI treatment on the number of PH3 positive cells in the epidermis, spinal cord, and mesenchyme. Error bars represent standard deviations of the mean (* P < 0.05).

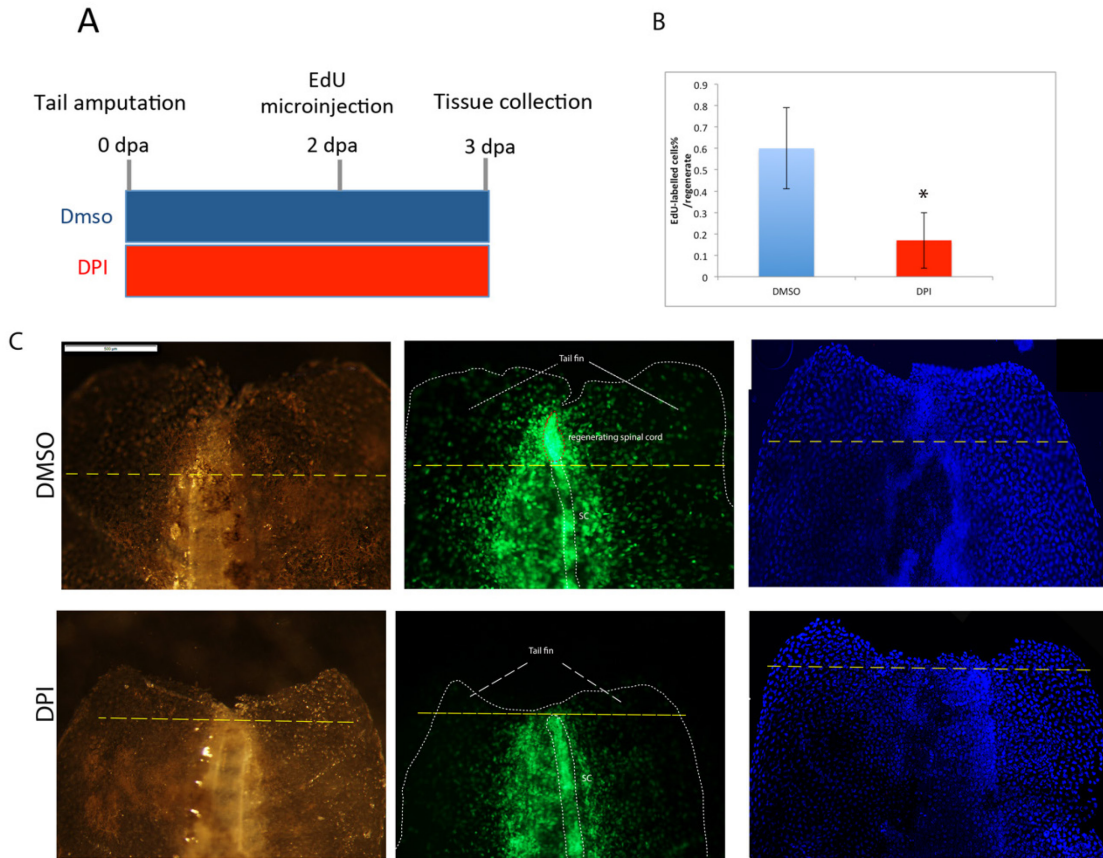


Figure 6.6 ROS signaling is required for DNA synthesis and cell cycle re-entry during axolotl tail regeneration. A) Sketch representing the experimental design of the experiment. B) EdU quantification results for control (n = 12) and DPI-treated (n = 15) embryos. Error bars represent standard deviations of the mean (* P < 0.05). C) Representative images of EdU labeled tails of DMSO embryos (top panel) and DPI- treated embryos (Bottom panel) at 3 dpa. SC: spinal cord. Scale bar = 500 mm.

CHAPTER 7: CONCLUSIONS AND FUTURE DIRECTIONS

There is growing evidence that the extraordinary ability of salamanders to regenerate whole organs depends in part upon salamander-specific genes not found in non-regenerative vertebrates (Zhao et al., 2016; Slack et al., 2017). Novel genes are known to emerge via different mechanisms, however the most prominent mechanism is gene duplication. Gene duplication provides new genetic material for evolution to modulate existing functions or creating new ones (Force et al., 1999). This dissertation describes results from a set of bioinformatic analyses that utilized salamander and vertebrate DNA/Protein databases to identify novel, paralogous genes that arose by gene duplication. The novel genes that were discovered likely encode proteins that have essential functions during tissue regeneration. As a result of my studies, a relatively large list of novel genes is now available to test this hypothesis in salamanders.

While bioinformatic analyses identified many interesting examples of gene duplication, I was very interested to examine *mmp* lineage-specific paralogs in more detail. MMPs are generally highly expressed during regeneration because they are needed to histolyze damaged tissues and modify the ECM to make the injury site permissive for regeneration. MMPs perform similar functions during wound healing in mammals but the process is associated with the formation of scar tissue. In contrast, axolotls heal scar-free. This potentially suggests that MMPs may function differently between mammals and salamanders. In Chapter 4, I performed bioinformatic and phylogenetic analyses to identify 24 MMP family members in the axolotl. I also showed that duplicated collagenases and stromelysins in the axolotl have orthologs in other salamanders but not in other

vertebrates. MMP duplications that evolved uniquely within salamanders may be associated with a mode of tissue histolysis and wound healing that is permissive for regeneration. Functional studies of MMP structural variations observed in salamanders may reveal strategies to modulate their activity in humans to promote scar-free healing.

While the ability to regenerate whole organs varies greatly among vertebrates, regeneration is regulated by highly conserved signaling pathways that all vertebrates share. This suggests that small but important differences in signal transduction cascades may underlie differences in regenerative ability. The discovery of two *jnk1/mapk8* paralogs supports this idea because duplication of *mapk8* might allow phosphorylation and activation of new target proteins, many of which are known to be transcription factors. It will be important to perform and assess the phenotypic effect of CRISPR gene knockouts of these *jnk1/mapk8* paralogs, and identify their gene targets. Chapter 5 reported global gene expression changes following JNK signaling inhibition during axolotl tail regeneration. The genes that were differentially expressed suggested that JNK signaling is essential for wound healing, response to cellular stress, immune response, and muscle remodeling; all of these processes are essential for providing a regeneration-permissive environment that facilitates dedifferentiation and blastema formation. Among the results obtained, was a surprising upregulation of core clock genes (*arntl*, *cry1*, *cry2*, *csnk1d*, *csnk1e*). Might there be a role for the circadian clock in tissue regeneration? Overall, the genes identified in this study provide novel insights and new targets for future studies of tissue regeneration.

Genes associated with ROS production (like *nox2*, *mpo*, *c9*) were down regulated in response to JNK inhibition. This motivated me to investigate ROS and determine if NOX

activity is required for regeneration (Chapter 6, Al Haj Baddar et al., 2019). Using superoxide anion dye (DHE, dihydroethidium), I found that ROS were produced at the injury site immediately after amputation and were sustained throughout the first day of tail regeneration. During the wound healing period between 0-1 dpa, phagocytic cells infiltrate the local injury site to remove tissue debris and elicit immune responses against pathogens (Chapter 5; Franklin et al., 2017; Godwin et al., 2013; Godwin et al., 2017). I pharmacologically inhibited NOX protein activity and ROS production by DPI and found that it inhibited tail regeneration; within the tail it inhibited cell proliferation and mitosis, especially in the spinal cord. Our results clearly show a NOX activity requirement (and presumably an early ROS requirement) for epimorphic regeneration that agrees with work performed in tadpole frogs and zebrafish (Love et al., 2013; Gauron et al., 2013). This suggests that ROS provides an essential cue to coordinate damage responses and instruct regeneration programs.

It is important to note that I developed several new assays for the axolotl embryo model during my dissertation research. In addition to optimizing dosage for the chemicals I used, I optimized methods for histology and generated the first anatomical images and descriptions for the axolotl embryo regeneration model (Chapter 6, Al Haj Baddar et al., 2019). I also optimized methods to determine the timing of wound closure and quantify cell proliferation (Chapter 6, Al Haj Baddar et al., 2019; Voss et al., 2019). As I continue my studies of axolotl regeneration into the future, I hope to develop reliable and efficient assays for additional biological processes, including apoptosis, necrosis, and senescence. In summary, I hope that my results will guide future work to help reveal mechanisms of tissue regeneration in the axolotl that can help promote regeneration in humans.

References

- Abdullayev, I., Kirkham, M., Bjorklund, A.K., Simon, A., Sandberg, R., 2013. A reference transcriptome and inferred proteome for the salamander *Notophthalmus viridescens*. *Exp Cell Res* 319, 1187-1197.
- Abu-Abed, S., Dolle, P., Metzger, D., Beckett, B., Chambon, P., Petkovich, M., 2001. The retinoic acid-metabolizing enzyme, CYP26A1, is essential for normal hindbrain patterning, vertebral identity, and development of posterior structures. *Genes & development* 15, 226-240.
- Al Haj Baddar, N.W., Chithrala, A., Voss, S.R., 2019. Amputation-induced reactive oxygen species signaling is required for axolotl tail regeneration. *Dev Dyn* 248, 189-196.
- Altschul, S.F., Gish, W., Miller, W., Myers, E.W., Lipman, D.J., 1990. Basic local alignment search tool. *J Mol Biol* 215, 403-410.
- Arenas Gomez, C.M., Woodcock, R.M., Smith, J.J., Voss, R.S., Delgado, J.P., 2018. Using transcriptomics to enable a plethodontid salamander (*Bolitoglossa ramosi*) for limb regeneration research. *BMC Genomics* 19, 704.
- Arikan, G.D., Isbir, S., Yilmaz, S.G., Isbir, T., 2019. Characteristics of Coronary Artery Disease Patients Who Have a Polymorphism in the Cholesterol Ester Transfer Protein (CETP) Gene. *In vivo (Athens, Greece)* 33, 787-792.
- Baddar, N.W., Woodcock, M.R., Khatri, S., Kump, D.K., Voss, S.R., 2015. Sal-Site: research resources for the Mexican axolotl. *Methods in molecular biology (Clifton, N.J.)* 1290, 321-336.
- Beck, C.W., Izpisua Belmonte, J.C., Christen, B., 2009. Beyond early development: *Xenopus* as an emerging model for the study of regenerative mechanisms. *Dev Dyn* 238, 1226-1248.
- Bedard K, Krause KH. 2007. The NOX family of ROS-generating NADPH oxidases: physiology and pathophysiology. *Physiological Reviews* 87:245-313.
- Bellayr, I.H., Mu, X., Li, Y., 2009. Biochemical insights into the role of matrix metalloproteinases in regeneration: challenges and recent developments. *Future medicinal chemistry* 1, 1095-1111.
- Bennett, B.L., Sasaki, D.T., Murray, B.W., O'Leary, E.C., Sakata, S.T., Xu, W., Leisten, J.C., Motiwala, A., Pierce, S., Satoh, Y., Bhagwat, S.S., Manning, A.M., Anderson, D.W., 2001. SP600125, an anthrapyrazolone inhibitor of Jun N-terminal kinase. *Proc Natl Acad Sci USA* 98, 13681-13686.

Bjursell, M., Ahnmark, A., Bohlooly, Y.M., William-Olsson, L., Rhedin, M., Peng, X.R., Ploj, K., Gerdin, A.K., Arnerup, G., Elmgren, A., Berg, A.L., Oscarsson, J., Linden, D., 2007. Opposing effects of adiponectin receptors 1 and 2 on energy metabolism. *Diabetes* 56, 583-593.

Blassberg, R.A., Garza-Garcia, A., Janmohamed, A., Gates, P.B., Brockes, J.P., 2011. Functional convergence of signalling by GPI-anchored and anchorless forms of a salamander protein implicated in limb regeneration. *Journal of cell science* 124, 47-56.

Bordzilovskaya NP, Dettlaff TA, Duhon ST, Malacinski GM. 1989. Developmental stage series of axolotl embryos, *Developmental Biology of the Axolotl*, Armstrong JB and Malacinski GM, Editors. Oxford University Press: New York pp. 201-219.

Bryant, D.M., Johnson, K., DiTommaso, T., Tickle, T., Couger, M.B., Payzin-Dogru, D., Lee, T.J., Leigh, N.D., Kuo, T.H., Davis, F.G., Bateman, J., Bryant, S., Guzikowski, A.R., Tsai, S.L., Coyne, S., Ye, W.W., Freeman, R.M., Jr., Peshkin, L., Tabin, C.J., Regev, A., Haas, B.J., Whited, J.L., 2017. A Tissue-Mapped Axolotl De Novo Transcriptome Enables Identification of Limb Regeneration Factors. *Cell Rep* 18, 762-776.

Caldon, C.E., Musgrove, E.A., 2010. Distinct and redundant functions of cyclin E1 and cyclin E2 in development and cancer. *Cell division* 5, 2.

Calve, S., Odelberg, S.J., Simon, H.G., 2010. A transitional extracellular matrix instructs cell behavior during muscle regeneration. *Dev Biol* 344, 259-271.

Casco-Robles, R.M., Watanabe, A., Eto, K., Takeshima, K., Obata, S., Kinoshita, T., Ariizumi, T., Nakatani, K., Nakada, T., Tsonis, P.A., Casco-Robles, M.M., Sakurai, K., Yahata, K., Maruo, F., Toyama, F., Chiba, C., 2018. Novel erythrocyte clumps revealed by an orphan gene *Newtic1* in circulating blood and regenerating limbs of the adult newt. *Sci Rep* 8, 7455.

Ceci, M., Mariano, V., Romano, N., 2018. Zebrafish as a translational regeneration model to study the activation of neural stem cells and role of their environment. *Reviews in the neurosciences* 30, 45-66.

Che, R., Sun, Y., Wang, R., Xu, T., 2014. Transcriptomic analysis of endangered Chinese salamander: identification of immune, sex and reproduction-related genes and genetic markers. *PloS one* 9, e87940.

Chernoff, E.A., O'Hara, C.M., Bauerle, D., Bowling, M., 2000. Matrix metalloproteinase production in regenerating axolotl spinal cord. *Wound Repair Regen* 8, 282-291.

Choi, K.S., Choi, H.J., Lee, J.K., Im, S., Zhang, H., Jeong, Y., Park, J.A., Lee, I.K., Kim, Y.M., Kwon, Y.G., 2016. The endothelial E3 ligase HECW2 promotes endothelial

cell junctions by increasing AMOTL1 protein stability via K63-linked ubiquitination. *Cellular signaling* 28, 1642-1651.

Chrystal, P.W. The role of jnk1 during zebrafish development. 2015. Newcastle University. <http://theses.ncl.ac.uk/jspui/handle/10443/3035>.

Church, D.M., Goodstadt, L., Hillier, L.W., Zody, M.C., Goldstein, S., She, X., Bult, C.J., Agarwala, R., Cherry, J.L., DiCuccio, M., Hlavina, W., Kapustin, Y., Meric, P., Maglott, D., Birtle, Z., Marques, A.C., Graves, T., Zhou, S., Teague, B., Potamouisis, K., Churas, C., Place, M., Herschleb, J., Runnheim, R., Forrest, D., Amos-Landgraf, J., Schwartz, D.C., Cheng, Z., Lindblad-Toh, K., Eichler, E.E., Ponting, C.P., Mouse Genome Sequencing, C., 2009. Lineage-specific biology revealed by a finished genome assembly of the mouse. *PLoS Biol* 7, e1000112.

da Silva, S.M., Gates, P.B., Brockes, J.P., 2002. The newt ortholog of CD59 is implicated in proximodistal identity during amphibian limb regeneration. *Developmental cell* 3, 547-555.

Darriba, D., Taboada, G.L., Doallo, R., Posada, D., 2012. jModelTest 2: more models, new heuristics and parallel computing. *Nat Methods* 9, 772.

Davis, R.J., 2000. Signal transduction by the JNK group of MAP kinases. *Cell* 103, 239-252.

Davoine, F., Lacy, P., 2014. Eosinophil cytokines, chemokines, and growth factors: emerging roles in immunity. *Front Immunol* 5, 570.

Denis, J.F., Levesque, M., Tran, S.D., Camarda, A.J., Roy, S., 2013. Axolotl as a Model to Study Scarless Wound Healing in Vertebrates: Role of the Transforming Growth Factor Beta Signaling Pathway. *Advances in wound care* 2, 250-260.

Di Meo, S., Reed, T.T., Venditti, P., Victor, V.M., 2016. Role of ROS and RNS Sources in Physiological and Pathological Conditions. *Oxid Med Cell Longev* 2016, 1245049.

Ding, R., Jin, S., Pabon, K., Scotto, K.W., 2016. A role for ABCG2 beyond drug transport: Regulation of autophagy. *Autophagy* 12, 737-751.

Dixon, J.E., Allegrucci, C., Redwood, C., Kump, K., Bian, Y., Chatfield, J., Chen, Y.H., Sottile, V., Voss, S.R., Alberio, R., Johnson, A.D., 2010. Axolotl Nanog activity in mouse embryonic stem cells demonstrates that ground state pluripotency is conserved from urodele amphibians to mammals. *Development* 137, 2973-2980.

Dong, C., Davis, R.J., Flavell, R.A., 2002. MAP kinases in the immune response. *Annu Rev Immunol* 20, 55-72.

Dresden, M.H., Gross, J., 1970. The collagenolytic enzyme of the regenerating limb of the Newt *triturus viridescens*. *Dev Biol* 22, 129-137.

- Dwaraka, V.B., Smith, J.J., Woodcock, M.R., Voss, S.R., 2018. Comparative transcriptomics of limb regeneration: Identification of conserved expression changes among three species of *Ambystoma*. *Genomics*.
- Echeverri, K., Tanaka, E.M., 2005. Proximodistal patterning during limb regeneration. *Dev Biol* 279, 391-401.
- Eckert, M.A., Coscia, F., Chryplewicz, A., Chang, J.W., Hernandez, K.M., Pan, S., Tienda, S.M., Nahotko, D.A., Li, G., Blazenovic, I., Lastra, R.R., Curtis, M., Yamada, S.D., Perets, R., McGregor, S.M., Andrade, J., Fiehn, O., Moellering, R.E., Mann, M., Lengyel, E., 2019. Proteomics reveals NNMT as a master metabolic regulator of cancer-associated fibroblasts. *Nature* 569, 723-728.
- Elewa, A., Wang, H., Talavera-Lopez, C., Joven, A., Brito, G., Kumar, A., Hameed, L.S., Penrad-Mobayed, M., Yao, Z., Zamani, N., Abbas, Y., Abdullayev, I., Sandberg, R., Grabherr, M., Andersson, B., Simon, A., 2017. Reading and editing the *Pleurodeles waltl* genome reveals novel features of tetrapod regeneration. *Nature communications* 8, 2286.
- Enyedi, B., Niethammer, P., 2015. Mechanisms of epithelial wound detection. *Trends Cell Biol* 25, 398-407.
- Fasciglione, G.F., Gioia, M., Tsukada, H., Liang, J., Iundusi, R., Tarantino, U., Coletta, M., Pourmotabbed, T., Marini, S., 2012. The collagenolytic action of MMP-1 is regulated by the interaction between the catalytic domain and the hinge region. *Journal of biological inorganic chemistry: JBIC: a publication of the Society of Biological Inorganic Chemistry* 17, 663-672.
- Fischer, A.H., Jacobson, K.A., Rose, J., Zeller, R., 2008. Hematoxylin and eosin staining of tissue and cell sections. *CSH Protoc* 2008, pdb prot4986.
- Force, A., Lynch, M., Pickett, F.B., Amores, A., Yan, Y.L., Postlethwait, J., 1999. Preservation of duplicate genes by complementary, degenerative mutations. *Genetics* 151, 1531-1545.
- Franklin, B.M., Voss, S.R., Osborn, J.L., 2017. Ion channel signaling influences cellular proliferation and phagocyte activity during axolotl tail regeneration. *Mech Dev* 146, 42-54.
- Gardiner, D.M., Blumberg, B., Komine, Y., Bryant, S.V., 1995. Regulation of *HoxA* expression in developing and regenerating axolotl limbs. *Development* 121, 1731-1741.
- Garza-Garcia, A., Harris, R., Esposito, D., Gates, P.B., Driscoll, P.C., 2009. Solution Structure and Phylogenetics of *Prod1*, a Member of the Three-Finger Protein Superfamily Implicated in Salamander Limb Regeneration. *PloS one* 4, e7123.

- Garza-Garcia, A.A., Driscoll, P.C., Brockes, J.P., 2010. Evidence for the local evolution of mechanisms underlying limb regeneration in salamanders. *Integr Comp Biol* 50, 528-535.
- Gauron, C., Rampon, C., Bouzaffour, M., Ipendey, E., Teillon, J., Volovitch, M., Vríz, S., 2013. Sustained production of ROS triggers compensatory proliferation and is required for regeneration to proceed. *Sci Rep* 3, 2084.
- Gemberling, M., Bailey, T.J., Hyde, D.R., Poss, K.D., 2013. The zebrafish as a model for complex tissue regeneration. *Trends in genetics: TIG* 29, 611-620.
- Geng, J., Gates, P.B., Kumar, A., Guenther, S., Garza-Garcia, A., Kuenne, C., Zhang, P., Looso, M., Brockes, J.P., 2015. Identification of the orphan gene *Prod 1* in basal and other salamander families. *Evodevo* 6, 9.
- Globus, M., Livsavage, R., 1975. Differentiation in vitro of innervated tail regenerates in larval *Ambystoma*. *J Embryol Exp Morphol* 33, 803-812.
- Godwin, J.W., Pinto, A.R., Rosenthal, N.A., 2013. Macrophages are required for adult salamander limb regeneration. *Proc Natl Acad Sci U S A* 110, 9415-9420.
- Goldsmith, C.S., Bell-Pedersen, D., 2013. Diverse roles for MAPK signaling in circadian clocks. *Adv Genet* 84, 1-39.
- Greer, J.M., Puetz, J., Thomas, K.R., Capecchi, M.R., 2000. Maintenance of functional equivalence during paralogous Hox gene evolution. *Nature* 403, 661-665.
- Grillo, H.C., Lapiere, C.M., Dresden, M.H., Gross, J., 1968. Collagenolytic activity in regenerating forelimbs of the adult newt (*Triturus viridescens*). *Dev Biol* 17, 571-583.
- Haas, B.J., Papanicolaou, A., Yassour, M., Grabherr, M., Blood, P.D., Bowden, J., Couger, M.B., Eccles, D., Li, B., Lieber, M., MacManes, M.D., Ott, M., Orvis, J., Pochet, N., Strozzi, F., Weeks, N., Westerman, R., William, T., Dewey, C.N., Henschel, R., LeDuc, R.D., Friedman, N., Regev, A., 2013. De novo transcript sequence reconstruction from RNA-seq using the Trinity platform for reference generation and analysis. *Nat Protoc* 8, 1494-1512.
- Hahn, C., Orr, A.W., Sanders, J.M., Jhaveri, K.A., Schwartz, M.A., 2009. The subendothelial extracellular matrix modulates JNK activation by flow. *Circ Res* 104, 995-1003.
- Hameed, L.S., Berg, D.A., Belnoue, L., Jensen, L.D., Cao, Y., Simon, A., 2015. Environmental changes in oxygen tension reveal ROS-dependent neurogenesis and regeneration in the adult newt brain. *Elife* 4.

Hasegawa, T., Hall, C.J., Crosier, P.S., Abe, G., Kawakami, K., Kudo, A., Kawakami, A., 2017. Transient inflammatory response mediated by interleukin-1beta is required for proper regeneration in zebrafish fin fold. *Elife* 6.

He, Y., Cai, C., Sun, S., Wang, X., Li, W., Li, H., 2016. Effect of JNK inhibitor SP600125 on hair cell regeneration in zebrafish (*Danio rerio*) larvae. *Oncotarget* 7, 51640-51650.

Huggins, C.J., Malik, R., Lee, S., Salotti, J., Thomas, S., Martin, N., Quinones, O.A., Alvord, W.G., Olanich, M.E., Keller, J.R., Johnson, P.F., 2013. C/EBPgamma suppresses senescence and inflammatory gene expression by heterodimerizing with C/EBPbeta. *Mol Cell Biol* 33, 3242-3258.

Huggins, P., Johnson, C.K., Schoergendorfer, A., Putta, S., Bathke, A.C., Stromberg, A.J., Voss, S.R., 2012. Identification of differentially expressed thyroid hormone responsive genes from the brain of the Mexican Axolotl (*Ambystoma mexicanum*). *Comp Biochem Physiol C Toxicol Pharmacol* 155, 128-135.

Hurles, M., 2004. Gene duplication: the genomic trade in spare parts. *PLoS Biol* 2, E206.

Huxley-Jones, J., Clarke, T.K., Beck, C., Toubaris, G., Robertson, D.L., Boot-Handford, R.P., 2007. The evolution of the vertebrate metzincins; insights from *Ciona intestinalis* and *Danio rerio*. *BMC Evol Biol* 7, 63.

Irizarry, R.A., Hobbs, B., Collin, F., Beazer-Barclay, Y.D., Antonellis, K.J., Scherf, U., Speed, T.P., 2003. Exploration, normalization, and summaries of high density oligonucleotide array probe level data. *Biostatistics* 4, 249-264.

Ishida, T., Nakajima, T., Kudo, A., Kawakami, A., 2010. Phosphorylation of Junb family proteins by the Jun N-terminal kinase supports tissue regeneration in zebrafish. *Dev Biol* 340, 468-479.

Iten, L.E., Bryant, S.V., 1976. Stages of tail regeneration in the adult newt, *Notophthalmus viridescens*. *The Journal of experimental zoology* 196, 283-292.

Itoh, Y., 2015. Membrane-type matrix metalloproteinases: Their functions and regulations. *Matrix biology: journal of the International Society for Matrix Biology* 44-46, 207-223.

Jackson, B.C., Nebert, D.W., Vasiliou, V., 2010. Update of human and mouse matrix metalloproteinase families. *Hum Genomics* 4, 194-201.

Jensen, E.C., 2013. Quantitative analysis of histological staining and fluorescence using ImageJ. *Anatomical record (Hoboken, N.J.: 2007)* 296, 378-381.

Jeong, W.J., Park, J.C., Kim, W.S., Ro, E.J., Jeon, S.H., Lee, S.K., Park, Y.N., Min, D.S., Choi, K.Y., 2019. WDR76 is a RAS binding protein that functions as a tumor suppressor via RAS degradation. *Nature communications* 10, 295.

Johnson, C.K., Voss, S.R., 2013. Salamander paedomorphosis: linking thyroid hormone to life history and life cycle evolution. *Curr Top Dev Biol* 103, 229-258.

Jopling, C., Sune, G., Faucherre, A., Fabregat, C., Izpisua Belmonte, J.C., 2012. Hypoxia induces myocardial regeneration in zebrafish. *Circulation* 126, 3017-3027.

Kato, T., Miyazaki, K., Shimizu-Nishikawa, K., Koshiba, K., Obara, M., Mishima, H.K., Yoshizato, K., 2003. Unique expression patterns of matrix metalloproteinases in regenerating newt limbs. *Dev Dyn* 226, 366-376.

Katoh, K., Standley, D.M., 2013. MAFFT multiple sequence alignment software version 7: improvements in performance and usability. *Mol Biol Evol* 30, 772-780.

Keinath, M.C., Timoshevskiy, V.A., Timoshevskaya, N.Y., Tsonis, P.A., Voss, S.R., Smith, J.J., 2015. Initial characterization of the large genome of the salamander *Ambystoma mexicanum* using shotgun and laser capture chromosome sequencing. *Sci Rep* 5, 16413.

Khalturin, K., Hemmrich, G., Fraune, S., Augustin, R., Bosch, T.C., 2009. More than just orphans: are taxonomically-restricted genes important in evolution? *Trends in genetics: TIG* 25, 404-413.

Kleinjan, D.A., Bancewicz, R.M., Gautier, P., Dahm, R., Schonhaler, H.B., Damante, G., Seawright, A., Hever, A.M., Yeyati, P.L., van Heyningen, V., Coutinho, P., 2008. Subfunctionalization of duplicated zebrafish pax6 genes by cis-regulatory divergence. *PLoS Genet* 4, e29.

Kozlov, A.M., Darriba, D., Flouri, T., Morel, B., Stamatakis, A., 2019. RAxML-NG: A fast, scalable, and user-friendly tool for maximum likelihood phylogenetic inference. *Bioinformatics*.

Kragl, M., Knapp, D., Nacu, E., Khattak, S., Maden, M., Epperlein, H.H., Tanaka, E.M., 2009. Cells keep a memory of their tissue origin during axolotl limb regeneration. *Nature* 460, 60-65.

Kumar, A., Godwin, J.W., Gates, P.B., Garza-Garcia, A.A., Brockes, J.P., 2007. Molecular basis for the nerve dependence of limb regeneration in an adult vertebrate. *Science* 318, 772-777.

Kyriakides, T.R., Maclauchlan, S., 2009. The role of thrombospondins in wound healing, ischemia, and the foreign body reaction. *J Cell Commun Signal* 3, 215-225.

- Leask, A., Abraham, D.J., 2003. The role of connective tissue growth factor, a multifunctional matricellular protein, in fibroblast biology. *Biochemistry and cell biology: Biochimie et biologie cellulaire* 81, 355-363.
- Ledo A.S., Washer S.J., Dhanaseelan, T., Chrystal, P, Papoutsis, T., Henderson D., Chaudhry. 2019. doi: <https://doi.org/10.1101/546184>.
- Levesque, M., Gatien, S., Finnson, K., Desmeules, S., Villiard, E., Pilote, M., Philip, A., Roy, S., 2007. Transforming growth factor: beta signaling is essential for limb regeneration in axolotls. *PloS one* 2, e1227.
- Liem, R.K., 2016. Cytoskeletal Integrators: The Spectrin Superfamily. *Cold Spring Harb Perspect Biol* 8.
- Lisse, T.S., King, B.L., Rieger, S., 2016. Comparative transcriptomic profiling of hydrogen peroxide signaling networks in zebrafish and human keratinocytes: Implications toward conservation, migration and wound healing. *Sci Rep* 6, 20328.
- Looso, M., Michel, C.S., Konzer, A., Bruckskotten, M., Borchardt, T., Kruger, M., Braun, T., 2012. Spiked-in pulsed in vivo labeling identifies a new member of the CCN family in regenerating newt hearts. *J Proteome Res* 11, 4693-4704.
- Looso, M., Preussner, J., Sousounis, K., Bruckskotten, M., Michel, C.S., Lignelli, E., Reinhardt, R., Hoffner, S., Kruger, M., Tsonis, P.A., Borchardt, T., Braun, T., 2013. A de novo assembly of the newt transcriptome combined with proteomic validation identifies new protein families expressed during tissue regeneration. *Genome Biol* 14, R16.
- Lopez, D., Lin, L., Monaghan, J.R., Cogle, C.R., Bova, F.J., Maden, M., Scott, E.W., 2014. Mapping hematopoiesis in a fully regenerative vertebrate: the axolotl. *Blood* 124, 1232-1241.
- Love, N.R., Chen, Y., Ishibashi, S., Kritsiligkou, P., Lea, R., Koh, Y., Gallop, J.L., Dorey, K., Amaya, E., 2013. Amputation-induced reactive oxygen species are required for successful *Xenopus* tadpole tail regeneration. *Nat Cell Biol* 15, 222-228.
- Lu, J., Chatterjee, M., Schmid, H., Beck, S., Gawaz, M., 2016. CXCL14 as an emerging immune and inflammatory modulator. *Journal of inflammation (London, England)* 13, 1.
- MacGrath, S.M., Koleske, A.J., 2012. Cortactin in cell migration and cancer at a glance. *Journal of cell science* 125, 1621-1626.
- Mastellos, D.C., Deangelis, R.A., Lambris, J.D., 2013. Complement-triggered pathways orchestrate regenerative responses throughout phylogenesis. *Semin Immunol* 25, 29-38.

Mathew, L.K., Sengupta, S., Kawakami, A., Andreasen, E.A., Lohr, C.V., Loynes, C.A., Renshaw, S.A., Peterson, R.T., Tanguay, R.L., 2007. Unraveling tissue regeneration pathways using chemical genetics. *The Journal of biological chemistry* 282, 35202-35210.

Marchesi, S.L., Steers, E., Marchesi, V.T., Tillack, T.W. 1970. Physical and chemical properties of a protein isolated from red cell membranes. *Biochemistry* 9, 50-57.

McCusker, C., Gardiner, D.M., 2011. The axolotl model for regeneration and aging research: a mini-review. *Gerontology* 57, 565-571.

McElroy, K.E., Denton, R.D., Sharbrough, J., Bankers, L., Neiman, M., Lisle Gibbs, H., 2017. Genome expression balance in a triploid trihybrid vertebrate. *Genome Biol Evol.*

McHedlishvili, L., Mazurov, V., Grassme, K.S., Goehler, K., Robl, B., Tazaki, A., Roensch, K., Duemmler, A., Tanaka, E.M., 2012. Reconstitution of the central and peripheral nervous system during salamander tail regeneration. *Proc Natl Acad Sci USA* 109, E2258-2266.

McLaughlin, K.A., Levin, M., 2018. Bioelectric signaling in regeneration: Mechanisms of ionic controls of growth and form. *Dev Biol* 433, 177-189.

Meda, F., Gauron, C., Rampon, C., Teillon, J., Volovitch, M., Vriza, S., 2016. Nerves Control Redox Levels in Mature Tissues Through Schwann Cells and Hedgehog Signaling. *Antioxidants & redox signaling* 24, 299-311.

Meda, F., Joliot, A., Vriza, S., 2017. Nerves and hydrogen peroxide: how old enemies become new friends. *Neural regeneration research* 12, 568-569.

Miyazaki, K., Uchiyama, K., Imokawa, Y., Yoshizato, K., 1996. Cloning and characterization of cDNAs for matrix metalloproteinases of regenerating newt limbs. *Proc Natl Acad Sci USA* 93, 6819-6824.

Monaghan, J.R., Athippozhy, A., Seifert, A.W., Putta, S., Stromberg, A.J., Maden, M., Gardiner, D.M., Voss, S.R., 2012. Gene expression patterns specific to the regenerating limb of the Mexican axolotl. *Biology open* 1, 937-948.

Monaghan, James Robert, "PHYSIOLOGICAL GENOMICS OF SPINAL CORD AND LIMB REGENERATION IN A SALAMANDER, THE MEXICAN AXOLOTL" (2009). University of Kentucky Doctoral Dissertations. Paper 703. http://uknowledge.uky.edu/gradschool_diss/703

Nagase, H., Visse, R., Murphy, G., 2006. Structure and function of matrix metalloproteinases and TIMPs. *Cardiovasc Res* 69, 562-573.

Niethammer, P., Grabher, C., Look, A.T., Mitchison, T.J., 2009. A tissue-scale gradient of hydrogen peroxide mediates rapid wound detection in zebrafish. *Nature* 459, 996-999.

Nowoshilow, S., Schloissnig, S., Fei, J.F., Dahl, A., Pang, A.W.C., Pippel, M., Winkler, S., Hastie, A.R., Young, G., Roscito, J.G., Falcon, F., Knapp, D., Powell, S., Cruz, A., Cao, H., Habermann, B., Hiller, M., Tanaka, E.M., Myers, E.W., 2018. The axolotl genome and the evolution of key tissue formation regulators. *Nature* 554, 50-55.

Ohno, S., Wolf, U., Atkin, N.B., 1968. Evolution from fish to mammals by gene duplication. *Hereditas* 59, 169-187.

Owusu-Ansah E, Yavari A, Banerjee U. 2008. A protocol for in vivo detection of reactive oxygen species. Protocol Exchange doi:10.1038/nprot.2008.23.

Ozkucur, N., Epperlein, H.H., Funk, R.H., 2010. Ion imaging during axolotl tail regeneration *in vivo*. *Dev Dyn* 239, 2048-2057.

Page, R.B., Boley, M.A., Kump, D.K., Voss, S.R., 2013. Genomics of a metamorphic timing QTL: *met1* maps to a unique genomic position and regulates morph and species-specific patterns of brain transcription. *Genome Biol Evol* 5, 1716-1730.

Pajtler, K.W., Weingarten, C., Thor, T., Kunkele, A., Heukamp, L.C., Buttner, R., Suzuki, T., Miyata, N., Grotzer, M., Rieb, A., Sprussel, A., Eggert, A., Schramm, A., Schulte, J.H., 2013. The KDM1A histone demethylase is a promising new target for the epigenetic therapy of medulloblastoma. *Acta neuropathologica communications* 1, 19.

Panda, S., Zhang, J., Yang, L., Anand, G.S., Ding, J.L. 2014. Molecular interaction between natural IgG and ficolin--mechanistic insights on adaptive-innate immune crosstalk. *Sci Rep* 4, 3675.

Pardo, F.N., Altirriba, J., Pradas-Juni, M., Garcia, A., Ahlgren, U., Barbera, A., Slebe, J.C., Yanez, A.J., Gomis, R., Gasa, R., 2012. The role of Raf-1 kinase inhibitor protein in the regulation of pancreatic beta cell proliferation in mice. *Diabetologia* 55, 3331-3340.

Pirotte, N., Stevens, A.S., Fraguas, S., Plusquin, M., Van Roten, A., Van Belleghem, F., Paesen, R., Ameloot, M., Cebria, F., Artois, T., Smeets, K., 2015. Reactive Oxygen Species in Planarian Regeneration: An Upstream Necessity for Correct Patterning and Brain Formation. *Oxid Med Cell Longev* 2015, 392476.

Ponomareva, L.V., Athipozhy, A., Thorson, J.S., Voss, S.R., 2015. Using *Ambystoma mexicanum* (Mexican axolotl) embryos, chemical genetics, and microarray analysis to identify signaling pathways associated with tissue regeneration. *Comp Biochem Physiol C Toxicol Pharmacol* 178, 128-135.

Pozner, A., Terooatea, T.W., Buck-Koehntop, B.A., 2016. Cell-specific Kaiso (ZBTB33) Regulation of Cell Cycle through Cyclin D1 and Cyclin E1. *The Journal of biological chemistry* 291, 24538-24550.

Putta, S., Smith, J.J., Walker, J.A., Rondet, M., Weisrock, D.W., Monaghan, J., Samuels, A.K., Kump, K., King, D.C., Maness, N.J., Habermann, B., Tanaka, E., Bryant, S.V., Gardiner, D.M., Parichy, D.M., Voss, S.R., 2004. From biomedicine to natural history research: EST resources for ambystomatid salamanders. *BMC Genomics* 5, 54.

Ravi, V., Bhatia, S., Gautier, P., Loosli, F., Tay, B.H., Tay, A., Murdoch, E., Coutinho, P., van Heyningen, V., Brenner, S., Venkatesh, B., Kleinjan, D.A., 2013. Sequencing of Pax6 loci from the elephant shark reveals a family of Pax6 genes in vertebrate genomes, forged by ancient duplications and divergences. *PLoS Genet* 9, e1003177.

Roy, S., Levesque, M., 2006. Limb regeneration in axolotl: is it superhealing? *TheScientificWorldJournal* 6 Suppl 1, 12-25.

Saadeddin, A., Babaei-Jadidi, R., Spencer-Dene, B., Nateri, A.S., 2009. The links between transcription, beta-catenin/JNK signaling, and carcinogenesis. *Molecular cancer research: MCR* 7, 1189-1196.

Sabin, K., Santos-Ferreira, T., Essig, J., Rudasill, S., Echeverri, K., 2015. Dynamic membrane depolarization is an early regulator of ependymogial cell response to spinal cord injury in axolotl. *Dev Biol* 408, 14-25.

Sader, F., Denis, J.F., Laref, H., Roy, S., 2019. Epithelial to mesenchymal transition is mediated by both TGF-beta canonical and non-canonical signaling during axolotl limb regeneration. *Sci Rep* 9, 1144.

Salic, A., Mitchison, T.J., 2008. A chemical method for fast and sensitive detection of DNA synthesis in vivo. *Proc Natl Acad Sci USA* 105, 2415-2420.

Santos-Ledo, A., Washer, S.J., Dhanaseelan, T., Chrystal, P., Papoutsis, T., Henderson, D., Chaudhry, B., 2019. An alternatively spliced zebrafish *jnk1a* transcript has an essential and non-redundant role in development of the first heart field derived proximal ventricular chamber. *bioRxiv*, 546184.

Scarl, R.T., Lawrence, C.M., Gordon, H.M., Nunemaker, C.S., 2017. STEAP4: its emerging role in metabolism and homeostasis of cellular iron and copper. *J Endocrinol* 234, R123-R134.

Schnapp, E., Kragl, M., Rubin, L., Tanaka, E.M., 2005. Hedgehog signaling controls dorsoventral patterning, blastema cell proliferation and cartilage induction during axolotl tail regeneration. *Development* 132, 3243-3253.

Schneider, C.A., Rasband, W.S., Eliceiri, K.W., 2012. NIH Image to ImageJ: 25 years of image analysis. *Nat Methods* 9, 671-675.

Shin, S., Jang, W., Kim, M., Kim, Y., Park, S.Y., Park, J., Yang, Y.J., 2018. Targeted next-generation sequencing identifies a novel nonsense mutation in SPTB for hereditary spherocytosis: A case report of a Korean family. *Medicine (Baltimore)* 97, e9677.

Shiu, S.H., Byrnes, J.K., Pan, R., Zhang, P., Li, W.H., 2006. Role of positive selection in the retention of duplicate genes in mammalian genomes. *Proc Natl Acad Sci U S A* 103, 2232-2236.

Shukla, V., Habib, F., Kulkarni, A., Ratnaparkhi, G.S., 2014. Gene duplication, lineage-specific expansion, and subfunctionalization in the MADF-BESS family patterns the *Drosophila* wing hinge. *Genetics* 196, 481-496.

Singel, K.L., Segal, B.H., 2016. NOX2-dependent regulation of inflammation. *Clin Sci (Lond)* 130, 479-490.

Slack, J.M., 2017. Animal regeneration: ancestral character or evolutionary novelty? *EMBO Rep* 18, 1497-1508.

Smith, J.J., Putta, S., Walker, J.A., Kump, D.K., Samuels, A.K., Monaghan, J.R., Weisrock, D.W., Staben, C., Voss, S.R., 2005. Sal-Site: integrating new and existing ambystomatid salamander research and informational resources. *BMC Genomics* 6, 181.

Smith, J.J., Putta, S., Zhu, W., Pao, G.M., Verma, I.M., Hunter, T., Bryant, S.V., Gardiner, D.M., Harkins, T.T., Voss, S.R., 2009. Genic regions of a large salamander genome contain long introns and novel genes. *BMC Genomics* 10, 19.

Smith, J.J., Timoshevskaya, N., Timoshevskiy, V.A., Keinath, M.C., Hardy, D., Voss, S.R., 2019. A chromosome-scale assembly of the axolotl genome. *Genome Res* 29, 317-324.

Sreekumar, P.G., Hinton, D.R., Kannan, R., 2011. Methionine sulfoxide reductase A: Structure, function and role in ocular pathology. *World J Biol Chem* 2, 184-192.

Stocum, D.L., 2017. Mechanisms of urodele limb regeneration. *Regeneration (Oxf)* 4, 159-200.

Stoick-Cooper, C.L., Moon, R.T., Weidinger, G., 2007. Advances in signaling in vertebrate regeneration as a prelude to regenerative medicine. *Genes & development* 21, 1292-1315.

Sugiura, T., Tazaki, A., Ueno, N., Watanabe, K., Mochii, M., 2009. *Xenopus* Wnt-5a induces an ectopic larval tail at injured site, suggesting a crucial role for noncanonical Wnt signal in tail regeneration. *Mech Dev* 126, 56-67.

Sun, Y.B., Xiong, Z.J., Xiang, X.Y., Liu, S.P., Zhou, W.W., Tu, X.L., Zhong, L., Wang, L., Wu, D.D., Zhang, B.L., Zhu, C.L., Yang, M.M., Chen, H.M., Li, F.,

Zhou, L., Feng, S.H., Huang, C., Zhang, G.J., Irwin, D., Hillis, D.M., Murphy, R.W., Yang, H.M., Che, J., Wang, J., Zhang, Y.P., 2015. Whole-genome sequence of the Tibetan frog *Nanorana parkeri* and the comparative evolution of tetrapod genomes. *Proc Natl Acad Sci USA* 112, E1257-1262.

Takahashi, J.S., 2016. Molecular Architecture of the Circadian Clock in Mammals, in: Sassone-Corsi, P., Christen, Y. (Eds.), *A Time for Metabolism and Hormones*, Cham (CH), pp. 13-24.

Tan, H., Chen, X., Lv, W., Linpeng, S., Liang, D., Wu, L., 2018. Truncating mutations of HIBCH tend to cause severe phenotypes in cases with HIBCH deficiency: a case report and brief literature review. *Journal of human genetics* 63, 851-855.

Tan, H.M., Low, W.Y., 2018. Rapid birth-death evolution and positive selection in detoxification-type glutathione S-transferases in mammals. *PloS one* 13, e0209336.

Tanaka, E., Galliot, B., 2009. Triggering the regeneration and tissue repair programs. *Development* 136, 349-353.

Tapia, N., Reinhardt, P., Duemmler, A., Wu, G., Arauzo-Bravo, M.J., Esch, D., Greber, B., Cojocaru, V., Rascon, C.A., Tazaki, A., Kump, K., Voss, R., Tanaka, E.M., Scholer, H.R., 2012. Reprogramming to pluripotency is an ancient trait of vertebrate Oct4 and Pou2 proteins. *Nature communications* 3, 1279.

Tasaki, J., Shibata, N., Sakurai, T., Agata, K., Umesono, Y., 2011. Role of c-Jun N-terminal kinase activation in blastema formation during planarian regeneration. *Development, growth & differentiation* 53, 389-400.

Thomas, P.D., Campbell, M.J., Kejariwal, A., Mi, H., Karlak, B., Daverman, R., Diemer, K., Muruganujan, A., Narechania, A., 2003. PANTHER: a library of protein families and subfamilies indexed by function. *Genome Res* 13, 2129-2141.

Timmer, J.R., Mak, T.W., Manova, K., Anderson, K.V., Niswander, L., 2005. Tissue morphogenesis and vascular stability require the Frem2 protein, product of the mouse myelencephalic blebs gene. *Proc Natl Acad Sci U S A* 102, 11746-11750.

Torres-Sanchez, M., Creevey, C.J., Kornobis, E., Gower, D.J., Wilkinson, M., San Mauro, D., 2019. Multi-tissue transcriptomes of caecilian amphibians highlight incomplete knowledge of vertebrate gene families. *DNA Res* 26, 13-20.

Tseng, A.S., Levin, M., 2012. Transducing bioelectric signals into epigenetic pathways during tadpole tail regeneration. *Anatomical record (Hoboken, N.J.: 2007)* 295, 1541-1551.

Vinarsky, V., Atkinson, D.L., Stevenson, T.J., Keating, M.T., Odelberg, S.J., 2005. Normal newt limb regeneration requires matrix metalloproteinase function. *Dev Biol* 279, 86-98.

- Voordeckers, K., Pougach, K., Verstrepen, K.J., 2015. How do regulatory networks evolve and expand throughout evolution? *Current opinion in biotechnology* 34, 180-188.
- Voss, S.R., Kump, D.K., Putta, S., Pauly, N., Reynolds, A., Henry, R.J., Basa, S., Walker, J.A., Smith, J.J., 2011. Origin of amphibian and avian chromosomes by fission, fusion, and retention of ancestral chromosomes. *Genome Res* 21, 1306-1312.
- Voss, S.R., Palumbo, A., Nagarajan, R., Gardiner, D.M., Muneoka, K., Stromberg, A.J., Athippozhy, A.T., 2015. Gene expression during the first 28 days of axolotl limb regeneration I: Experimental design and global analysis of gene expression. *Regeneration (Oxf)* 2, 120-136.
- Voss, S.R., Ponomareva, L.V., Dwaraka, V.B., Pardue, K.E., Baddar, N., Rodgers, A.K., Woodcock, M.R., Qiu, Q., Crowner, A., Blichmann, D., Khatri, S., Thorson, J.S., 2019. HDAC Regulates Transcription at the Outset of Axolotl Tail Regeneration. *Sci Rep* 9, 6751.
- Voss, S.R., Prudic, K.L., Oliver, J.C., Shaffer, H.B., 2003. Candidate gene analysis of metamorphic timing in ambystomatid salamanders. *Molecular ecology* 12, 1217-1223.
- Voss, S.R., Shaffer, H.B., 1997. Adaptive evolution via a major gene effect: paedomorphosis in the Mexican axolotl. *Proc Natl Acad Sci U S A* 94, 14185-14189.
- Voss, S.R., Smith, J.J., 2005. Evolution of salamander life cycles: a major-effect quantitative trait locus contributes to discrete and continuous variation for metamorphic timing. *Genetics* 170, 275-281.
- Wagner, A., 2008. Gene duplications, robustness and evolutionary innovations. *BioEssays: news and reviews in molecular, cellular and developmental biology* 30, 367-373.
- Wang, S., Zhu, X. Q., & Cai, X. 2017. Gene duplication analysis reveals no ancient whole genome duplication but extensive small-scale duplications during genome evolution and adaptation of *Schistosoma mansoni*. *Frontiers in cellular and infection microbiology*, 7, 412.
- Walford, G.A., Gustafsson, S., Rybin, D., Stancakova, A., Chen, H., Liu, C.T., Hong, J., Jensen, R.A., Rice, K., Morris, A.P., Magi, R., Tonjes, A., Prokopenko, I., Kleber, M.E., Delgado, G., Silbernagel, G., Jackson, A.U., Appel, E.V., Grarup, N., Lewis, J.P., Montasser, M.E., Landenvall, C., Staiger, H., Luan, J., Frayling, T.M., Weedon, M.N., Xie, W., Morcillo, S., Martinez-Larrad, M.T., Biggs, M.L., Chen, Y.D., Corbaton-Anchuelo, A., Faerch, K., Gomez-Zumaquero, J.M., Goodarzi, M.O., Kizer, J.R., Koistinen, H.A., Leong, A., Lind, L., Lindgren, C., Machicao, F., Manning, A.K., Martin-Nunez, G.M., Rojo-Martinez, G., Rotter, J.I., Siscovick, D.S., Zmuda, J.M., Zhang, Z., Serrano-Rios, M., Smith, U., Soriguer, F., Hansen, T., Jorgensen, T.J.,

Linnenberg, A., Pedersen, O., Walker, M., Langenberg, C., Scott, R.A., Wareham, N.J., Fritsche, A., Haring, H.U., Stefan, N., Groop, L., O'Connell, J.R., Boehnke, M., Bergman, R.N., Collins, F.S., Mohlke, K.L., Tuomilehto, J., Marz, W., Kovacs, P., Stumvoll, M., Psaty, B.M., Kuusisto, J., Laakso, M., Meigs, J.B., Dupuis, J., Ingelsson, E., Florez, J.C., 2016. Genome-Wide Association Study of the Modified Stumvoll Insulin Sensitivity Index Identifies BCL2 and FAM19A2 as Novel Insulin Sensitivity Loci. *Diabetes* 65, 3200-3211.

Wang, J., Karra, R., Dickson, A.L., Poss, K.D., 2013. Fibronectin is deposited by injury-activated epicardial cells and is necessary for zebrafish heart regeneration. *Dev Biol* 382, 427-435.

Weidinger, A., Kozlov, A.V., 2015. Biological Activities of Reactive Oxygen and Nitrogen Species: Oxidative Stress versus Signal Transduction. *Biomolecules* 5, 472-484.

Weston, C.R., Davis, R.J., 2002. The JNK signal transduction pathway. *Curr Opin Genet Dev* 12, 14-21.

Wilson, R., Golub, S.B., Rowley, L., Angelucci, C., Karpievitch, Y.V., Bateman, J.F., Fosang, A.J., 2016. Novel Elements of the Chondrocyte Stress Response Identified Using an in Vitro Model of Mouse Cartilage Degradation. *J Proteome Res* 15, 1033-1050.

Wingler, K., Altenhoefer, S.A., Kleikers, P.W., Radermacher, K.A., Kleinschnitz, C., Schmidt, H.H., 2012. VAS2870 is a pan-NADPH oxidase inhibitor. *Cellular and molecular life sciences: CMLS* 69, 3159-3160.

WWW.ambystoma.org

Yang, E.V., Bryant, S.V., 1994. Developmental regulation of a matrix metalloproteinase during regeneration of axolotl appendages. *Dev Biol* 166, 696-703.

Yang, E.V., Gardiner, D.M., Carlson, M.R., Nugas, C.A., Bryant, S.V., 1999. Expression of Mmp-9 and related matrix metalloproteinase genes during axolotl limb regeneration. *Dev Dyn* 216, 2-9.

Yin, F.F., Wang, N., Bi, X.N., Yu, X., Xu, X.H., Wang, Y.L., Zhao, C.Q., Luo, B., Wang, Y.K., 2016. Serine/threonine kinases 31(STK31) may be a novel cellular target gene for the HPV16 oncogene E7 with potential as a DNA hypomethylation biomarker in cervical cancer. *Virology journal* 13, 60.

Yoo, S.K., Freisinger, C.M., LeBert, D.C., Huttenlocher, A., 2012. Early redox, Src family kinase, and calcium signaling integrate wound responses and tissue regeneration in zebrafish. *The Journal of cell biology* 199, 225-234.

Yun, M.H., Davaapil, H., Brockes, J.P., 2015. Recurrent turnover of senescent cells during regeneration of a complex structure. *Elife* 4.

- Yun, M.H., Gates, P.B., Brockes, J.P., 2014. Sustained ERK activation underlies reprogramming in regeneration-competent salamander cells and distinguishes them from their mammalian counterparts. *Stem cell reports* 3, 15-23.
- Zeke, A., Misheva, M., Remenyi, A., Bogoyevitch, M.A., 2016. JNK Signaling: Regulation and Functions Based on Complex Protein-Protein Partnerships. *Microbiology and molecular biology reviews: MMBR* 80, 793-835.
- Zhang, J. Z. 2003. Evolution by gene duplication: an update. *Trends Ecol. Evol.* 18, 292–298. doi: 10.1016/S0169-5347(03)00033-8.
- Zhang, Q., Wang, Y., Man, L., Zhu, Z., Bai, X., Wei, S., Liu, Y., Liu, M., Wang, X., Gu, X., Wang, Y., 2016. Reactive oxygen species generated from skeletal muscles are required for gecko tail regeneration. *Sci Rep* 6, 20752.
- Zhang, W., Bouchard, G., Yu, A., Shafiq, M., Jamali, M., Shrager, J.B., Ayers, K., Bakr, S., Gentles, A.J., Diehn, M., Quon, A., West, R.B., Nair, V., van de Rijn, M., Napel, S., Plevritis, S.K., 2018. GFPT2-Expressing Cancer-Associated Fibroblasts Mediate Metabolic Reprogramming in Human Lung Adenocarcinoma. *Cancer research* 78, 3445-3457.
- Zhang, W., Guo, Y., Li, J., Huang, L., Kazitsa, E.G., Wu, H., 2016. Transcriptome analysis reveals the genetic basis underlying the seasonal development of keratinized nuptial spines in *Leptobranchium boringii*. *BMC Genomics* 17, 978.
- Zhao, A., Qin, H., Fu, X., 2016. What Determines the Regenerative Capacity in Animals? *BioScience* 66, 735-746.
- Zheng, J., Lu, W., Wang, C., Xing, Y., Chen, X., Ai, Z., 2017. Galectin-3 induced by hypoxia promotes cell migration in thyroid cancer cells. *Oncotarget* 8, 101475-101488.
- Zuehlke, A.D., Beebe, K., Neckers, L., Prince, T., 2015. Regulation and function of the human HSP90AA1 gene. *Gene* 570, 8-16.

Curriculum Vitae
Nour W. AL Haj Baddar

EDUCATION

- 2019** University of Kentucky, Department of Biology, Ph.D. candidate.
- 2009** University of Jordan, Amman, Jordan.
- 2006** B.Sc., Biomedical Sciences, University of Jordan, Amman, Jordan.

PUBLICATIONS

Al Haj Baddar N.W., Torres Sanchez M., Kump D. K., Keach L., Woodcock M. R., and S. Randal Voss. Identification of Axolotl Matrix Metalloproteinases Gene Family Reveals Novel Salamander-Specific *MMP3* Gene Duplication. *In prep.*

Voss, S. R., Ponomareva L., Dwaraka, V., Pardue, K., **Al Haj Baddar, N.**, Rodgers A., Woodcock R., Qiu Q., Crouner A., Blichmann D., Khatri S., Thorson, J. (2019). HDAC Regulates Pathways Associated with Tissue Regeneration at the Time of injury. Scientific Reports. *In press.*

Al Haj Baddar, N. W.*, Chithrala, A., and Voss, S. R. (2018). Amputation-induced Reactive Oxygen Species Signaling is Required for Axolotl Tail Regeneration. *Dev. Dyn.* doi:10.1002/dvdy.5

Al Haj Baddar, N. W., Woodcock, M. R., Khatri, S., Kump, D. K., Voss, S. R. (2015). Sal-site: Research Resources for the Mexican Axolotl. In A. Kumar and A. Simon (Eds). *Salamanders in Regeneration Research: Methods and Protocols* (pp. 321-336). New York, NY: Springer Science + Business Media.

Al Haj Baddar, N., Disi A., Aburjai A., and Taha M. (2011). Thujone corrects cholesterol and Triglyceride Profiles in Diabetic Rat Model. *Natural Product Research Journal*.25: 1180-1184.

Al Haj Baddar, N., Disi A., Aburjai T., and Taha M. (2010). The entitled patent Thujone corrects Cholesterol and Triglyceride Profiles in Diabetic Rat Model has been registered by JU intellectual property office at The University of Jordan.

*: Corresponding Author

TEACHING AND RESEARCH EXPERIENCE

- 2019** Teaching Assistantship, Cell biology BIO 315, Department of Biology, University of Kentucky.

- 2018** Teaching Assistantship, Principles of Biology BIO 155, Department of Biology, University of Kentucky.
- 2015- 2017** Research Assistantship, Dr. Randal Voss's Lab, Department of Biology, University of Kentucky.
- 2014- 2015** Teaching Assistantship, Cell Biology BIO 315, Department of Biology, University of Kentucky.
- 2013- 2014** Teaching Assistantship, Evolution BIO 303, Department of Biology, University of Kentucky.
- 2011- 2013** Teaching Assistantship, Principles of Biology BIO 155, Department of Biology, University of Kentucky.
- 2010** Lab Supervisor, Department of biology, University of Jordan.
- 2010** Biomedical lab technician, Arab Medical Laboratory, Amman, Jordan.
- 2006- 2009** Teaching Assistantship, Department of Biology, University of Jordan.
- 2005** Biomedical Laboratories training, University of Jordan Hospital, Amman, Jordan.